Design and Motion Control of a 6-UPS Fully Parallel Robot for Long Bone Fracture Reduction

A thesis presented in partial fulfillment of the requirements for the degree of

Master of Engineering

In
Mechatronics

at
Massey University
Albany, New Zealand.

Yimin Wu

2007

ACKNOWLEDGEMENTS

I would like to thank those who have helped me throughout the project. I would firstly like to thank my wife, Mei and also my mother, RongXiang for looking after my newborn daughter, ChuQi. Without their help I could not have concentrated on the project. I would like to thank Professor Peter Xu and Dr Johan Potgieter who are my project supervisors. The project could not have been completed without their advice and guidance.

To the following engineering staff members, Dr Olaf Diegel, Gordon Warren, Eddy Rogers and Raymond Hoffmann, I would like to express my gratitude for all their time spent in making the heavy robot framework and giving me lots of suggestions in mechanical design.

I would also like to thank my friends, BiQing Chen, Steven, and all other postgraduates for the happy time shared during the project and the chance to exchange strange and wonderful ideas.

Last, but not least, I would like to thank my lovely princess, ChuQi, for all the joy she has brought to my life. I would like to dedicate the thesis to her.

ABSTRACT

The incidences of long bone fractures in New Zealand are approximately 1 in 10,000. Long bones such as tibia and femur have complicated anatomic structures, making the realignment of these long bone fractures reliant on the skill of the surgeon. The drawbacks of current practice result in long time exposure to radiation, slow recovery and possible morbidity. A semi-automated long bone fracture reduction system based on a 6-DOF parallel robot platform has been in development since 2004.

The developed 6-DOF parallel robot platform comprises of six linear actuators with rotary incremental encoders. To implement a realignment of long bone fractures, a framework for the 6-DOF platform robot has been developed. The inverse kinematics and singularity of the 6-DOF parallel robot has been studied to obtain the actions and Jacobin matrices.

In motion control a multiple axis motion controller and amplifiers were used for 6-DOF parallel robot. PID tuning algorithms were developed based on the combination of the general tuning result and the contour control principle. The PID parameters have been validated by a numbers of experiments.

The practical realignment of bone fractures requires a "Pull-Rotate-Push" action implemented by the 6-DOF parallel robot. After calibration, the reduction trajectories were generated accurately. The actual trials on the artificial fractures have shown that the robot developed is capable of performing the required reduction motion.

TABLE OF CONTENTS

LIST of FIGURES

LIST of TABLES

Chapter 1 Introduction

1.1 Introduction

1.1.1 Definition

A long bone fracture realignment medical robot system is under development at Massey University in Auckland. This robot system is expected to be a semi-automated fracture reduction system interacting with a Human-Machine (HM) interface. After planning and simulation through HMI in an offline mode, the repositioning movements planned by the surgeon will be performed on a robot platform whose end-effector is attached to the patient's foot. With the aid of this system, an actual manipulation of the fracture fragments will become more accurate, safe and more efficient compared with current manual procedures. The old system relies on the surgeon's experience and ability to interpret X-rays, a higher volume of X-ray exposure rate on the patients, higher risk possibility of other infections, human fatigue and lengthy operations.

1.1.2 System structure

The fracture realignment procedures consist of a planning phase (or teaching) and an operational phase. According to these two phases, the entire system has been developed as shown in Figure1.1 (Graham et. al., 2005).

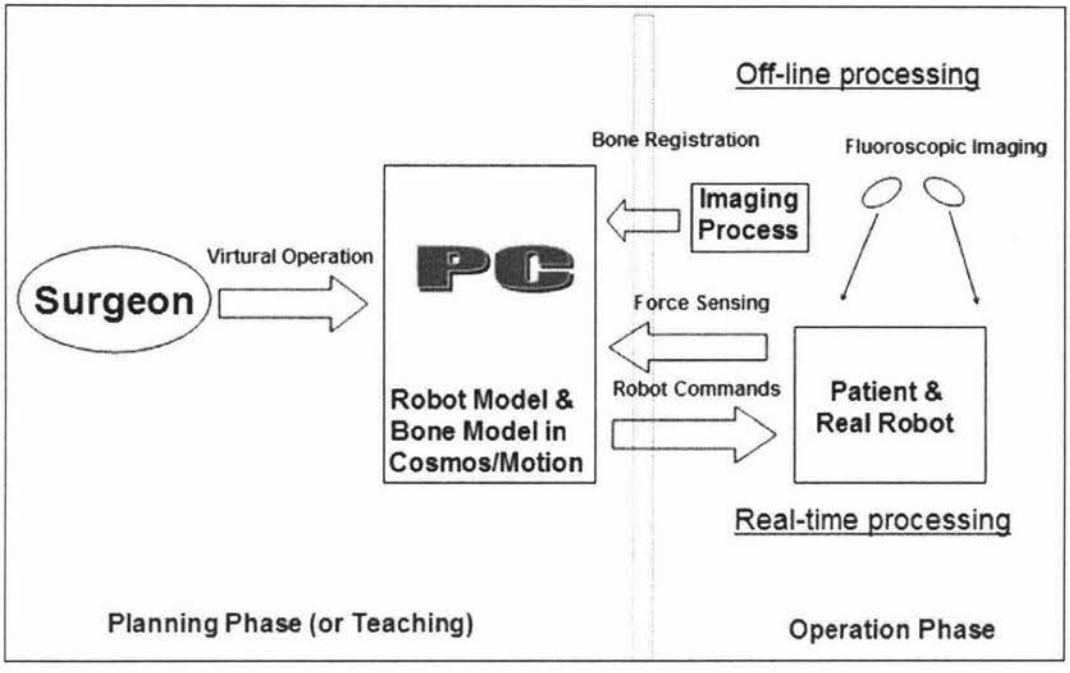

Figure 1.1 Overview of the proposed system structure

To achieve the required robot system, the following functional modules should be developed.

System modeling & software engineering is the primary module, which integrates the other subsystems for signal inputting, motion analysis, trajectory generation, motion implementation, feedback and emergency procedures.

X-ray Image processing for geometric model of fractures is to take advantage of existing digital fluoroscopic images to reconstruct fractures in a three-dimensional environment. An effective procedure is required to reduce fluoroscopic images taken, and the format of the relative displacement of fractures needs to be represented in homogenous transformations.

Motion implementation emphasizes that a compact/portable 6-DOF (Degree-Of-Freedom) parallel robot is used to provide spatial mobility for fracture reduction. The frame of robot, formation, kinematics and dynamics analysis are required to manipulate the fractures realignment in a controlled fashion.

Human machine interface for surgeons differs from an engineer's requirements. A software environment is required to be developed for surgical procedures, in which the geometric fractures can be modeled from X-ray images, and the fractures'

biomechanics and robotic dynamics can be visualized, simulated and animated. A graphical user interface (GUI) for the surgeon's convenience of planning and decision making is essential.

1.1.3 Project aim

This thesis is concerned with the motion implementation of a standardized 6-DOF parallel robot for the use in the surgical environment. In 2004, a 6-DOF parallel Stewart-Gough platform was introduced into this project. This Stewart Gough platform comprises of six linear actuators attached between a top and base plate. The ends of each linear actuator are equipped with a 3-DOF joint and a 2-DOF joint. In principle, the linear extension and retraction of the six actuators gives the platform six degrees-of-freedom positioning capabilities, consisting of three translational and three rotational degree-of-freedoms (Harib and Srinivasan, 2003).

This platform was constructed and single motor was tested. As a platform, it was not working in a control fashion. The trial and evaluation of the prototype system did not begin in a real operation theatre environment, the robot framework in term of real environment was missing and the analysis of the kinematics and performance was not completed. All these issues are required to be studied deeply before the platform would get into a working system. In view of this, this project was aimed to work out the solution for these issues clearly and provide more valuable experiences and sources for the future system integration.

1.2. Background

1.2.1 The current bone realignment procedure

The initial requirements of the robot were specified by a surgeon, who hoped Massey University to develop a robot system for image-guided orthopedic surgery. The surgical procedure is described as below.

The patient's foot is attached to a traction machine connected to the patient's table through a 2-DOF linkage. The traction machine is able to slide along one of links to adjust linear displacement according to patient leg length and has the purpose of pulling the broken bone fragments into partial alignment. This is the main method of realigning during the operation (Figure1.2).

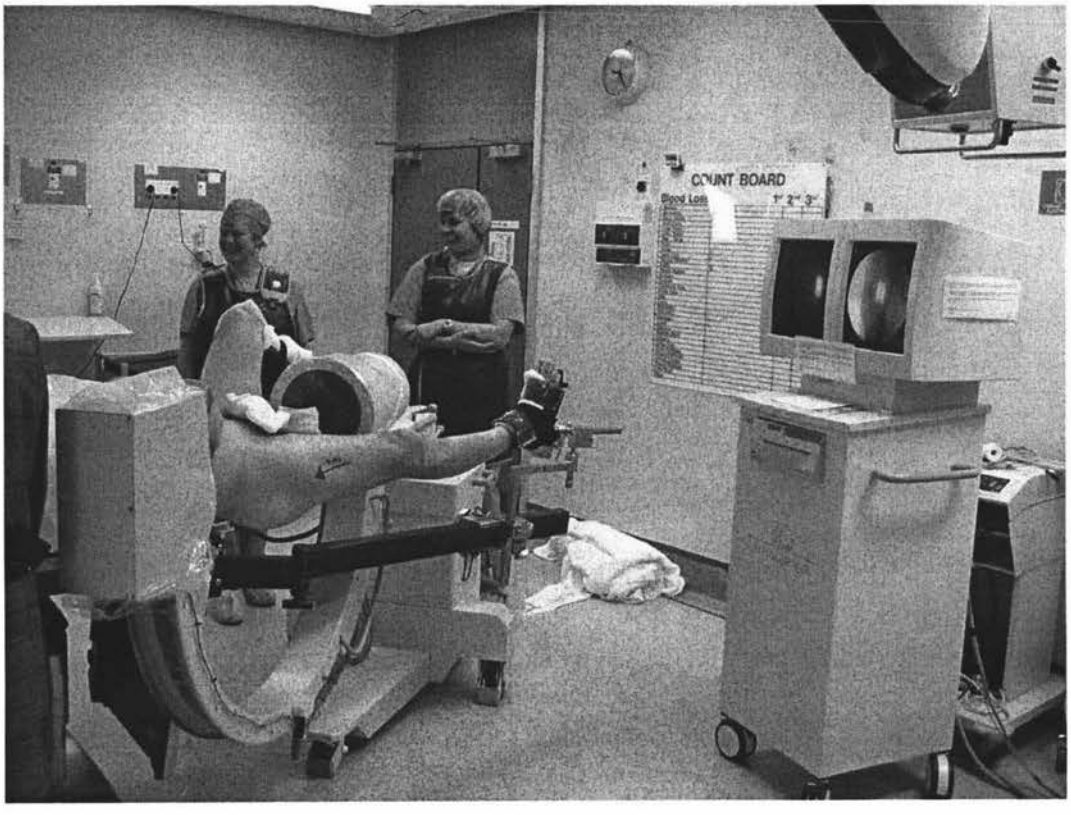

Figure 1.2 Long bone fracture realignment operation

The alignment of the broken bones is viewed in real time using a fluoroscope that is the large cylindrical instrument with a low power portable x-ray machine that can take short burst images that provide a video display of the position of the broken bone fragments to surgeons during the operation. Using resource provided by fluoroscope, the surgeon manipulates the broken bones manually to achieve the best possible realignment. The feedback is acted on manually by the surgical assistants to align the bone parts back into the best possible alignment. Once aligned, the surgeon pins the bones into position and the operation is complete. After the operation the patient's leg is placed in a cast.

The traction machine has a rack and pinion mechanism that provides the axial force to pull the leg. The foot is attached to the foot holster and the traction machine assembly is rigidly attached to the operating table (Figure 1.3).

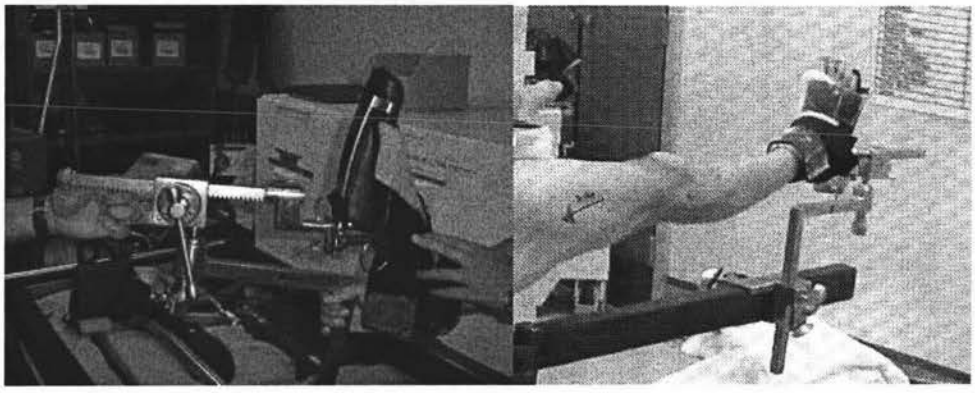

Figure 1.3 Traction machine and operation

1.2.2 Contribution by preceding students

In the past three years, a number of undergraduates have contributed to the project to various extents. Swanson (Swanson 2004) designed in SolidWorks model and built 6-DOF parallel robot. Torrance (Torrance 2004) developed a motion control system and tried on single actuator closed loop control. Ashish (Ashsih 2005) built a Hall-effect position sensor for the actuators.

1.2.3 Objectives

In early 2006, it was expected that the robot prototype should perform facture alignment procedures in a controlled fashion in the real environment and the performance of platform would be evaluated after experimentation.

To this end, objectives were identified as follows,

- Investigation and improvement of the existing design
- Design and building of a physical framework where the robot is attached
- Interfacing sensors to the motion controller
- PID tuning with effective load for all six actuators

- Trajectory generation and implementation by the robot within predefined error limitations
- Platform demonstration and simulation
- Performance evaluation and analysis
- Trouble shooting and future improvement

Chapter 2 Literature review

2.1 Overview of parallel robots

2.1.1 Parallel robots: definition

General parallel manipulators can be defined as follows: A generalized parallel manipulator is a closed-loop kinematic chain mechanism whose end-effectors are linked to the base by several independent kinematic chains (Merlet 2000).

This type of mechanism is interesting for the following reasons:

- A minimum of two chains allows to distribute the load on the chains.
- The number of actuators is minimal.
- The number of sensors necessary for the closed-loop control of the mechanism is minimal.
- When the actuators are locked, the manipulator remains in its position; this is an important safety aspect for certain application, such as medical robot.

Parallel robot can be therefore be defined as follows:

A parallel robot is made up of an end-effector with n degrees of freedom, and of a fixed base, linked together by at least two independent kinematic chains. Actuation takes place through n simple actuators (Merlet 2000).

Parallel robots for which the number of chains is strictly equal to the number of DOF of the end-effector are called fully parallel manipulators (Merlet 2000).

A fully parallel manipulator is described into Eq. (1.1) by Gosselin (Gosselin 1988).

$$p\,(n-6) = -6 \qquad (1.1)$$

Where, p represents the number of chains and n the number of rigid bodies within a chain.

2.1.2 Parallel robot vs. serial robot

A fully parallel robot with 6-DOF has six serial chains in parallel, and only one joint in each chain is actuated. The Gough-Stewart platform is the one of the representative fully parallel robot introduced by Gough (1956) as an aircraft simulation mechanism, also called as 6-UPS robot which is related to its structure by some literatures. Of course, other parallel structures are possible and many exist in practice (Figure 2.1).

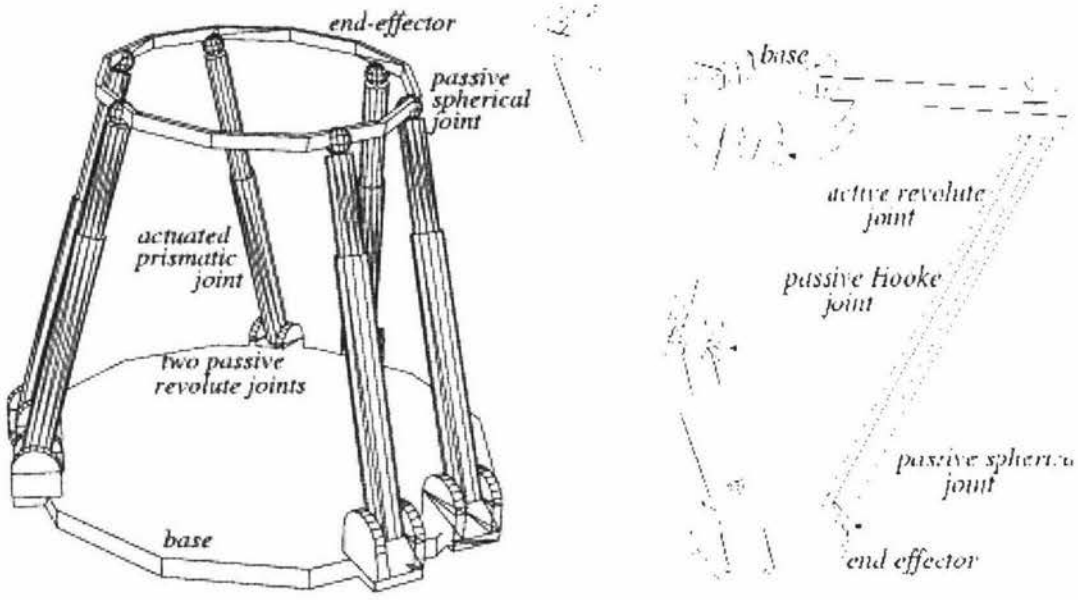

(a) Fully parallel Stewart-Gough platform (b) parallel HEXA platform

Figure 2.1 Structures of fully parallel platform (Bruyninckx 2005)

In recent years, the Stewart Platform mechanism has attracted considerable attention in view of its application to 6 DOF machine tool structures rather than serial robots that are constituted of a succession of rigid bodies, each of them being linked to its predecessor and its successor by a one DOF joint (Merlet 2000).

The main reasons for the overwhelming success of the serial robot design (over 99% of installed industrial robots) are:

- A larger workspace compared to the space occupied by the robot itself

- Kinematics designs that simplify the mathematics of the robot's geometry enormously.
- Higher rigidity and strength to weight ratio

The main drawback of a serial robot is low intrinsic rigidity, so that heavy links and joints must be used to obtain a reasonable effective rigidity at the end point. These pros and cons are exactly the opposites of those of parallel manipulators.

The fully parallel designs have all actuators in or near the base, which results in a very low inertia of the part of the robot that has actually to be moved. Hence, a higher bandwidth can be achieved with the same actuation power. This is why parallel structures are used for, for example, flight simulators and ABB Flexi Picker robots.
A parallel structure supports its end-effector in multiple places, which yields a stiffer and hence more accurate manipulator for the same weight and cost, and which causes the positioning errors generated in each leg to "average out," again increasing the accuracy. However, experiments with real prototypes show that parallel structures currently do not live up to these expectations: their accuracy and stiffness are about an order of magnitude worse than for classical serial machines. The reasons are: (Bruyninckx, 2005).

- The compliance of the ball screws in the prismatic joints,
- The complexity of the construction with many passive joints that all have to be manufactured and assembled with strict tolerances,
- The complexity of kinematic calibration of this structure
- The high forces that some passive joints have to resist.

In addition, another major disadvantage of parallel manipulators is their small workspace: legs can collide, and there are many passive joints in the structure that all introduce joint limit constraints. This is especially the case with the spherical "ball-in-socket" joints used in most implementations, (Bruyninckx 2005).

2.2 Architectures

2.2.1 Notation of parallel robots

There are many ways to describe the mechanical architecture of a parallel robot. For example, a Gough platform can be denoted either as 6-6 robot (because there are six attachment points connecting on the end of top plate and end plate) or as a 6-UPS (where U represents Universal joint, followed by a prismatic that is itself connected by a ball-and-socket joint or spherical joint) or as 3T-3R (having three translational and three rotational DOF (Merlet 2000).

For convenience, this thesis will use 6-UPS robot for a Gough-Stewart platform unless otherwise stated, "fully parallel robot" will be regarded as 6-UPS robot or Gough-Stewart platform because this project has already used it as a system structure.

2.2.2 6-DOF manipulators

As mentioned early, 6-DOF manipulator can be presented by several physical forms in term of their chains constitution. Such that forms are RRPS, RPRS, PRRS, RRRS types where R denotes revolution joint. All the mechanisms using these generators will belong to the same class as the Gough-Stewart platform, but that doesn't mean they have equivalent performance because of different leg structure (Merlet 2000).

2.2.3 6-UPS robot (Gough-Stewart platform)

6-UPS robot is also called hexapod, which is the most commonly used architecture and has been used in numerous applications and prototype. The first design for industrial purpose was done early 1950s, by Gough in UK for tire testing machine. In 1956, Stewart finished a design for a flight simulator. The first application of this type of parallel manipulator probably was contributed by McCallion in the end of 1970s.

This platform (Figure 2.2) is linked to the base by 6 chains. The base plate is connected to the end of a prismatic actuator through a universal joint, while the chains

are attached to the top plate by a spherical joint. The top plate is able to reach anyplace within workspace droved by the prismatic joint which allows the change of the length of the links.

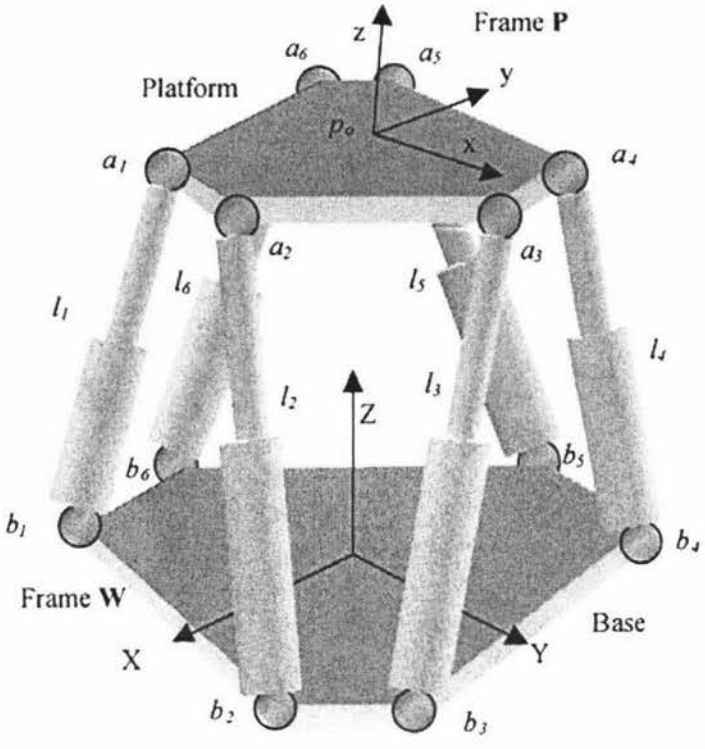

Figure 2.2 General structure of Gough Stewart platform (Harib and Srinivasan 2003)

In general, the linear actuation of the link could be provided either hydraulically, electrically or pneumatically and usually includes a ball screw-nut mechanism to convert motor shaft rotation to linear displacement. With position sensor equipped, the displacement can be controlled precisely according to real requirement.

2.3 Existing applications of 6-UPS robot

2.3.1 Spatial application

Besides tire testing machine and flight simulator mentioned before, a very successful utilization of 6-UPS robot is as a pointing device for telescopes that has

been installed at Cerro Armazones observatory in Chile (APEX assembly 2003) (Figure 2.3).

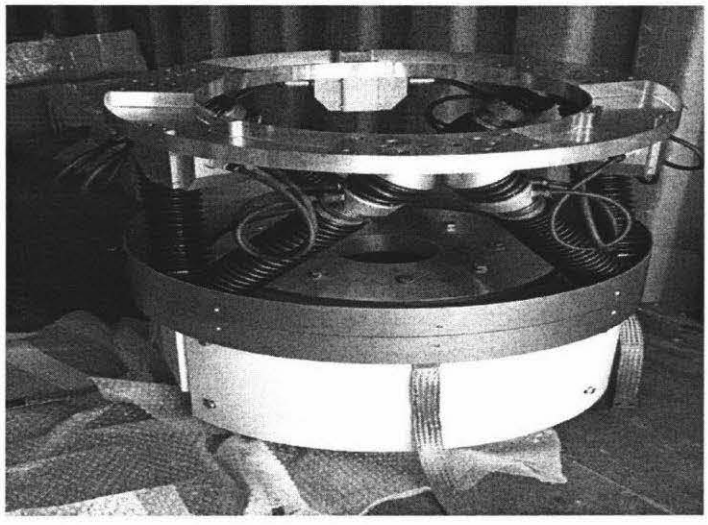

Figure 2.3 A telescope pointing system (APEX assembly 2003)

2.3.2 Vibration

The characteristics of high bandwidth of parallel structures make them good candidates for vibration damping done by MicroMega (MicroMega 2003) (Figure 2.4).

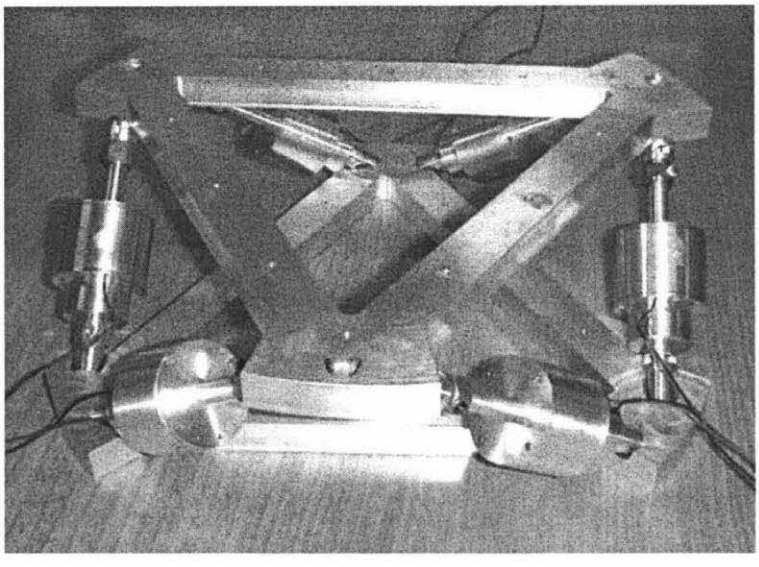

Figure 2.4 A vibration damping (Micromega Dynamics)

2.3.3 Medical application

A MARS robot is mounted on the patient's bony structure near the surgical site. This robot has been used as a surgical tool guiding spinal pedicle screw placement and is sold by Mazor as the Spine Assist robot (Shoham 2003). A similar robot for knee arthroplasty, the Mini Bone Attached Robotic System is currently being developed at CMU (Lisien et al. 2004) (Figure 2.5).

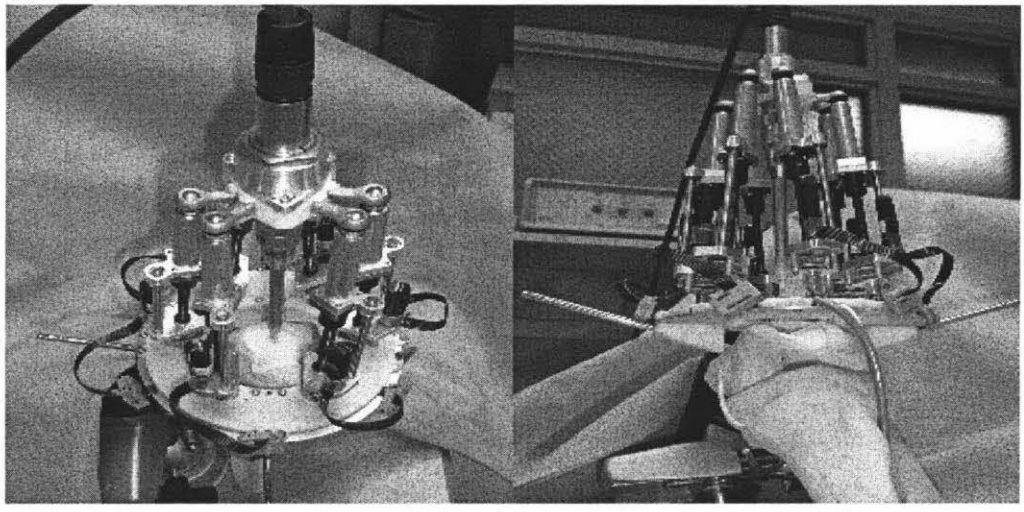

Figure 2.5 Mini bone-attached robotic systems (Lisien et.al. 2004)

Chapter 3 Analysis and design of the parallel robot

3.1 Introduction

A 6-UPS (Gough-Stewart) platform was designed and assembled at Massey University in 2004. As an operating mechanism, this platform is required to integrate with the entire system. Furthermore, the six linear actuators need to be positioned precisely for motion control. The analysis of the robot is necessary for further study. The advantage to do the above is to obtain useful control data from the mathematical model as well as to verify the platform performance through theoretical methods.

A further objective is for the entire robot to be attached to a working frame for the purpose of simulating real surgical environment. The framework to support the platform requires a combination of stability and flexibility with adequate mechanical strength.

3.2 Analysis of the 6-UPS robot

3.2.1 Coordinate system assignment

To fully describe a 6-UPS robot, a six-coordinate system is needed. Three of these coordinates are used for describing the positional displacement of a reference point in the top plate (the moving part) with respect to the base plate (the fixed part). The other three coordinates are angular displacements to describe the orientation of the moving part with reference to the fixed part (Harib and Srinivasan 2003).

In robotics, Euler angles are widely used to represent orientations transformation. For convenience, in this thesis, Z-Y-X Euler angle (α, β, γ) convention is selected from a set of 24 conventions (Craig 2005). They are defined in Figure 3.1:

> Start with the frame coincident with a know frame {A}. Rotate {B} first about Z_B by an angle α, then about Y_B by an angle β, and, finally, about X_B by an angle γ.

Figure 3.1 shows the axes of frame B during this rotation process.

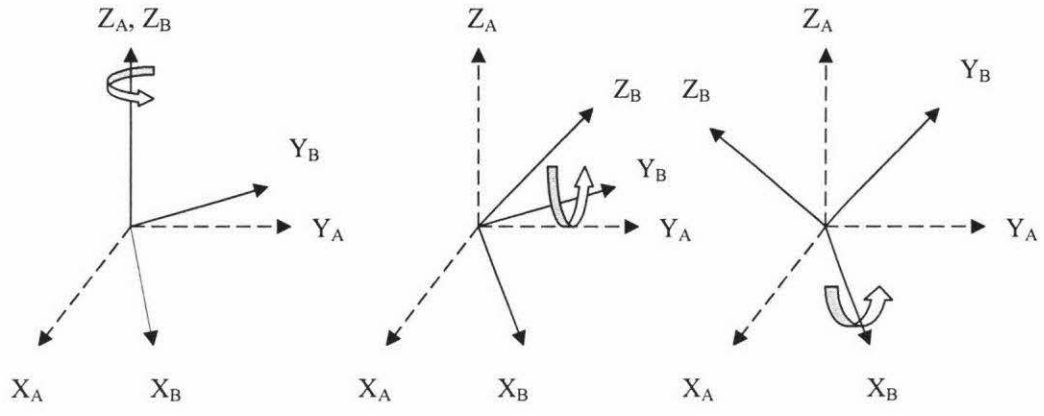

Figure 3.1 Z-Y-X Euler system

Particularly, for 6-UPS robot, frame {A} and {B} represent the base and top plate respectively. Only one difference from the above figure, the origin of frame A and B are not in coincidence, which indicates the origin of frame B has a translation with respect to the origin of frame A (Figure 3.2)

Since each vertex of link is a known value with respect to the plane that it locates, once coordinate system confirmed, the joints space kinematics of the robot are easily determined.

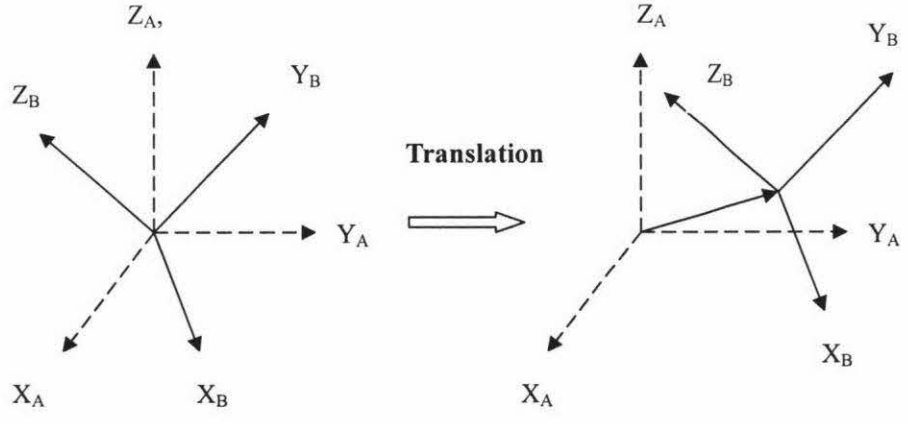

Figure 3.2 Translational Z-Y-X Euler system

The position of frame B is specified as a vector x $(X, Y, Z)^T$ described by frame A. The orientation of frame B with reference to frame A is expressed in a matrix ${}^{A}_{B}R$ which is derived in term of Euler angles in the next section. So a generalized coordinate vector q can be described in the following matrix as $q = (X, Y, Z, \alpha, \beta, \gamma)^T$, the joint space coordinate vector l is defined as $l_i = (l_1, l_2, l_3, l_4, l_5, l_6)^T$ where l_i for $i = 1 \quad 6$ are the lengths of the six links of 6-UPS.

3.2.2 Inverse kinematics

The inverse kinematics problem of 6-UPS robot is concerned with the determination of the displacements of the six links corresponding to a given Cartesian position of the top plate in terms of three positional displacements and three Euler angular displacements (Harib and Srinivasan 2003). The inverse kinematics for a 6-UPS robot has a unique solution (Bruyninckx 2005). This study has a realistic meaning for robot operation, which is what displacement should be fed into each linear actuator while the robot is trying to pull the fractured bone from the fracture area back to the original position or those transitional points in the trajectory.

To achieve the aim, a simplified vectorial structure is presented for one of links of the 6-UPS robot (Figure 3.3).

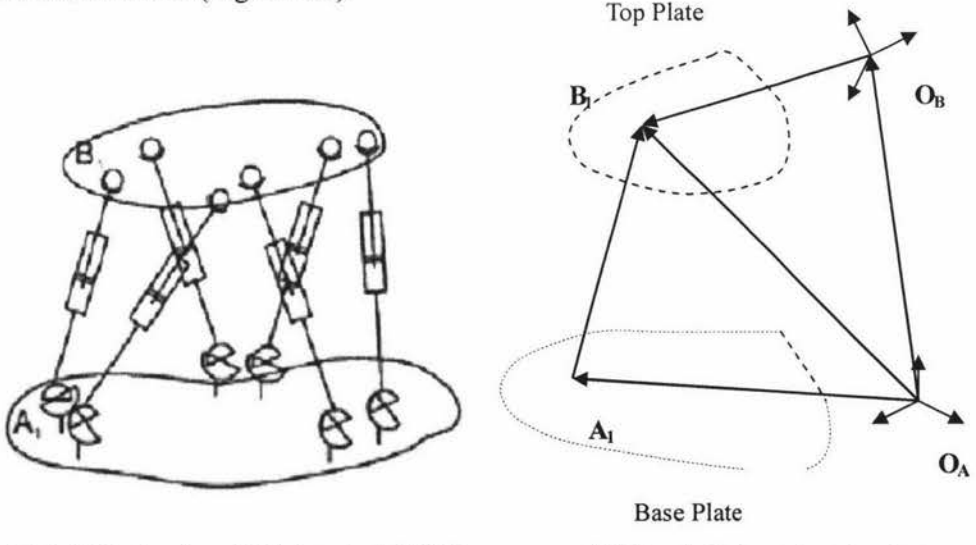

(a) 6-UPS structure (Sabater et.al. 2006) (b) Single link vector structure

Figure 3.3 Vecotrial structure for inverse kinematics

Referring to the above diagram, the solution of the inverse kinematics of 6-UPS robot is to get the length of A_1B_1. Where, O_A and O_B are the origin of frame A and B, O_AA_1 and O_BB_1 are two known vectors with respect to the frame A and frame B respectively. According to the principle of vector addition and Z-Y-X Euler orientation angle, O_AB_1 which represents the position of B_1 with reference to frame A calculated as:

$$O_AB_1 = O_AO_B + {}^A_BR\ O_BB_1 \qquad (3.1)$$

Eq.(3.1) is theoretical solution for 6-UPS robot, which is also proved in (Merlet 2000). Where, ${}^A_BR(\alpha, \beta, \gamma)$ is the orthogonal rotation matrix that can be calculated as follow: R_Z is the rotation matrix about the z axis, R_Y is the rotation matrix about the y axis, R_X is the rotation matrix about the x axis, which

$$ {}^A_BR(\alpha, \beta, \gamma) = R_Z(\alpha)\, R_Y(\beta)\, R_X(\gamma) $$

$$ = \begin{bmatrix} C\alpha C\beta & C\alpha S\beta S\gamma - S\alpha C\gamma & C\alpha S\beta C\gamma + S\alpha S\gamma \\ S\alpha C\beta & S\alpha S\beta S\gamma + C\alpha C\gamma & S\alpha S\beta C\gamma - C\alpha S\gamma \\ -S\beta & C\beta S\gamma & C\beta C\gamma \end{bmatrix} \qquad (3.2)$$

Where, $C\alpha = Cos\alpha, S\alpha = Sin\alpha$, and so on (Craig 2005).

As mentioned, O_AA_1, O_BB_1, are the known positions of A_1, B_1 described by frame A and frame B respectively, which their coordinates are constant value from the original design (Table 3.1). O_BO_A represents the vertical height of robot platform that needs to be assigned according to requirement.

Table 3.1: Coordinates of vertexes in the frame A and frame B

Vertexes	Frame A	Vertexes	Frame B
A1	(220,0)	B1	(150,0)
A2	(110,192.525)	B2	(129.90, 75)
A3	(-110,192.525)	B3	(-75,129.90)
A4	(-220,0)	B4	(-129.90,75)
A5	(-110,-192.525)	B5	(-75,-129.90)
A6	(110,-192.525)	B6	(0,-150)

Therefore, referring back to Eq. (3.1), (3.2) and Table 3.1, the position of B_1 with reference to frame A, namely O_AB_1 is can be obtained. Consequently, the length of leg can be calculated effortlessly for any given position of the moving platform as:

$$A_1B_1 = O_AB_1 - O_AA_1 \tag{3.3}$$

Similarly, the principle of Eq. (3.3) can also be applied to other links. This algorithm has been coded in MATLAB program (Appendix A) for all inverse calculations. While running this program, a user just needs to follow the prompts and enter the desired Euler angle (α, β, γ) and the origin O_B described by frame A-O_AO_B, and then the lengths of six links will be shown on the screen. When the robot is at the home position, it has an angle set (α=15°, β=0°, γ=0°) and O_AO_B (0, 0,500), which means O_A and O_B are in concentric with a distance along Z axis of 500mm, the inverse solution yields the six actuations in the range of 507.09~507.43mm.

3.2.3 Singularity

Singularity is about the special positions of the moving plate, in which the robot is uncontrollable and loses its rigidity. Since singularity can never be eliminated, avoidance should be considered in the design stage and control algorithm. Singularity analysis is important for several reasons:

- Freedom loss: the pose of the moving platform has a loss of instantaneous motion of one or more degrees (Donelan 2005).
- Control issues: the robot is uncontrollable. The actual trajectory is away from commanded trajectory with an unacceptable error.
- Safety consideration: element of the robot such as joints may be subjected to very large forces, even causing a breakdown of the robot..

For the above-mentioned reasons, the singularity of a parallel robot has been studied by many researchers. One of the singularity analysis methods for the 6-UPS robot is related to Jacobian matrix. Singularity occurs in the configurations where the determinant of Jacobian matrix vanishes. Hence, to find those conditions which

make the determinant of Jacobian matrix become zero is the key of singularity analysis. In this section, Jacobian matrix will be derived and studied. In addition, some contributions on the singularity analysis by the previous researches will be presented.

(A) Jacobian matrix

To derive Jacobian matrix for singularity analysis, it is useful to express the angular velocity $\omega = (\omega_X, \omega_Y, \omega_Z)^T$ of the top plate with respect to frame A (base plate) as a function of the first time derivatives of the Euler angles $(\dot{\alpha}, \dot{\beta}, \dot{\gamma})$. Referring to Figure 3.3, consider the Z-Y-X Euler angles

$$ {}^{A}_{B}R(\alpha, \beta, \gamma) = R_Z(\alpha) R_Y(\beta) R_X(\gamma) \qquad (3.4) $$

The angular velocity of frame B with respect to frame A described in frame A is the sum of components due to the rotation of each individual Euler angle, which is

$$ \omega = \dot{\alpha} e_3 + \dot{\beta} R_\alpha e_2 + \dot{\gamma} R_\alpha R_\beta e_1 \qquad (3.5) $$

In which the first term is related to the rotation α around the $Z_A \in A$ axis. The rotation occurs around $R_\alpha e_2$ the rotated version of Y_1. The Y axis of the rotated frame after the yaw rotation has been applied. Finally the roll γ occurs around the axis $R_\alpha R_\beta$ e_1, the image of X_A under the first two rotations (Chen 2005).

Expanding Eq. (3.5) yields

$$ \omega = \begin{pmatrix} \omega_X \\ \omega_Y \\ \omega_Z \end{pmatrix} = \dot{\alpha} \begin{pmatrix} 0 \\ 0 \\ 1 \end{pmatrix} + \dot{\beta} \begin{pmatrix} -S\alpha \\ C\alpha \\ 0 \end{pmatrix} + \dot{\gamma} \begin{pmatrix} C\partial C\beta \\ S\alpha C\beta \\ S\beta \end{pmatrix} $$

$$ = \begin{pmatrix} 0 & -S\alpha & C\alpha C\beta \\ 0 & C\alpha & S\alpha C\beta \\ 1 & 0 & -S\beta \end{pmatrix} \begin{pmatrix} \dot{\alpha} \\ \dot{\beta} \\ \dot{\gamma} \end{pmatrix} = R_{3\times 3} \begin{pmatrix} \dot{\alpha} \\ \dot{\beta} \\ \dot{\gamma} \end{pmatrix} \qquad (3.6) $$

In Figure3.3, the coordinates of the i[th] attachment point B_i on the top plate, described with respect to frame B as ${}^{B}B_i=(x, y, z)^T$, are obtained with respect to the base plate coordinate system A (${}^{A}B_i$):

$$ {}^{A}B_i = O_A B_i = O_A O_B + {}^{A}_{B}R \; O_B B_i \tag{3.7} $$

Once the position of the attachment point ${}^{A}B_i$ is determined, the vector L_i of link i is obtained as

$$ L_i = {}^{A}A_i - {}^{A}B_i \tag{3.8} $$

Where ${}^{A}A_i$ is a known 3-vector that represents the coordinates of the base attachment point A_i with respect to frame A (Tab 3.1). The scalar length l_i of link i can be computed as follows.

$$ l_i = \sqrt{L_i \cdot L_i} \tag{3.9} $$

Therefore, the unit vector along the axis of the prismatic joint of link i is computed as

$$ n_i = L_i / l_i \tag{3.10} $$

The velocity of point B_i is obtained by differentiating B_i with respect to time,

$$ \dot{B}_i = \omega \times {}^{A}_{B}R \; {}^{A}B_i + \dot{H} \tag{3.11} $$

where H represents $O_A O_B$ $(X, Y, Z)^T$, the origin O_B described by frame A, the projection of this velocity vector on the axis of the prismatic joint of link i yields the extension rate of link i

$$ \dot{l}_i = \dot{B}_i \cdot n_i = \omega \times {}^{A}_{B}R \; {}^{A}B_i \cdot n_i + \dot{H} \cdot n_i \tag{3.12} $$

or

$$ \dot{l}_i = \dot{B}_i \cdot n_i = \omega \cdot \left({}^{A}_{B}R \; {}^{A}B_i \right) \times n_i + \dot{H} \cdot n_i \tag{3.13} $$

where for a triple scalar product ($\boldsymbol{a}$ x $\boldsymbol{b}$) · $\boldsymbol{c}$, the dot and cross products can be interchanged yielding $\boldsymbol{a}$ · ($\boldsymbol{b}$ x $\boldsymbol{c}$), as long as the order of the vectors is not changed (Harib and Srinivasan 2003). For the purpose of deriving the Jacobian matrix of the robot, it is useful to write the equation for the six links, in matrix form, as

$$\dot{l}_i = \begin{pmatrix} n_1^T & \left({}_B^A R \, {}^A B_1 \times n_1 \right)^T \\ \vdots & \\ n_6^T & \left({}_B^A R \, {}^A B_6 \times n_6 \right)^T \end{pmatrix} \begin{pmatrix} \dot{H} \\ \omega \end{pmatrix}$$

$$= J_1 \begin{pmatrix} \dot{H} \\ \omega \end{pmatrix} \tag{3.14}$$

Where

$$J_1 = \begin{pmatrix} n_1^T & \left({}_B^A R \, {}^A B_1 \times n_1 \right)^T \\ \vdots & \\ n_6^T & \left({}_B^A R \, {}^A B_6 \times n_6 \right)^T \end{pmatrix} \tag{3.15}$$

Now substituting H$(X, Y, Z)^T$ and ω Equation (3.6) into the equation (3.14) yields

$$\dot{l}_i = \begin{pmatrix} n_1^T & \left({}_B^A R \, {}^A B_1 \times n_1 \right)^T \\ \vdots & \\ n_6^T & \left({}_B^A R \, {}^A B_6 \times n_6 \right)^T \end{pmatrix} \begin{pmatrix} \dot{X} \\ \dot{Y} \\ \dot{Z} \\ \omega \end{pmatrix}$$

$$= \begin{pmatrix} n_1^T & \left({}_B^A R \, {}^A B_1 \times n_1 \right)^T \\ \vdots & \\ n_6^T & \left({}_B^A R \, {}^A B_6 \times n_6 \right)^T \end{pmatrix} \begin{pmatrix} \dot{X} \\ \dot{Y} \\ \dot{Z} \\ R_{3\times3} \begin{pmatrix} \dot{\alpha} \\ \dot{\beta} \\ \dot{\gamma} \end{pmatrix} \end{pmatrix} = \begin{pmatrix} n_1^T & \left({}_B^A R \, {}^A B_1 \times n_1 \right)^T \\ \vdots & \\ n_6^T & \left({}_B^A R \, {}^A B_6 \times n_6 \right)^T \end{pmatrix} \begin{pmatrix} I_{3\times3} & & O_{3\times3} & \\ & 0 & -S\alpha & C\alpha C\beta \\ O_{3\times3} & 0 & C\alpha & S\alpha C\beta \\ & 1 & 0 & -S\beta \end{pmatrix} \begin{pmatrix} \dot{X} \\ \dot{Y} \\ \dot{Z} \\ \dot{\alpha} \\ \dot{\beta} \\ \dot{\gamma} \end{pmatrix}$$

$$= J_1 J_2 \dot{q} = J \dot{q} \tag{3.16}$$

where q is a generalized coordinate vector described as $(X, Y, Z, \alpha, \beta, \gamma)^T$ and J_2 is defined as

$$J_2 = \begin{pmatrix} I_{3\times3} & & O_{3\times3} & \\ & 0 & -S\alpha & C\alpha C\beta \\ O_{3\times3} & 0 & C\alpha & S\alpha C\beta \\ & 1 & 0 & -S\beta \end{pmatrix} \tag{3.17}$$

Eq.(3.16) presents the solution to the inverse rate kinematics problem. $J = J_1\ J_2$ is the Jacobian matrix of this 6-UPS robot. The mechanism is in a singular position when $Det\ (J^{-1}) = 0$. Such a condition will occur as either J_1 or J_2 is singular.

However, the conditions for J_1 involve a complicated polynomial computation. On the other hand, J_2 is singular for $\beta = \pi/2$, the procedure can be done in *MATLAB* symbolic calculation as:

$$\begin{aligned} Det\ (J_2^{-1}) &= -Sin^2\alpha Cos\beta - Cos^2\alpha Cos\beta \\ &= -Cos\beta\ (Sin^2\alpha + Cos^2\alpha\ ) \\ &= -Cos\beta \end{aligned} \tag{3.18}$$

So when $\beta = \pi/2$, $Det\ (J_2^{-1}) = 0$. This means singularity will occur in the current system configuration.

(B) Experienced singular configuration

In addition, for a 6-UPS robot, some known configurations causing singularities have been found by many researchers, which are summarized as follows:

- A singularity occurs when the moving plate is rotated ± 90 degree about the Z-axis. In that case, α is arbitrary and other rotational angles are zero. This kind of singularity is called Fichter's singularity (Fichter 1986).
- A singular configuration occurs where the moving plate can rotate about the line intersected by all six legs (Hunt 1978).
- The plates are in the same plane (Bruyninckx 2005).
- When the plates are similar in structure, 6-UPS robot is singular in the significant region of the workspace, which is the so-called architecture singularity(Ma and Angeles 1990):

1) When the plates are regular polygons, 6-UPS is singular in the whole workspace.
2) When the plates are irregular polygons, and
    a) If the centers of both plates are coincident;
    b) If the orientation of the plates are same

3.3 Framework design

3.3.1 Current operating framework

The current operating framework for surgery consists of a traction device, a mobile patient table, linkages, and joints and supporting accessories (Figure 3.4), which can support a series of operating positions according to different fracture situations and patient's physical diversity. Considering the traction device to be replaced by a 6-DOF robot, the characteristics of the framework are summarized as follows:

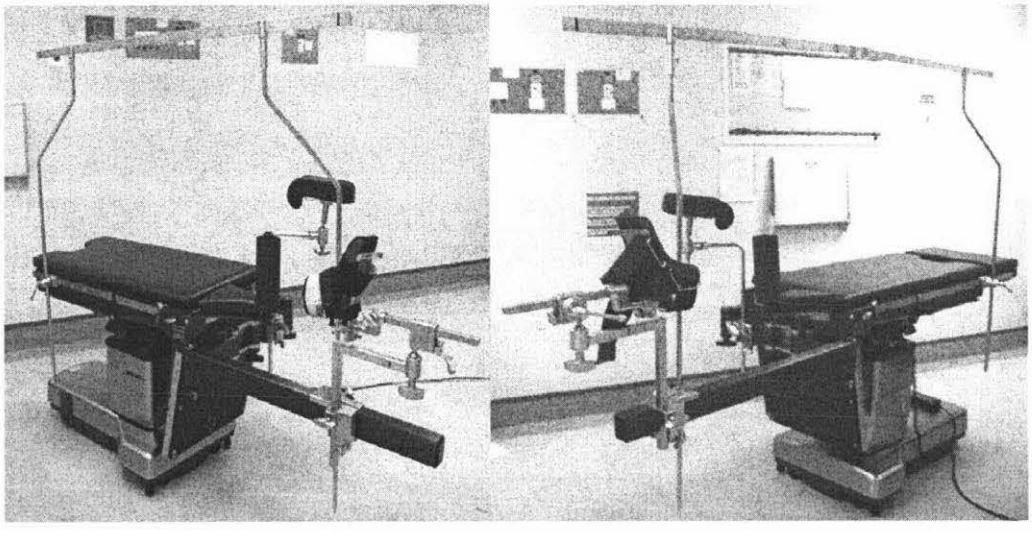

Figure 3.4 Current operating table for surgery

- A two-bar linkage with 2-DOF supporting traction device.
- The traction device has one DOF of sliding along the link (Horizontal).
- The traction device has a height adjustment (Vertical).
- The patient table is mobile and portable.

- Some special accessories are designed helpfully for positioning and patient comfort.

3.3.2 Design concept

As a prototype, the key of the design is to embody the above characteristics. Considering the physical dimensions and mass of 6-UPS platform robot, a strong supporting framework is necessary for the robot as well as the original degrees of freedom and flexibility.

Conceptual design was firstly carried out in SolidWorks with main specifications as shown in Figure 3.5 and Table 3.2.

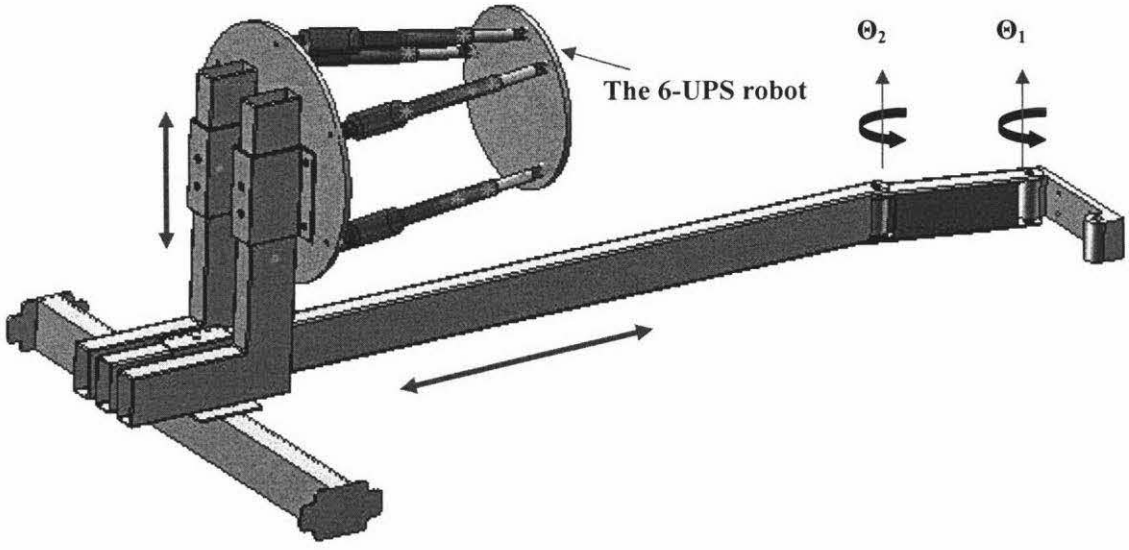

Figure 3.5 SolidWorks model of robot framework

Table 3.2 Parts details

Serial No	Part name	Description	Quantity
1	Link 1 in 2-DOF	Consists of 2-DOF linkage	1
2	Link 2 in 2-DOF	Consists of 2-DOF linkage	1
3	L shaped beam	Support mechanism	2

4	Coupler	Support mechanism	1
5	Crossbeam	Load supporter	1
6	Jockey Stander	Robot height adjustment	1
7	Jockey wheel	Framework mobile mechanism	2
8	Cylinder joint	Revolute joint	2
9	Mounting plate	Mounting 2-DOF on the table	1
10	Φ 16 bolt	Joints fasten	4
11	Φ 12 bolt	Fixing robot	14
12	6-UPS robot	Robot platform	1
13	Mobile table	Patient table	1

(A) 2-DOF linkage

The 2-DOF linkage is used to connect patient's table to the robot supporting frame. The design idea is to make a rigid, strong 'long bar' to form the main link in the framework (Figure 3.6). The two revolution joints provide the linkages from the table attachment to a 'short bar' and from the 'short bar' to the 'long bar'.

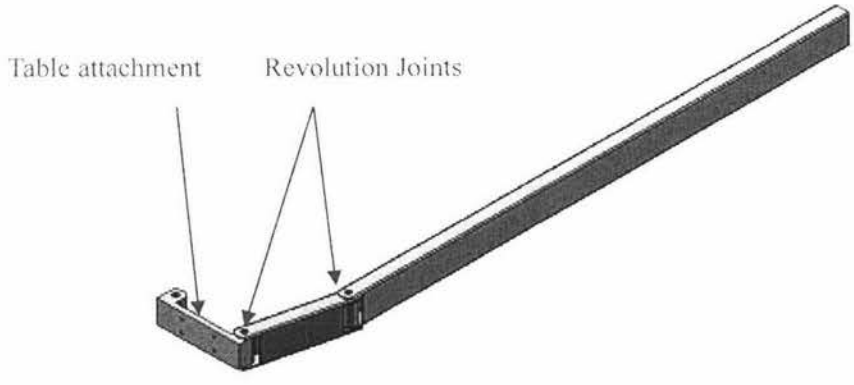

Figure 3.6 Design of the 2-DOF main linkages and the attachment

(B) Crossbeam and L shaped beam

To support a total weight over 19.2 kg, a crossbeam designed for supporting the 6- DOF robot and 2-DOF linkage is shown in Figure 3.5. As specified early, it should both support the maximum load in the framework and keep adequate mobility by attaching two jockey wheels at the end.

(C) Coupling mechanism

The coupling device is a mechanism that was designed to link the actual robot to the 'L' shaped beam. Its function is the height adjustment along L shape beam (Figure 3.5).

(D) Jockey stander and jockey wheel

As mentioned early, to make the height of the platform adjustable and the framework mobile, one jockey stander was installed on L shaped beam as well as a pair of jockey wheel attached on both ends of crossbeam.

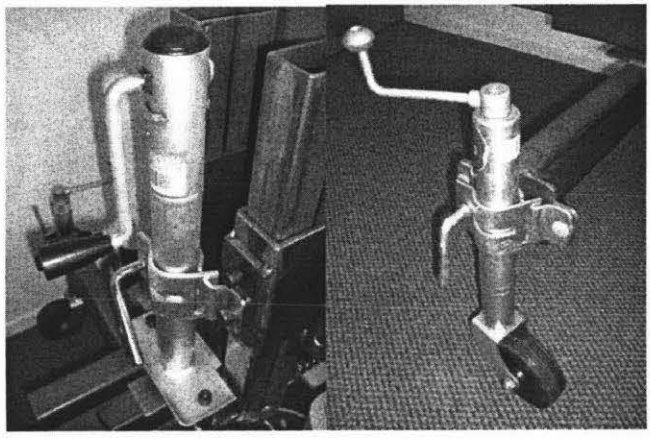

Figure 3.7 Jockey stander and jockey wheel

(E) Mobile table

As a required, the table needs to be rigid and strong to withstand the applied weight and torque. The table also has to be heavy enough and have a lockable roller stand to move around.

A garage tool trolley was chosen as the solution. Equipped with lockable wheels, it is able to provide enough stability and rigidity for the entire platform and the 2-DOF linkage also can be mounted effectively on its surface. The table also provides an enough space to place a computer and controller on, which means the portability would be realized.

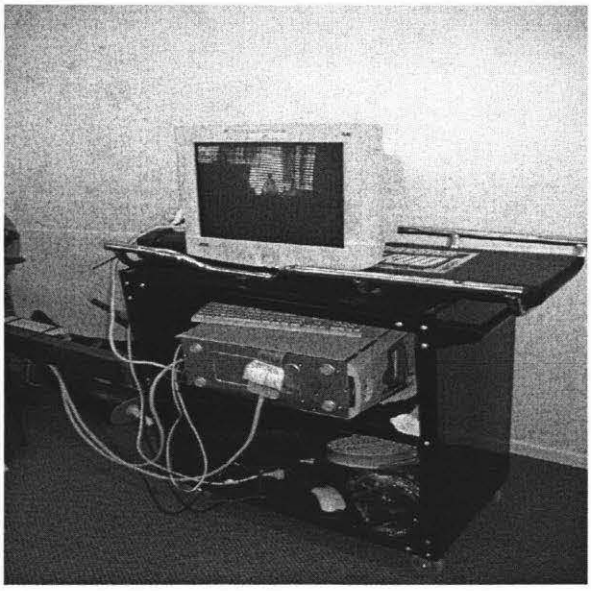

Figure 3.8 Mobile table

3.3.3 Implementation and assembly

(A) Materials

The main materials chosen for links, crossbeam and L shaped beam are made from steel En (9)/ AISI 1060, and its specification is shown in Table 3.3..

Table 3.3: Physical properties of EN 9 carbon steel

Materials	Density	Unit weight	Modulus of elasticity	Modulus of Rigidity
Steel, Carbon	7.7 Mg/m3	0.28Ib/in3	207 Gpa	79Gpa

(B) Production

According to the conceptual design and SolidWorks models, the 2-DOF link bars were firstly produced. 4 of Ø16 bolts fasten links and cylindrical bearing in axial so that consists of a 2-DOF linkage (Figure 3.9).

The shaped beam was welded onto the steel sleeve of $130 \times 100 \times 150$ mm. The purpose was to put the 2-DOF link through to perform the required link length adjustment. The sleeve type attachment interfacing located between in dual L shaped beams was specially fabricated, so that the main 'long bar' can be secured and put

through the sleeve. As a result, the platform system could be securely locked into a shape desired according to the physical dimension of the patient.

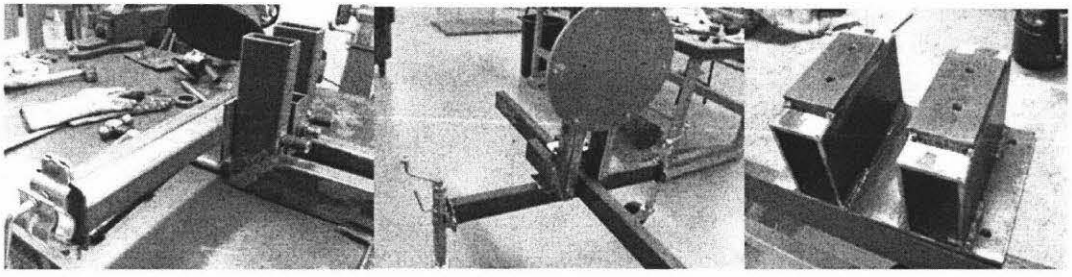

A) Welding L and crossbeam B) Jockey stander and wheel C) Sleeve mechanism

Figure 3.9 Production of framework

The jockey wheel and stand have also been assembled for ease and adjustability of the height, which adds mobility and adjusting capability to the platform system.

(C) Other accessories

A few racks and handles would still be required for securing the patient's feet. As for the prototype, they were not included in the design.

Two artificial fractures are shown in Figure 3.10, one being a manikin and the other real bones. The femur was cut into two pieces, one being fixed into manikin and another on the table.

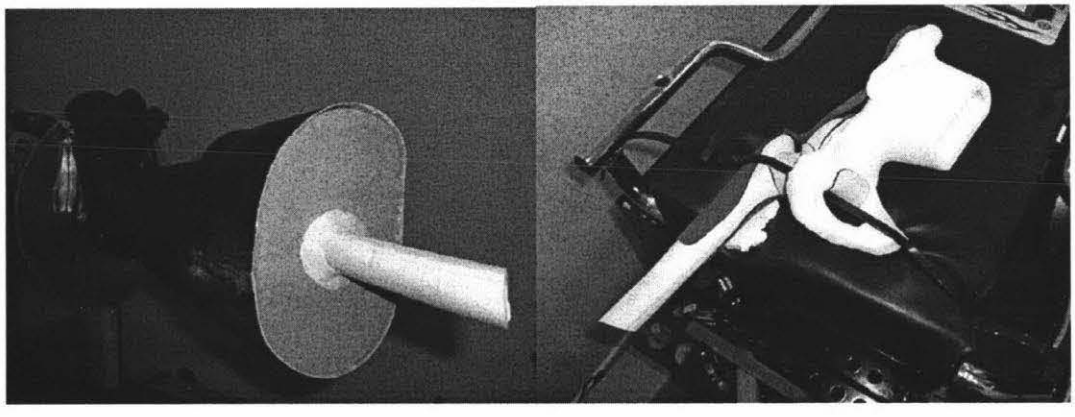

Figure 3.10 Manikin and the fixed sciatic joint

(D) Assembly

The whole system including the framework and the robot is shown in Figure 3.11.

The technical parameters for the framework are shown in Table 3.4.

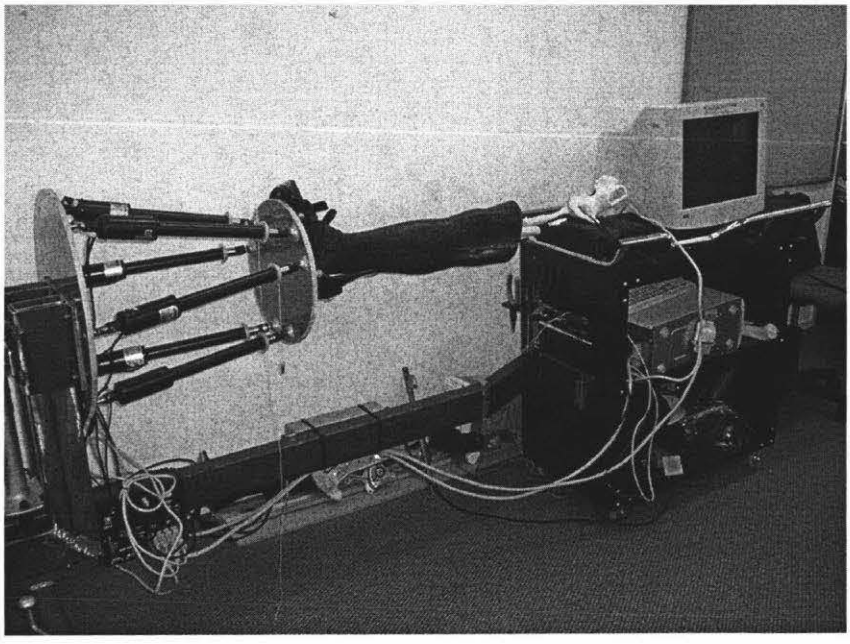

Figure 3.11 Assembled robot with framework

Table 3.4 Components of the system

Serial No	Part name	Dimension (L x W x H)mm	Weight	Quantity
1	Link 1 in 2-DOF	350 x 100 x 50	2.7kg	1
2	Link 2 in 2-DOF	1730 x 100 x 50	10.4 kg	1
3	L shaped beam	350 x 600 x 50	6.6kg	2
4	Coupler	290 x 180 x 115	6.2kg	1
5	Crossbeam	1012 x100 x50	7.8kg	1
6	Jockey Stander	N/A	3.5kg	1
7	Jockey wheel	N/A	4.2kg	2
8	Cylinder joint	Φ50 x 90	1.2kg	2
9	Mounting plate	300 x 90 x 65	5.7kg	1
10	Φ 16 bolt	Φ 16	78gm	4
11	Φ 12 bolt	Φ 12	55gm	14
12	6-UPS robot	N/A	19.2kg	1
13	Mobile table	N/A	N/A	1

3.4 Performance analysis.

3.4.1 Workspace

The workspace of this framework can be regarded as a 2-D area similar to the one for a standard two-links manipulator, which depends on the 2-DOF linkage transformation. Theoretically, the reachable workspace consists of a ring of outer radius L1+L2, and inner radius $|L1-L2|$, where L1 is one link length and L2 another link length. However, in practice, considering the physical constraints of revolution joints, the real reachable workspace is less than theoretical. With $0 \leq \theta_1 \leq 165$ degree for link L1, the workspace is shown in Figure 3.12.

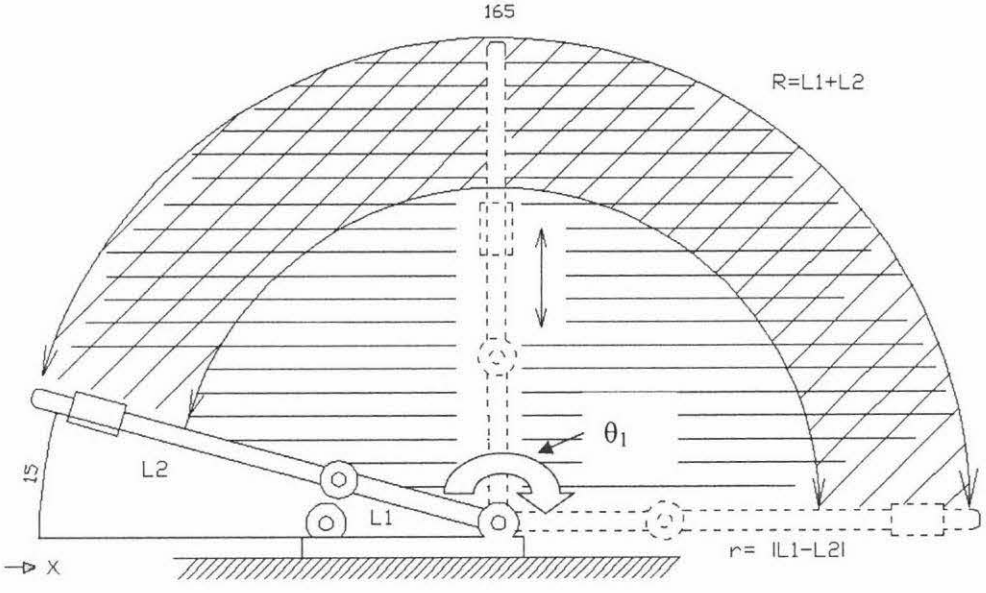

Figure 3.12 Workspace for framework (Top View)

However, different from two links manipulator, with coupling mechanism design, the robot is able to translate along the longer link, that means the end-effector can reach the inside of $|L1-L2|$ according to patient's leg length. This results in the maximum reachable area in a semicircular area of radius L1+L2. Therefore, the workspace of the framework would provide enough space for surgical requirements. In addition, for 6-UPS robot, it also can provide 3-D workspace, whose parameters are given in Figure 3.13.

6-UPS Parallel Robot Workspace	
Rotation Z – α	± 35
Rotation Y – β	± 10
Rotation X – γ	± 10
Translation Z	± 200
Translation Y	± 100
Translation X	± 100

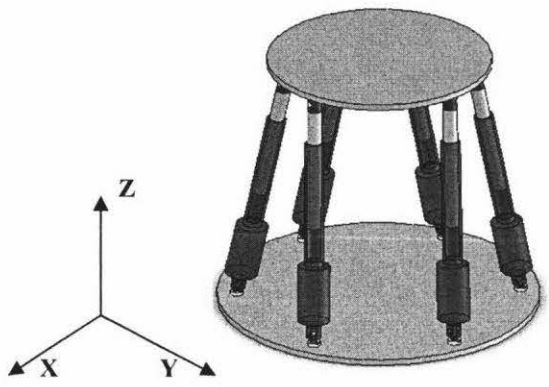

Figure 3.13 6-UPS Parallel Robot Workspace

3.4.2 Height adjustment

There are three Jockey standers and Jockey wheels attached onto the L shaped beam and at the ends of the crossbeam. For the Jockey stander, the maximum adjustable distance (vertical) is 40cm with maximum load of 350 kg. Similarly, two Jockey wheels have a 30 cm operational displacement with 350kg load capacity.

During the operation, two Jockey wheels are not supposed to do more vertical adjustment because another end of the link is fixed on the mobile table, an over adjusting would cause the longer link to not be in a horizontal plane as well as the introduction of unnecessary stress in the joints.

However, the constraint does not affect the performance. The reasons are: firstly, the main function of the Jockey wheels is to support the framework and realize the portability. Secondly, the Jockey stander provides adequate displacement for height adjustment.

3.5 Conclusion

In this chapter, a 6-UPS (Gough-Stewart) platform has been introduced, followed by a theoretical analysis, which involves coordinate system assignment, inverse kinematics and singularity study.

Euler Z-Y-X angle system has been chosen as a reference rotation system. Inverse kinematics analysis has been performed in Matlab. The Jacobian matrix has been

derived for singularity study. The derived results, combined with other singular conditions in literature provide a clear reference for the further study. Secondly, one of the objectives, the design of the framework for the robot has been described. In terms of practical requirements, the conceptual design has been presented in SolidWorks model. The real framework was produced. To verify the stability and flexibility of this framework, a performance analysis was conducted following the design.

Chapter 4 Motion control for the 6-UPS parallel robot

4.1 Introduction

Motion control is defined as a method of using computer-controlled mechanisms to drive an object's movement so that it is continuously repeatable within an acceptable error range. Particularly, for a fracture realignment parallel robot, all six linear actuators joined into the robot can be controlled precisely to follow a generated trajectory. Visually, the robot passes through a series of transitional positions, to perform a "Pull-Rotate-Push" action and return back to the required location.

This chapter first presents the motion control architecture and then the Galil system that implements the motion control. The selection of a control model and PID tuning algorithm is also included in this chapter.

4.2 Motion control architecture

4.2.1 Controller architecture

In the early stage of this project a DMC-1700/1800 series controller was specified for motion control. The hardware architecture is that of a two-level hierarchy, which comprises of a Pentium 4 1.6GHz Desktop computer serving as the top level master and a 68331 Microcontroller acting as a slave.

The master relays commands to the Microcontroller through its internal PCI bus protocol. The 68331 Microcontroller is capable of supporting up to 8 axes. Encoder signals are sampled and transferred to the microcontroller through a high speed motor encoder interface so that the microcontroller is able to read to obtain the current actuator position.

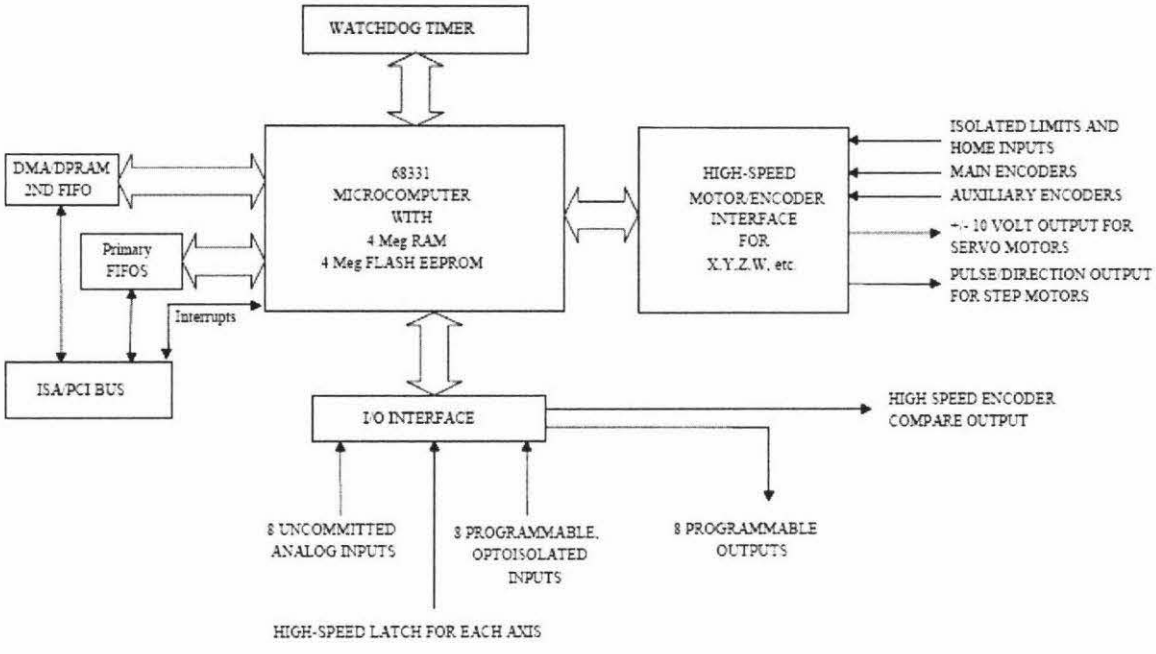

Figure 4.1 DMC-1700/1800 controllers Architecture (Galil 2005)

The elements shown in Figure 4.1 with its function brief are listed below:

- Microcomputer section: a specialized 32-bit Motorola 68331 Series microcomputer with 512K byte RAM and 512K byte Flash EEPROM.
- Motor Interface: performs quadrature decoding of each encoder at up to 12 MHz.
- Communication: contains primary and secondary communication channels, which are using 1 FIFO and DMA or DPRAM or a Polling FIFO for data transformation.
- General I/O: provides interface circuitry for 8 bi-directional, optoisolated inputs, 8 TTL outputs, and 8 analog inputs with 12-Bit ADC (16-bit optional).

4.2.2 Motion system architecture

In Figure 4.2, the motion system architecture is denoted by a functional block diagram. With the usual motion control procedure, the computer carries out all the "high-level" operations of the overall control system and trajectory planning. When a motion is required, MATLAB performs the inverse kinematics computation, and then a desired trajectory is planned in SolidWorks and a trajectory via points every 256

milliseconds is generated for the controller. Finally the generated trajectory is interpreted into the DMC terminal language and sent to DMC-1800 controller one by one. Once the controller receives the command, it will pass the command to the actuator amplifier (shown "Driver" in Figure4.2).

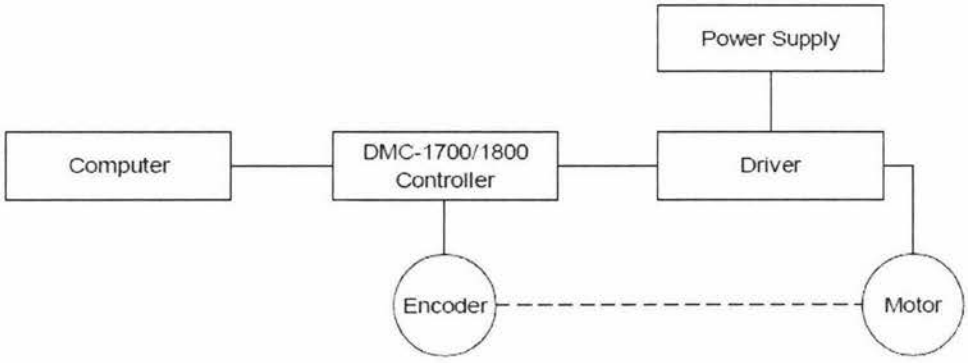

Figure 4.2 Architecture Motion control system (Galil 2005)

PWM is the method used to control the motor velocity. Each actuator has a built in rotary encoder. The position of the motor is transferred into a pair of quadrature electrical signals as a feedback signal sent back to the controller. When an over error limit is reached, controller stops and reports an error to the computer operating terminal. In addition, a power supply is needed to power the system with high stability, and built in protection setting.

4.3 Motion system elements

In Figure 4.2, a motion control system includes amplifiers, power supply, motors, motion controller and encoders. The system was selected due to a variety of specifications that are described below.

4.3.1 Motor (actuator)

A linear actuator consists of a DC motor and transmission mechanism. The DC motor converts current into torque and a transmission mechanism transfers rotary motion into linear motion. Each axis of motion requires a motor sized properly to move the load at the required speed and acceleration.

LA22 is an in-line actuator produced by LINAK. A small overall dimension was the reason to be selected by preceding students. The disadvantage of this kind of actuator is the lack of position encoder, for which a development of encoder is needed.

LA22 series linear actuators have many types classified by voltage level, spindle pitch and back fixture etc. The selected model no is LA22E000-052002410. The technical specifications are summarized as below.

- 24 V DC permanent magnet motor
- Max. Thrust 400 N
- Stainless steel piston rod and piston rod eye made of reinforced plastic.
- Duty cycle: Max. 10%
- Ambient temperature +5° to +40° C.
- Compact construction/design
- Protection class: IP 51
- Color: black
- 1.0 m straight cable without plug
- Speed max. 37 mm/s
- Extremely quiet operation
- Max. Stroke length 200 mm

The dimension of LA22E000-052002410 and the back fixture are shown in Figure 4.3.

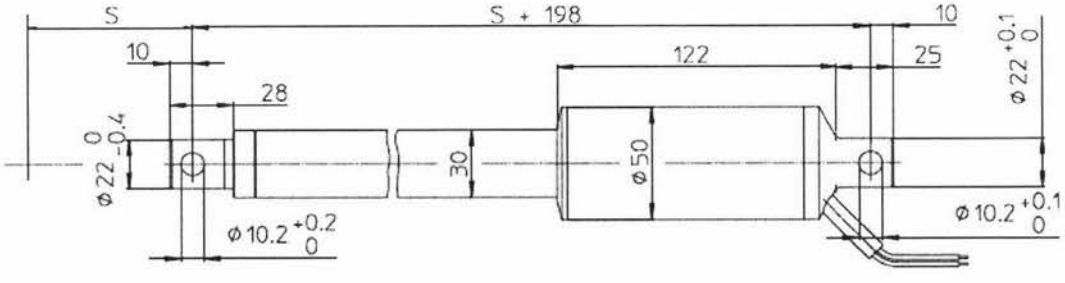

Figure 4.3 Dimension and back fixture for LA22

The relationship between speed vs. load and current vs. load are drawn down in Figure 4.4.

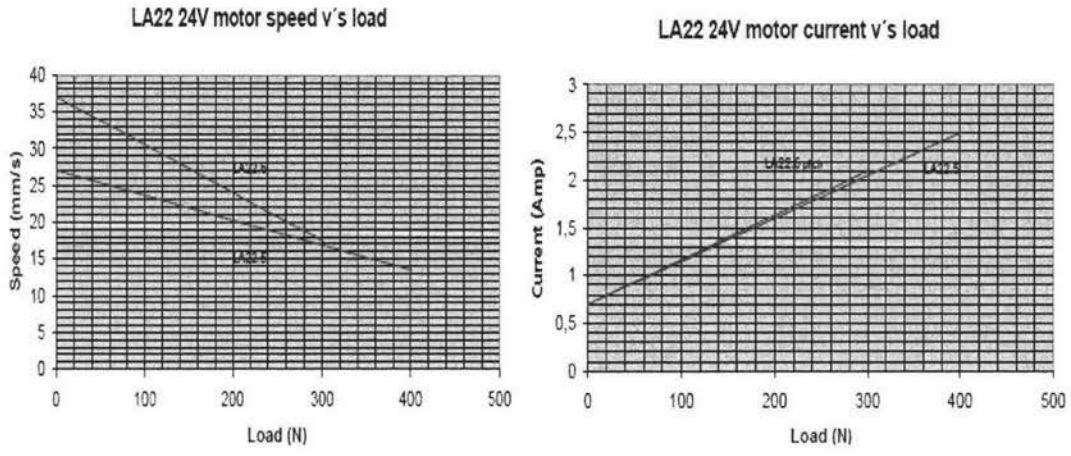

Figure 4.4 Speed vs. load and current vs. load

4.3.2 Amplifier (Driver)

The control signals from computer are amplified to drive actuators. A DMC 1800 controller is interfaced with the Galil's AMP-19540/19520. The Galil's AMP-19540is a 4-axis amplifier and another 2-axis amplifier the Galil's AMP-19520 is needed. Both of these are able to drive brush or brushless motors up to 500 Watts. With a cable connecting to DMC-1800controllers, it provides a cost-effective controller/drive solution for multi-axis applications.

The AMP-19540/19520 is brush/brushless trans-conductance PWM amplifier. The amplifier operates in torque mode and will output a motor current proportional to the command signal input. Its electrical specifications are:

Input Voltage: 18~80 VDC

Continuous Current: 7amps

Peak Current: 10amps

Amplifier Gain: 0.4/0.7/1.0 A/V (adjustable)

Switching Freq: 60 kHz

The AMP-19540 enclosure has dimensions of 6.8" x 8.75" x 1". It interfaces to Galil's DMC-18xx PCI bus controller with a single, 100-pin high density SCSI cable. Signals for each axis are brought out through D-type connectors located on the AMP-19540/20. For each axis, the power amplifier converts a +/-10 Volt signal from

the controller into current to drive the motor. Other auxiliary connectors for interfacing are available on the panel.

4.3.3 Switching power supply

In Figure 4.4 actuator load vs. current, the maximum current for 24VDC linear actuator is 2.5 Amps. Thus, the minimum current specification for 24VDC power supply should be satisfied with a sum of current, where all six actuators are working in the maximum current. Therefore, the minimum current capacity for power supply:

I_{total} = *the number of actuators x the maximum current occurred in single motor*

$= 6 \times 2.5$

$= 15\ (A)$

Considering a redundancy for system, a safety factor of 1.5~2.5 should time this calculated value and eventually, the current capacity for power supply is:

$I_{cap} = 1.5\sim2.5 \times I_{total}$

$= 1.5\sim2.5 \times 15$

$= 22.5\sim37.5\ (A)$

A 750W single output switching power supply supplied by MeanWell meets the requirement(Table 4.1 and Figure 4.5).

Table4.1 Specifications of Power supply

Manufacturer: Mean Well

Output Specifications:	
Output Voltage:	24 Volts DC
Voltage ADJ.Range	22 ~ 26.4 Volts DC
Min Current:	0 Amps
Max Current:	31.3 Amps
Power:	751.2 Watts
Input Specifications:	

Input frequency range	47 ~ 63Hz
Over load	105 ~ 125 % rated output power, 27.6 ~ 32.4V
Dimension and Weight	278 x 127 x 63.5mm, 2.9 kg
Other features	Protections: Short circuit/Over load/Over voltage/Over temperature Forced air cooling by built-in DC ball bearing fan

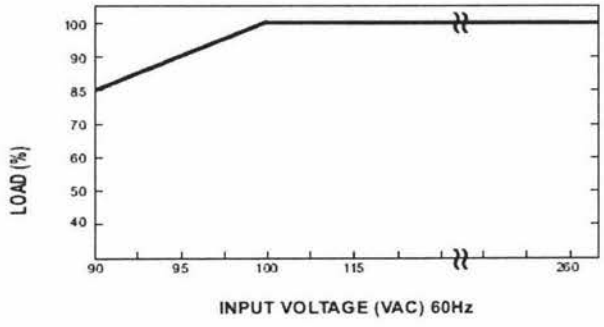

Figure 4.5 SP-750-24 static characteristics (Mean Well 2005)

4.3.4 DMC-1800 motion control card

Using two 19540/19520 amplifiers, the DMC-1860 motion control card is able to control up to 6 individual LINAK LA22 actuators to implement any allowable 6-DOF movement in specified work space.

The DMC-1860 control card based PCI is Galil's full-featured multi-axis motion controllers. Designed to fit in a single PCI slot of a PC, the DMC-1860 controller accommodate 6-axis formats and allow control of step or servo motors on any combination of axes. Any mode of motion can be programmed including linear and circular interpolation, contouring, electronic gearing and e-cam. Programming the DMC-1800 is simplified with two-letter, intuitive commands and a full set of software tools such as WSDK for servo tuning and analysis, ActiveX Tool Kit for Visual Basic users and a C-Programmers Tool Kit (Galil 2005).

The main technical specifications are below:

- Motorola 32-bit microcomputer

- Two communications channels
- Multiple models of Motion
- Dual encoder (for axes configured as servo)—Channel A, A-,B, B-
- Forward and reverse limit inputs—opto-isolated on DMC-18x0
- Home input—opto-isolated on DMC-18x0
- Analog motor command output with 16-bit DAC resolution
- PID filter (proportional-integral-derivative) with velocity and acceleration
- Digital input/output and analogue input/output

One of the important features of DMC 1800 series control card is to provide an internal watch dog timer, which checks for proper microprocessor operation. The timer toggles the Amplifier Enable Output (AEN), which can be used to switch the amplifiers off in the event of a serious controller failure. A reset is required to restore the controller to normal operation (Galil 2005). The meaning for 6-UPS robot is to avoid a potential danger and damage to robot when the actual motion trajectory is far away from the commanded trajectory.

4.3.5 Encoder

The encoders are a key element in the motion control system, which translate motion into electrical pulses fed back into the controller. Therefore, the quality of the encoder feedback will directly affect at the motion performance such as accuracy, stability and smoothness etc. The LA22 linear actuator does not provide a built-in encoder for position feedback, an encoder had to be developed.

(A) Quadrature signal and current encoder

The DMC control card accepts feedback from either a rotary or linear encoder with two channels in quadrature, known as CHA and CHB. This type of electrical signal is known as a quadrature encoder (Figure 4.6). Quadrature encoders may be either single-ended (CHA or CHB) or differential (CHA, CHA-, CHB, CHB-). Encoders may also have a third channel (or index) for synchronization. The

DMC-1700/1800 can also interface to encoders with pulse and direction signals (Galil 2005).

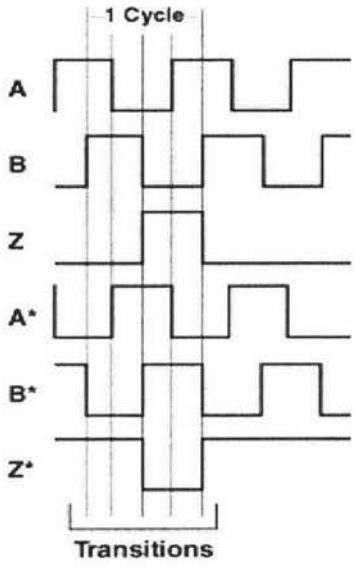

Definition

The output from encoders and many other types of measurement devices is known as a "quadrature" signal. A quadrature signal consists of two square waves 90° out of phase. The input channel on encoder interface board counts the square wave transitions and determines direction by comparing whether channel A is leading channel B or vice-versa.

Differential encoders provide a complimentary signal for each of the three standard signals. Differential transmission prevents signal degradation in applications where the signal is to be sent over long distances.

Figure 4.6 Single-ended and differential Quadrature signals (Cyber Research 2007).

Employing the Hall Effect principle, the encoder used in this project consists of a small PCB circuit surrounding the shaft and a set of semicircular magnetic arrays (Figure 4.7). The PCB circuit located on the motor surface (fixed) and the magnets arrays were arranged around the shaft surface (rotating). Two 3141 hall-effect sensors placed at ninety degrees from each other were able to encode the rotation of the linear actuators motor shaft into a pair of quadrature signals.

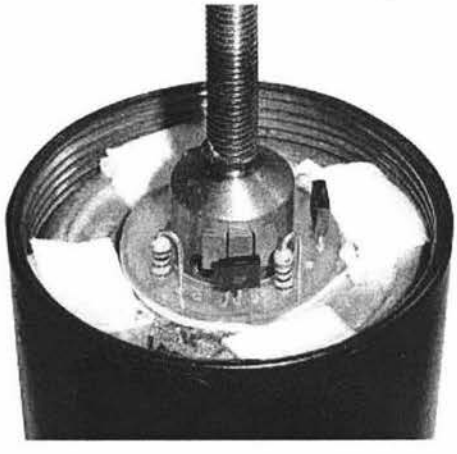

Figure 4.7: Hall Effect encoder

As the motor rotates with the magnets, the magnetic fields generated by magnets arrays will periodically come into vicinity of the sensors, which pull a higher voltage value from approximate 4.99 Volts down to 430 milli-Volts. Such this voltage change could be detected as a digital signal change (from 1 to 0) by DMC controller via amplifier interface. However, the distance between magnets and 3141 hall sensor is critical, the effective range is within 5mm or less depending on the intensity of magnetic field and sensors.

The 3141 hall-effect switch is monolithic integrated circuits with tighter magnetic specifications, including a voltage regulator for operation with supply voltages of 4.5 to 24 volts and an open-collector output to sink up to 25 mA. The supplier is Allegro Microsystems Inc. A 3141 Hall-Effect switch and the position sensor circuit are shown in Figure 4.8.

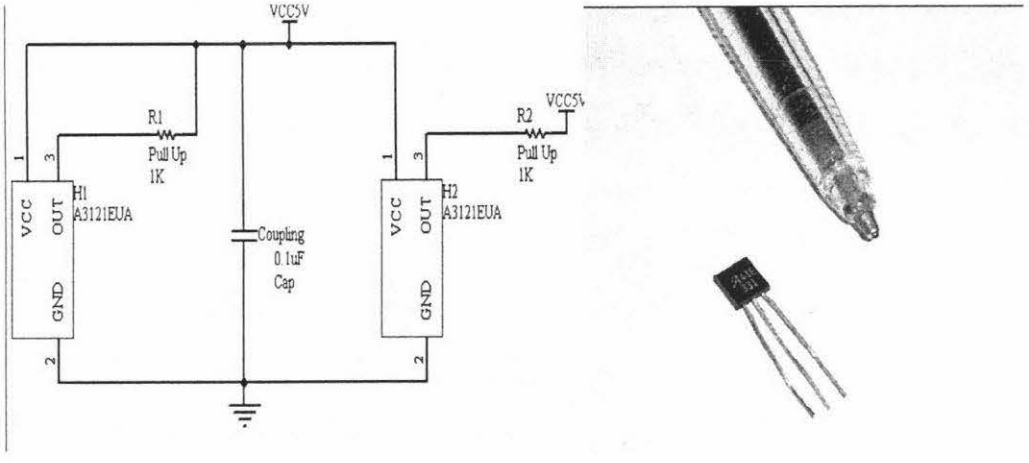

Figure 4.8 Position sensor circuit and 3141 Hall-Effect sensor

The reason to place the magnets in a 180 degree array around the shaft is to obtain a correct quadratrue signal sequence by eliminating the undesired while motor is in rotating. A correct quadrature sequence should be 10,11,01,00 circularly whichever the leader is. Such undesired states disturb this sequence and result in a transitional state. For example, the sequence becomes 10, 00, 11, 00, 01, 00 . Two scenarios related to the state transition are demonstrated in Figure 4.9.

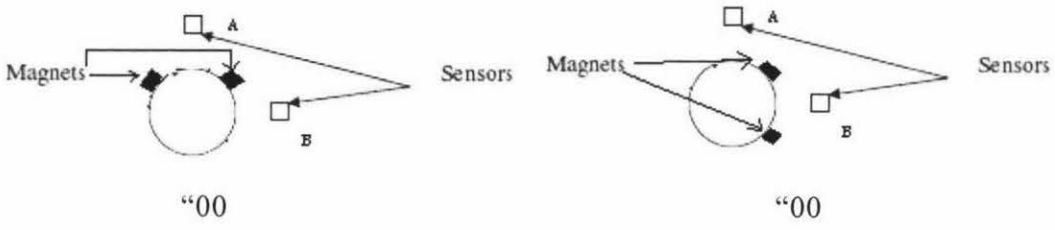

Figure 4.9 Two transitional positions generate undesired "00 state

(B) Improvement on the encoder

However, the encoders did not work properly during the testing. The big issue was the lack of stability and reliability, which results in the loss of the control of the actuator. Detected using an oscilloscope, two outputs of encoder was either 4.98V (which is regarded as "0 in logic) or 0 mv (which is regarded as "1 in logic) at any same time. The reasons were found eventually after opening and checking the actuators. They were:

- Open circuit: a ring shape PCB circuit of encoder is shown in Figure 4.10. The gray area is the cross section of the shaft, the outer ring is the anode (+5V) and the inner ring is the cathode (0 V). To obtain a better effect from magnets, the Hall sensor needs be installed as close to the shaft as possible. In reality, this gap is less than 1mm. However, the shaft was not concentric with the PCB ring since the shaft had been pre-machined and introduced deformation. As a result, the edge of ring was rubbed and cut off eventually by shaft.

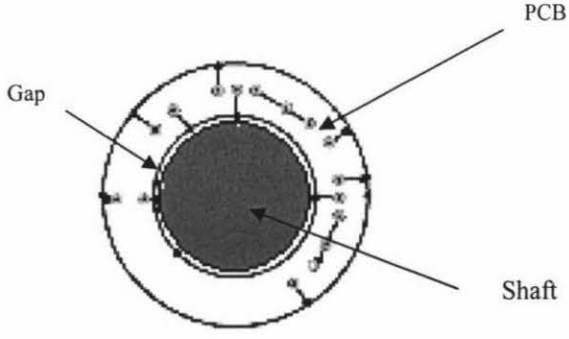

Figure 4.10 View of Cross section of shaft

- Short circuit: In Figure 4.7, the white item beneath the PCB ring was attached using double sided tape. The pins of the electronic components could easily touch the motor shaft causing a short circuit. Another reason was that the cable of the encoder has no electrical protection as it passes through the hole on the cylinder which has a sharp edge at the 90 degree corner.
- Fixing failure: PCB ring merely was stuck by double sided tape. This loose base caused the ring to move relative to the shaft.
- Sensor damage: 3 out of the 6 actuators suffered sensor damage because of limited space.
- Loss of Magnets: some tiny magnets fell off from the shaft.

The solution to this problem was to design another encoder or repair the existing ones.

The encoders were subsequently repaired as follows.

First of all, the PCB containing all the elements of the position sensor needs to be firmly fixed onto the motor casing so that the negative effects from vibrating and shaking generated by the rotating shaft would be eliminated as much as possible. To achieve it, a plastic layer was placed under the PCB. The purpose of the plastic insulation layer was to isolate the PCB from the motor casing to avoid short circuit and to provide a reliable base for the mounting of the PCB. The plastic layer was fixed on the motor casing using a kind of polymer binder instead of double sided tape, since drilling a hole on the casing might potentially damage the motor.

In the mean time, a layer of silicon was used to fill the gap between the PCB and the plastic layer. The advantages of using silicon are to enhance the electrical insulation, fix the encoder on the PCB and have a safe distance from the motor shaft. The disadvantage of this improvement is that the plastic layer and silicon occupy more space and make the maintenance difficult. The improved encoder is shown in Figure 4.11.

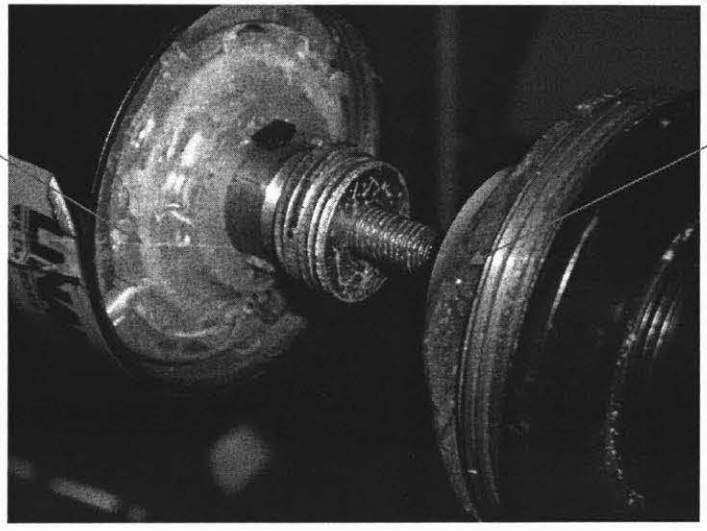

Figure 4.11 Improved position sensor

Secondly, a heat shrink tubing was covered around the encoder cable to enhance insulation, which considerably reduces the possibility of the cable cut off by the sharp edge.

Thirdly, the shafts were calibrated in the workshop and the magnets were taken off and cleaned. The surface of the shaft was cleaned by alcohol.

Finally, the damaged 3141 Hall-effect was replaced by an Allegro A1101~A1106 series Hall-effect switch. A1101~1106 series has better specification than the 3141 series hall-effect switch, the integrated voltage regulator permits operation from 3.8V to 24V and wider applicable range of magnetic field. To reduce the risk of the damage due to impact, the installation height has been closed down to the surface as low as possible. The real effect is shown in Figure 4.11.

A repetitive testing for all the encoders was carried out after the improvement, and the result showed that the encoders were working much better that before. The stability and reliability were improved up to adequate condition.

(C) Encoder interfacing to amplifier

The designed encoder has only 4 wires, which are +5VDC, 0V, channel A and channel B. The resolution of the current encoder is 4 counts per cycle. Since the pitch of powered screw is 0.8mm, therefore, one count is equal to 0.2mm in linear displacement.

For sake of the convenience, DMC places all encoders and auxiliary interface onto the AMP-19540/19520 panel. +5VDC and ground are supplied through 100-pin high density connector from the computer. The connector standard employs a 15-pin high density Female D-type connecter. The configurations of the pins and layout are listed as follows (Table4.1).

Table4.1 15-Pins definition

1.I+	6. I-	11. AA+
2. B+	7. B-	12. AB-
3.A+	8. A-.	13. Hall B
4.AB+	9. AA-	14. Hall C
5.Ground	10. Hall A	15. +5 V

Hence pin 2, 3, 5, and 15 can be used for encoder input. A D-15 high density male adapter with 1.5m cable connects encoder with amplifier panel.

4.4 Motion control mode

4.4.1 Overview of control mode

The DMC-1800 series controller provides several modes of motion control, including independent positioning and jogging, coordinated motion, electronic cam motion, and electronic gearing. Since each mode is accommodated to different applications, thus choosing an appropriate mode of motion becomes one of the tasks. A summary of modes of motion is listed in Table 4.2.

Since LA22 linear actuator comes with 24VDC standard servo motor, some modes of motion such as SPM (Stepper Position Maintenance Mode) and Dual Loop Mode won't be presented in the table.

Table 4.2 Control modes

Summary of Mode of motion			
No.	**Mode of motion**	**Description**	**Comments**
1	Independent Axis Positioning	Absolute or relative positioning where each axis is independent and follows prescribed velocity	Used for actuators testing and debugging, but not for trajectory

		profile.	following.
2	Independent Jogging	Velocity control where no final endpoint is prescribed. Motion stops on Stop command.	Used for actuators dynamic testing , but few use in this project
3	Position Tracking	Absolute positioning mode where absolute position targets may be sent to the controller while the axis is in motion.	Velocity mode can not be used for trajectory following.
4	Contour Mode	Motion Path described as incremental position points versus time.	Exact mode for trajectory following
5	Linear interpolation	2, 3 or 4 axis coordinated motion where path is described by linear segments.	Prescribed velocity mode can not be used for trajectory following.
6	Coordinated Motion	2-D motion path consisting of arc segments and linear segments, such as engraving or quilting.	Prescribed velocity mode can not be used for trajectory following.
7	Electronic Gearing	Electronic gearing where slave axes are scaled to master axis which can move in both directions	Gear ratio for 6 actuators can not be specified during the trajectory following
8	Electronic Cam	Following a trajectory based on a master encoder position	Another ramification of Electronic Gearing
9	Independent Motion Smoothing	Smooth motion while operating in independent axis positioning	A auxiliary function can be used to reduced vibrations during the trajectory following
10	Vector Smoothing	Smooth motion while operating in vector or linear interpolation positioning	Auxiliary function for Vectors and interpolation mode
11	Gantry Mode	Gantry - two axes are coupled by gantry	Not for 6 axes operation

4.4.2 Selection of control mode

From the above table, it is obvious that the different properties of motion determine different modes of motion. For 6-UPS parallel robot, there might have several modes of motion corresponding to different applications.

- Single actuator testing with/without load applied: in this case, the testing trajectory might be point to point, standard mathematic curves such as step, sinusoids and a specified trajectory. Therefore, the mode for this kind of motion could be independent Axis Positioning, independent Jogging and contour mode.
- Actuators follows a specific trajectory: because the 6-UPS is rigid frame with a unique inverse kinematics solution in the 3-D space, the trajectory for each actuator is critical, as a result, only the contour mode could be used in this situation.
- Debugging and calibration: Independent Axis Positioning only could be used for 6-UPS debugging and calibration.

4.4.3 Independent Axis Positioning (IAP)

In IAP mode, the motion between the specified axes is independent, and each axis follows its own profile. The desired absolute position (PA) or relative position (PR), slew speed (SP), acceleration ramp (AC), and deceleration ramp (DC) need to be specified for each axis before a motion starts. On begin (BG), the DMC-1700/1800 profiler generates the corresponding trapezoidal or triangular velocity profile and position trajectory (Figure 4.12). The controller determines a new command position along the trajectory every sample period until the specified profile is complete. Motion is complete when the last position command is sent by the DMC-1700/1800 profiler (Galil 2005).

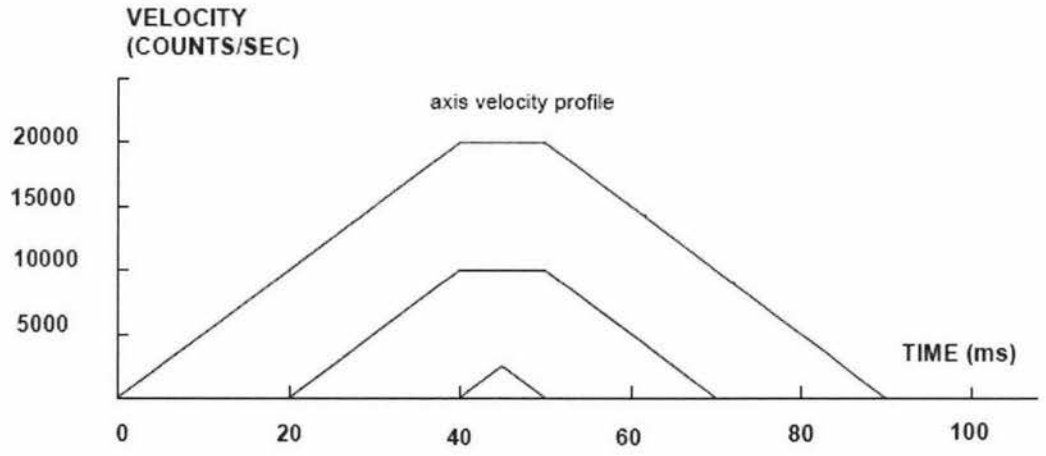

Figure 4.12 Velocity profile in trapezoidal and triangular (Galil 2005)

The Begin (BG) command can be issued for all axes either simultaneously or independently. The speed (SP) and the acceleration (AC) can be changed at any time during motion. However, the deceleration (DC) and position (PR or PA) cannot be changed until motion is complete The Stop command (ST) can be issued at any time to decelerate the motor to a stop before it reaches its final position.

An incremental position movement (IP) may be specified during motion as long as the additional move is in the same direction. As the desired position increment, n specified, the new target is equal to the old target plus the increment, n. An example specifies a relative position movement on X axe listed as below:

```
#A Begin Program
PR 2000          Specify relative position movement of 2000 counts for X axes.
SP 100           Specify speed of 100 counts / sec
AC 500000        Specify acceleration of 50counts / sec2 for axe
DC 500000        Specify deceleration of 50 counts / sec2 for axe
BG X             Begin motion on the X axis
```

4.4.4 Contour mode

Contour mode allows any arbitrary position curve to be prescribed for 1 to 8 axes. This is ideal for following computer generated paths or user defined profiles. The path is not limited to straight line and arc segments and the path length may be infinite (Galil 2005). Therefore, it is the most appropriate motion control mode for the robot trajectory following.

The Contour Mode is specified with the command, CM. A contour is described by position increments which are described with the command, CD x,y,z,w over a time interval, DT n. The parameter, n, specifies the time interval. The time interval is defined as 2^n ms, where n is a number between 1 and 8. The controller performs linear interpolation between the specified increments, where one point is generated for each millisecond (Gaili 2005).

The user can specify the desired increment for each segment, and then the controller builds the motion profile by stepping from each segment to the next in the time specified. This characteristic is very important to the trajectory following of the parallel robot, which requires each actuator to reach the specified position in the same time interval.

For example, the trajectory shown in Fig. 4.13, the position X may be described by the points:

Point 1 X=0 at T=0ms

Point 2 X=48 at T=4ms

Point 3 X=288 at T=12ms

Point 4 X=336 at T=28ms

The same trajectory may be represented by the increments

Increment 1 DX=48 Time=4 DT=2

Increment 2 DX=240 Time=8 DT=3

Increment 3 DX=48 Time=16 DT=4

The programmed commands to specify the above example are:

```
#A
CMX          Specifies X axis for contour mode
DT 2         Specifies first time interval, 22 ms
CD 48;       WC Specifies first position increment
DT 3         Specifies second time interval, 23 ms
CD 240;      WC Specifies second position increment
DT 4         Specifies the third time interval, 24 ms
CD 48;       WC Specifies the third position increment
DT0;         CD0 Exits contour mode
EN
```

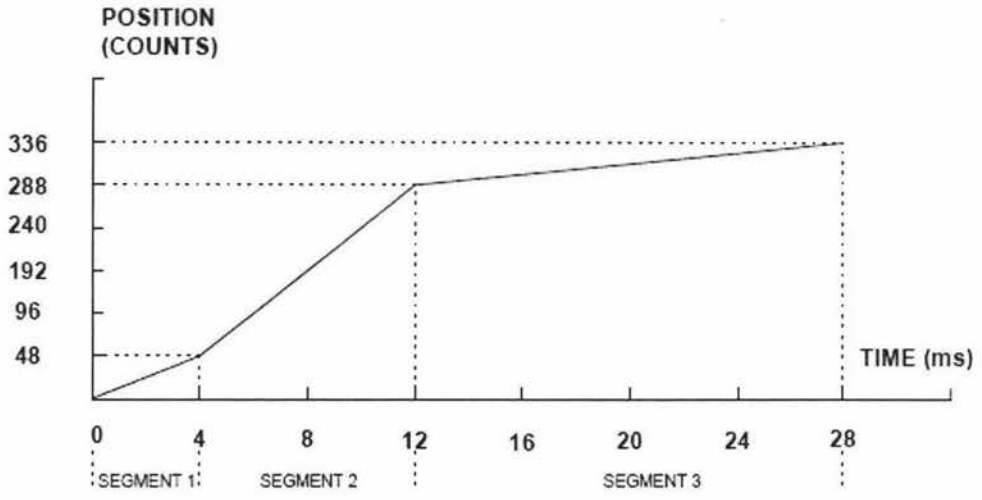

Figure 4.13 Trajectory in contour mode (Gaili 2005)

4.5 PID Tuning

Since the encoder improvement and the mode for motion control are completed, the main task of the motion control is to find a set of PID parameters for all six actuators, namely, PID tuning (Proportional, Integral and Derivative). The meaning of PID tuning is that the actuators are capable of following the generated trajectory with controlling the error within an acceptable limit. In practice, this is the requirement for the success of robot application.

Single actuator PID tuning was done earlier without load applied on. However, after assembly, the factors such weights of parts, reaction force between actuators etc. would make the situation substantially different from the earlier tuning. Moreover, another obstacle is that a fully PID tuning could not be done directly on the robot platform because a reduced angular range of 15 degree of spherical joint provides a limited workspace for testing. Thus, a reasonable methodology for PID tuning has to be defined before an operation may be fulfilled.

4.5.1 Methodology

For the motion of the medical robot, the most concern is that the robot should be able to follow commanded trajectories accurately. Another important concern is that

small overshoot should be maintained. This is because in reality the robot should not extend beyond the set point which results in great amount of unwanted force in the bone fragments. On other hand, the operating time or the speed is not an important aspect of system performance.

In practice, the accuracy requirement of the robot was set around +/- 5mm. Note that this limit is set at the end of bone fragments not for each linear actuator displacement. However, this is confusing specification, since the robot configuration is in conic form for side view, and there always is an angle existing between the axial line of actuator and patient's foot that normally is perpendicular to the top plate. Such configuration, when a small movement occurs at the top plate, will cause a big displacement on the linear actuators. The longer the leg length, the bigger the displacement will be.

The methods of tuning the control system can be classified into mathematical model analysis and automatic tuning, which are discussed in the following.

4.5.2 Mathematical modeling

A mathematical modeling for single actuator motion control, which includes controller, amplifier and other elements expressed into a block diagram as shown in Figure 4.14.

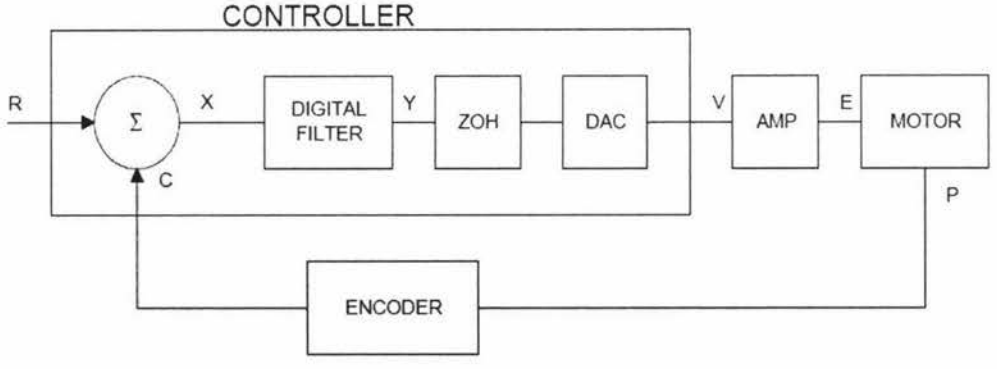

Figure 4.14 System modeling for single actuator

To find an appropriate PID setting for the system, first of all, the system's Laplace transform should be performed. The procedures of building transfer function as follows.

The relationship between amplifier (current drive model) and motor (Fig.4.14) is described by

$$P/V = Ka\ Kt / Js^2 \qquad (4.1)$$

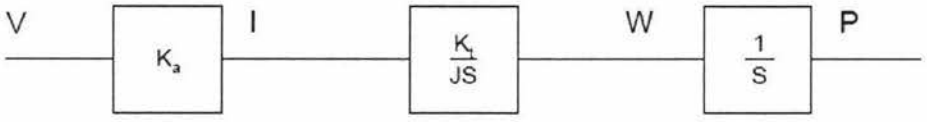

Figure 4.15 Amplifier and motor in System modeling (Galil 2005)

Where, Ka is a gain (A/V) of current amplifier, Kt denotes torque constant (Nm/A) and J is Combined inertia of motor and load ($kg.m^2$).

The Hall-effect encoder built only generates 1 pulse per revolution for each channel. Therefore, the position resolution is increased to 4 quadrature counts/rev. The model of the encoder can be represented by a gain of

$$K_f = 4/2\pi \text{ (count/ rad)} \approx 0.6369 \qquad (4.2)$$

The DAC converter is capable of converting 16-bit number to an analog voltage. The input range of the numbers is 65536 and the output voltage range is +/-10V or 20V. Therefore, the effective gain of the DAC is

$$K= 20/65536 = 0.0003 \text{ V/count} \qquad (4.3)$$

The digital filter has the transfer function given by DMC-1800:

$$G(s) = (P + SD + I/S) * a/(S+a) \qquad (4.4)$$

Where, $P = 4K_P$, $D = 4T \times KD$, $I = KI/2T$, $a = 1/T^* \ln 1/B$, T=0.001s is the sampling period, and B is the pole setting determined by PL, a low pass setting instruction in program. K_P, K_I, K_D are PID parameters.

The ZOH represents the effect of the sampling process, where the motor command is updated once per sampling period. The effect of the ZOH can be modeled by the transfer function

$$H(s) = 1/ (1+ST/2) \qquad (4.5)$$

Putting all above equations into the block diagram yields Fig. 4.16.

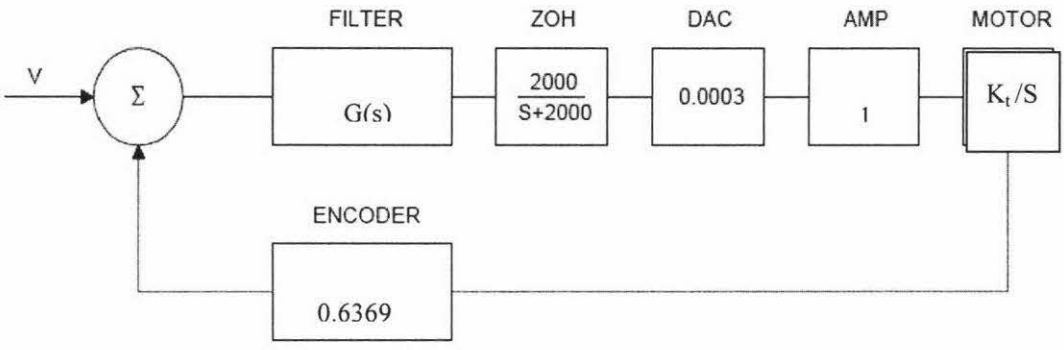

Figure 4.16 Actuator control diagram

If Kt and J are known, Ziegler-Nichols ruler can be used to find K_P, K_I, and K_D seeking. The second method of Ziegler-Nichols ruler is explained as follows.

First set $KD = 0$, $Ki = \infty$, only using the proportional control action only and increase K_P, from 0 to a critical value *Kcr* where the output first exhibits sustained oscillations. Thus, the critical gain *Kcr* and the corresponding period *Pcr* are experimentally determined. The value of the parameters K_P, K_I, and K_D can be set according to a specified formula (Ogata 1997).

4.5.3 Automatic tuning in WSDK

There are six different tuning methods included in WSDK32 software. Each method approaches the tuning process in a different way and may give different results.

- Auto Crossover Frequency
- Crossover Frequency
- General Tuning
- Conservative Tuning
- Point to Point Tuning
- Manual Tuning

Along with the tuning methods, a step response test may also be performed in order to evaluate the dynamic behaviors of the system. The test displays the actual position of the motor as a function of time. A well-tuned motor would show a slight overshoot and a shorter settle time.

To implement a PID tuning of the robot, the tuning procedure can be carried out in the following two stages:

Stage 1: With an effective load, singe actuator PID tuning will be performed in automatic with step response firstly. When the parameters tp be chosen are close to the final, the results can be verified in different places in 3-D space. The effective load can be estimated based on static force analysis. The top plate weight is 3kg approximately, on average, each actuator at least supports statically 0.5kg in vertical configuration. By scaling, the weight applied on the single actuator can be up to 3kg. For this purpose, a series of specified weights have been machined into two classes: 0.5kg and 1kg. With a long screw, the maximum load applied on the actuator can be up to 5kg (Figure 4.17).

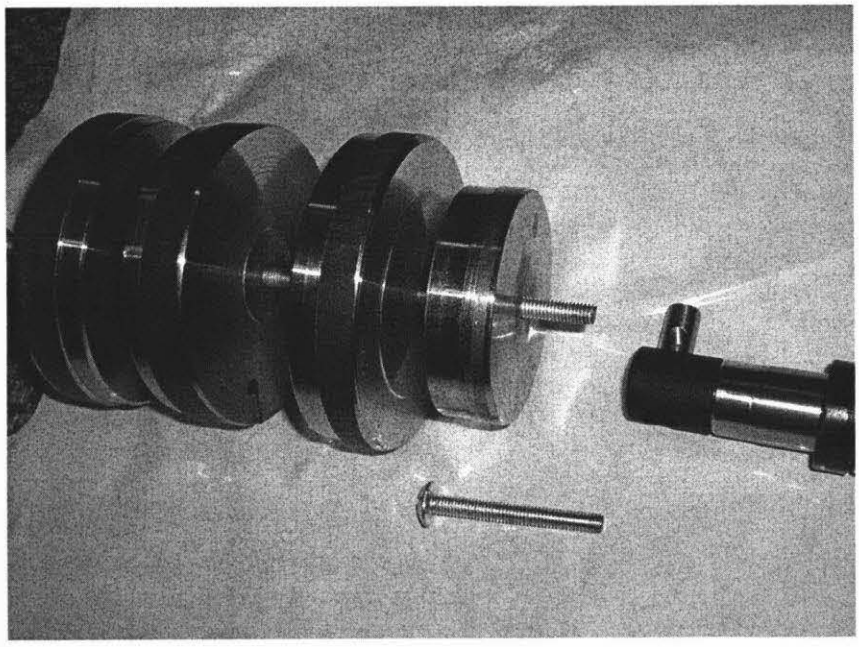

Figure 4.17 Combinable weights for PID testing

Stage 2: if the PID parameters verified in the stage 1, the separated actuator will be assembled back into the robot and undergo another step response testing. The above tuning is performed for all the six actuators. In the end, a generated trajectory from Solidworks model will be applied to controller for verifying the PID setting. If the performance satisfied, the tuned PID gains will be taken.

(A) Automatic crossover frequency

Automatic Crossover Frequency is defined as the maximum frequency to which a system can respond without a loss of gain. The Auto Crossover Frequency routine attempts to determine the PID parameters that correspond to this maximum frequency (measured in units of radians/ second).

The step response also can be selected and shown during the testing. The parameters of step are adjustable in Edit option. In the case, three consecutive steps input with a magnitude of 40 counts (40 counts x 0.2mm= 8mm) are used for testing.

Figure 4.18 shows the automatic crossover frequency in action for step responses of 40 counts with an applied load of 0.5kg and 2kg.

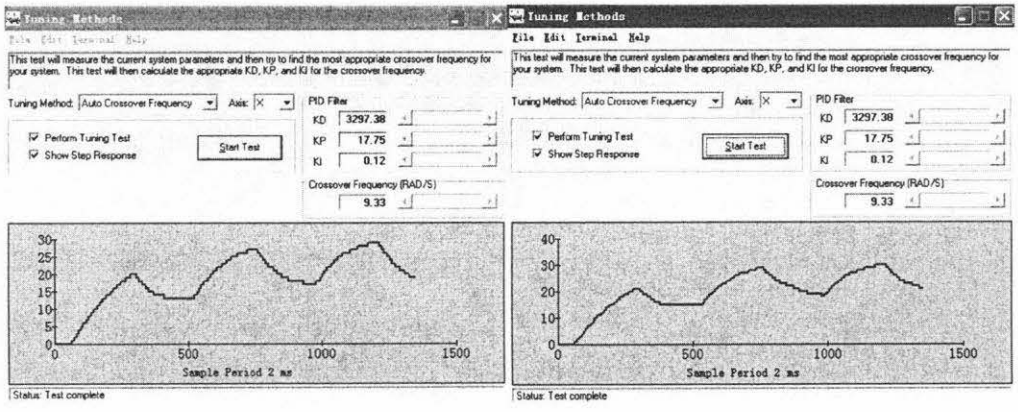

Figure 4.18 Auto Cross Frequency tuning

The step response shows that there is a serious deformation because the system has lost control, which represents the step responses do not reach the commanded value of 40 counts and their sizes are not consistent. Both of two cases are similar and reveal this method failed to find PID parameters.

(B) Crossover frequency

The crossover frequency routine will let user define a crossover frequency (rad /sec), and then attempts to tune the axis to provide the best system response at that frequency. The value of the crossover frequency should be set to the bandwidth of the system for best results. The lower frequencies tend to cause over damping in the system, resulting in a slower and more sluggish response. Higher frequencies produce

faster system response, but because it tends to under damp, it may cause the system overshoot.

As the method is another form of automatic Crossover Frequency, in practice, the results are similar to Figure 4.18.

(C) General Tuning

The General Tuning routine is best suited for velocity mode amplifiers, although it will work for systems with various types of drives and amplifiers. This routine tunes the system by increasing the gain until instability occurs and then backs the gain down. In the test, WSDK finds the best KP for a given value of KD. Once the best KP is found, KD is increased and WSDK finds the best KD gain. This process is repeated until KD cannot be increase further without causing instability in the system. WSDK then decrease KP and KD to stable values. At the last WSDK determines the highest stable value for KI.

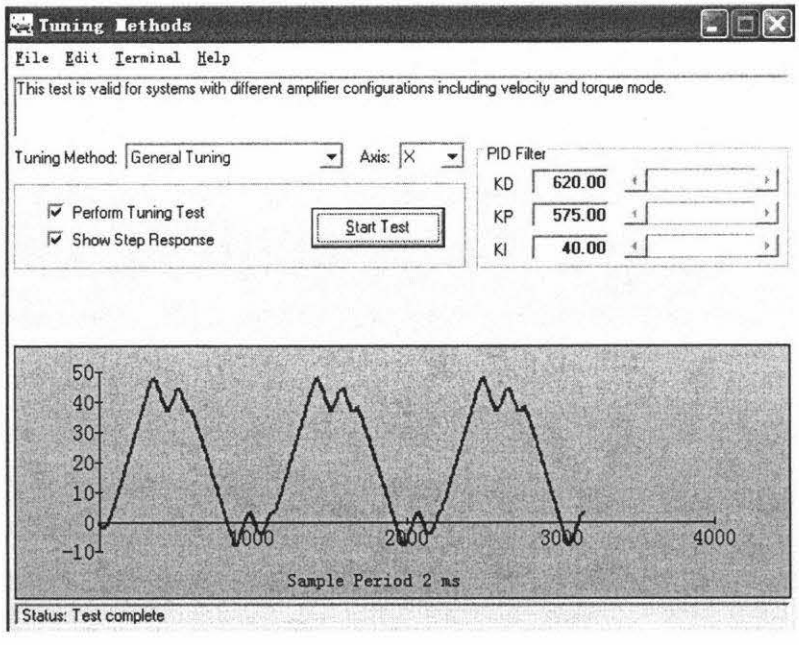

Figure 4.19 General tuning with 1kg of load

As shown in Figure 4.19, the General Tuning gets much better performance than that of the previous two tuning methods. The standard rectangle step of 40 counts has become a sawtooth wave and the peak and the trough have an overshoot. The dwell time of 200ms is unstable because of an inappropriate PID setting. Furthermore, the

actuator continues to oscillate after the test is complete until the controller is reset. This indicates the actuator has lost control.

The similar result has been obtained after unloading load and applying 0.5kg of load. Therefore, General Tuning is not appropriate for this application.

(D) Curve follower

The curve follower selects the best PID parameters that results in a minimum error along a curve. From Figure 4.20, this tuning method can not find a right setting for the system. The steady-state error was 186 counts (186 x 0.2mm = 37.2mm) occurred in a trajectory of 400 counts, which considerably exceed the error limit.

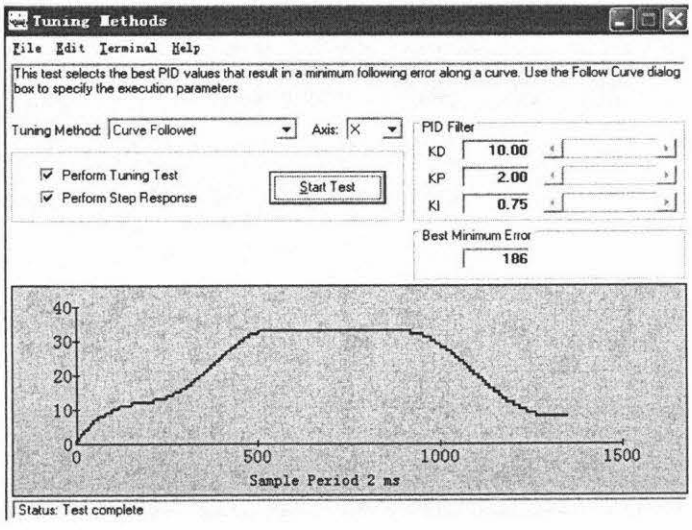

Figure 4.20: Curve follower with 1kg of load

(E) Point to Point Tuning

This tuning method allows the user to define "settling", the user specifies the error limit and time for which the system must stay within those limits. The program then iterates through the PID parameters within the specified range to determine which combination results in the fastest settling time. The larger the error limit and the shorter the time the system must stay within those limits, the faster the settling time. The result shows a big error of over 80 counts occurred during the test (Figure 4.21)

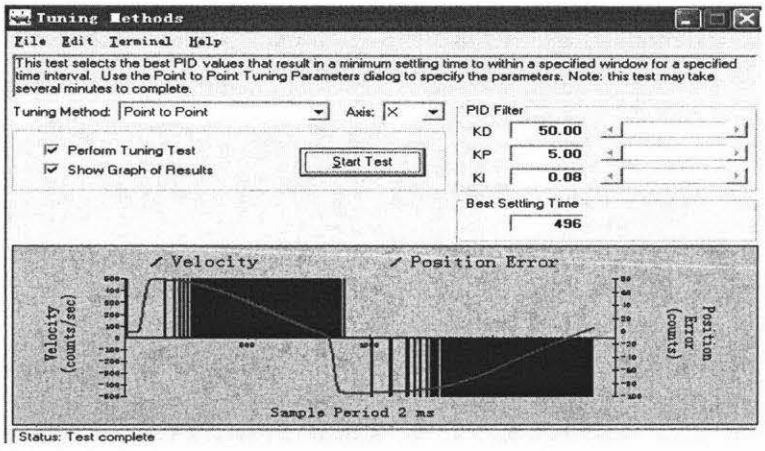

Figure 4.21 Point to Point tuning with 1kg of load

(F) Manual Tuning

This method allows user to choose PID parameters of system but is not an auto-tuning routine. Whenever the PID settings are assigned, the new values will be sent to the controller. An instant feedback regarding the effect of each parameter will be shown on the screen. This method is effective as an appropriate PID setting is closed so that a slight change can be optimized.

4.5.4 Consideration and solution

Having failed in tuning the actuator using automatic and mathematic methods, another solution that has to be considered for tuning is based on the previous tests. Among those tests, the general tuning has been shown better than the others. So if the parameters are put into the WSDK manual tuning, and change them in terms of the properties of PID parameters, the solution might be obtained.

Theoretically, a proportional gain KP has an effect of reducing the rise time and steady-state error but increase potentially the overshoot. A derivative gain KD has a control action, sometimes called rate control, when being added to a proportional controller, and provides a mean of obtaining a controller with high sensitivity. An advantage of it is that it responds to the rate of change of the actuating error and can produce a significant correction before the magnitude of the actuating error become too large. Thus, derivative control has the effect of increasing the stability of the system, reducing the overshoot, and improving the transient response.

An integral control (KI) has the effect of eliminating the steady-state error, but it may lead to oscillatory response of slowly decreasing or even increasing amplitude (Michigan 1997). A brief of the actions of KP, KI, and KD is listed as below (Table 4.3).

Table 4.3: Properties of PID parameters (Michigan 1997)

Close Loop response	Rise time	overshoot	settling time	Steady-state error
KP↑	Decrease	Increase	Small Change	Decrease
KI↑	Decrease	Increase	Increase	Eliminate
KD↑	Small Change	Decrease	Decrease	Small Change

Referring to Figure 4.19 for General Tuning, the overshoot could be reduced by increasing KD and decreasing KP, the oscillation could be eliminated by reducing KI value. The manual tuning procedure is fulfilled in the following algorithm:

- Copy the values from general tuning into manual tuning section.
- Set a step input of 40 counts
- Reduce integral KI until the oscillations vanish.
- Increase derivative KD to reduce the overshoot as much as possible
- Reduce regularly proportional gain until the actuator can reach step input without worse rising time
- According to Table 4.3, adjust each parameter regularly and record it, find out the range for each parameters
- Apply a weight of 0.5kg, 1kg, 3kg and 5kg to actuator and repeat the above procedure and record the result.

By using the procedure, the parameters of PID have been successfully obtained for the actuator control system. With different weights applied, KP = 180~550, KD=500~4901 and KI=0.01~0.12. If KP increased up to 1000 (with 5kg weight), the overshoot increased but still acceptable. Higher KD could reduce overshoot significant but cause noise and a little vibration. KI must be less than 0.12 otherwise there is a small amplitude of oscillation. The reason of wider range for each parameter is determined by the precise of encoder. Higher resolution of encoder could reduce the

bandwidth of parameters significant. One of manual tuning with 3kg of load is shown in Figure 4.22. The left figure shows the comparison between actual and commanded error, which is limited in +3 ~-3 counts (-0.6mm~0.6mm).

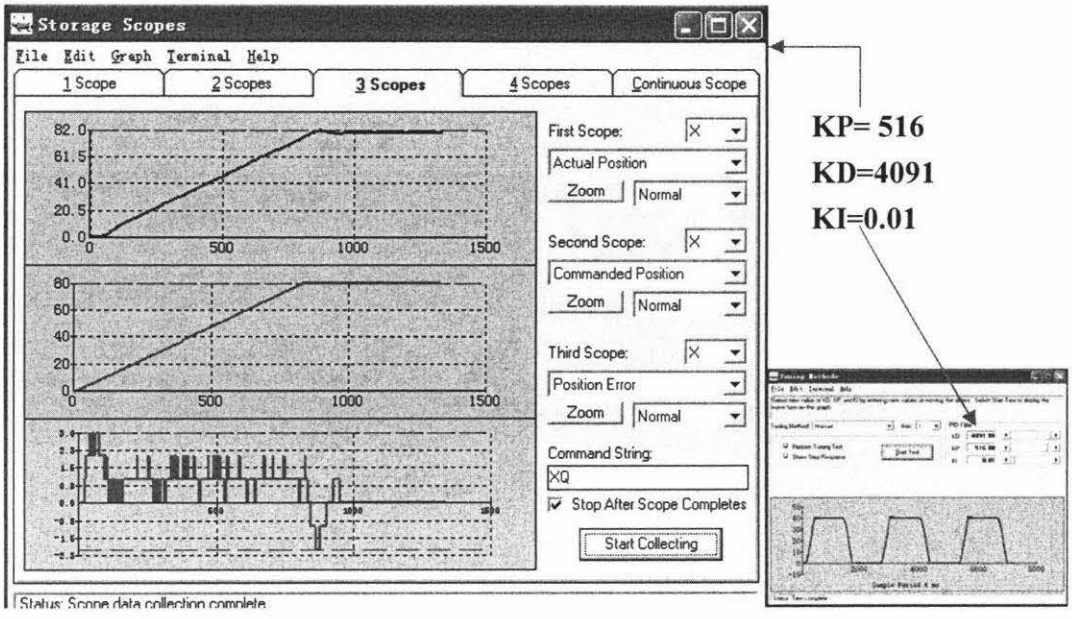

Figure 4.22: Tuning result and step response

4.5.5 Verification of PID parameters

Although the values of PID have been found, it is still necessary for all actuators to verify the PID setting through experiments with specified functional curves in the different 3D spatial poses before putting all actuators back into the real robot.

First of all, all of six actuators need to be tested, where a range from 0.5kg to 5kg of weights will be applied. To simulate a scenario as close to real robot operation as possible, according to different force directions, a single actuator might be configured into four poses in 3D space as horizontal, upward, downward and arbitrary position. The four configurations with applied weights are shown in Figure 4.23.

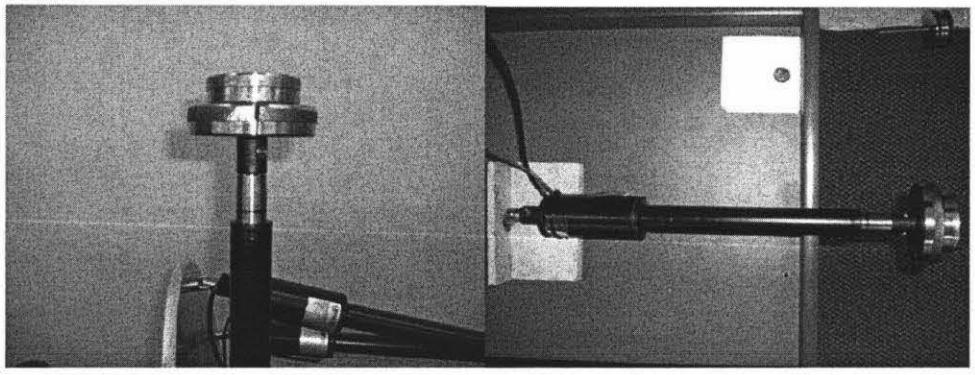

A) Upward B) Horizontal

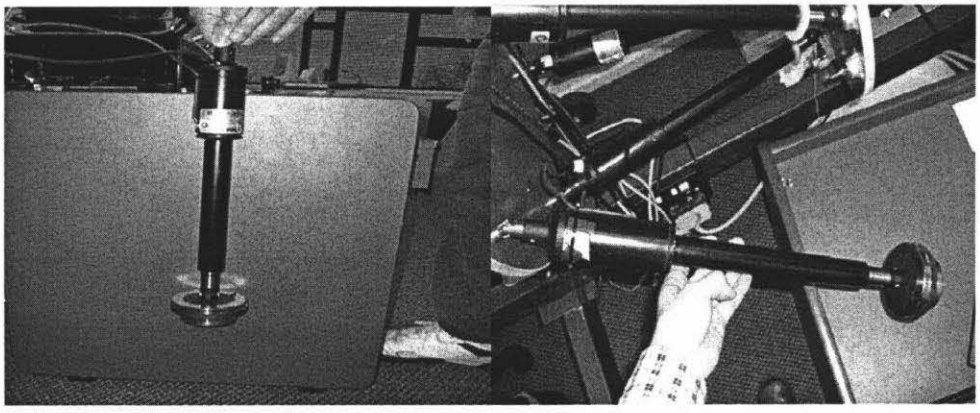

C) Downward D) Arbitrary

Figure 4.23 Four configurations of actuator in 3D space

To test PID setting completely, three functional curves, i.e., step response, standard sinusoidal waveform and a path generated form contour mode, are specified. The specifications of three samples are as follows (Figure 4.24).

Step input with an amplitude of 80 counts. This step input is edited in DMC smart terminal and produced in WSDK32. The description in command is:

# Step	Definition
PR 80	80counts step
SP80	Speed
SHX	Enable servo
BGX	Begin motion

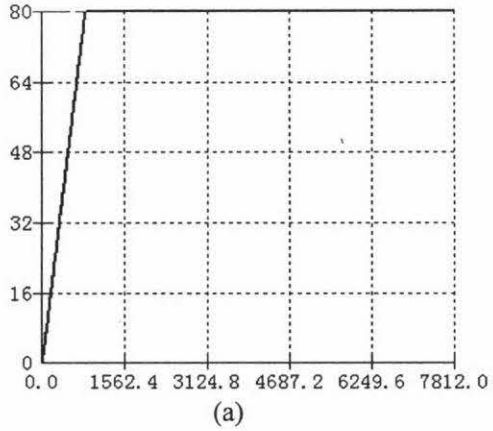

(a)

Standard sinusoidal waveform with 100 counts of amplitude can be programmed with Vector mode in DMC terminal and generated in WSDK

#SINE	Definition
VMX	Vector mode
VA1024	Acceleration
VD1024	Acceleration
VS126	Vector speed
CR100,-90, 3600	Amplitude, degree etc.
VE	End mode
BGS	Begin

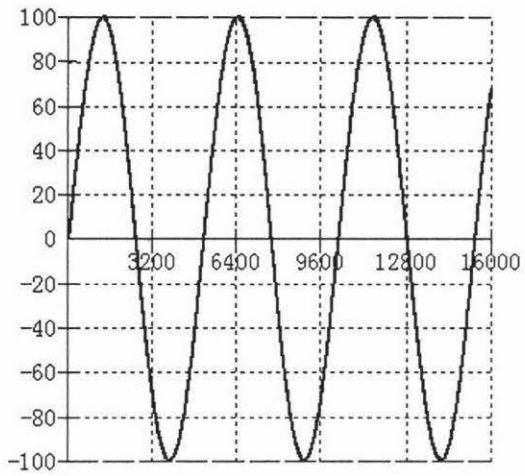

(b)

The generated path is produced in contour mode, and comprised of several linear displacements. The program is given below:

linear path

CMX	Specifies contour mode
DT 2	time interval, 4 ms
CD 48; WC	first position increment
DT 3	time interval, 8 ms
CD 240; WC	second position increment
DT 4	the third time interval, 16 ms
CD 48; WC	the third position increment
DT0; CD0	Exits contour mode
EN	

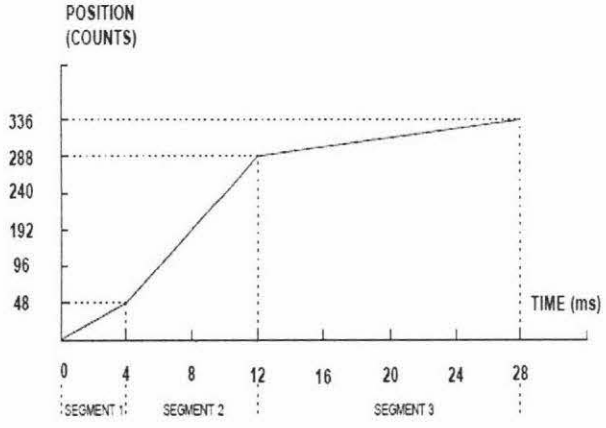

(c)

Figure 4.24 Three testing trajectories

According to the above procedure, one example of the actuator's partial results for following the sinusoidal waveform is listed in Table 4.4.

Table 4.4: PID testing and verification

Record of PID Testing and Verification					
Date: 06 July 06				**Actuator Number: 05**	
Start time: 9:45 am			**Testing sample: Sine input (+100~-100 counts)**		
No.	**Actuator**	**Weight**	**PID Parameters**	**Pass or Fail?**	**Error boundary**

	Placement	(kg)	KP	KD	KI	Comments	(unit : count)
1	H	0.5	30	270	0.01	F	+20 ~ -20
2	V	0.5	30	270	0.01	F	+23 ~ -23
3	H	0.5	180	270	0.01	P	+5 ~ -8
4	V	0.5	180	270	0.01	P	+5 ~ -8
5	H	0.5	500	270	0.01	P	+3 ~ -4
6	V	0.5	500	270	0.01	P	+5 ~ -6
7	H	0.5	500	500	0.01	P	+4 ~ -4
8	V	0.5	500	500	0.01	P	+3 ~ -3
9	H	0.5	500	1000	0.01	P	+1 ~ -1
10	V	0.5	500	1000	0.01	P	+1 ~ -1
11	H	0.5	500	2000	0.01	P	+2 ~ -2
12	V	0.5	500	2000	0.01	P	+1 ~ -2
13	H	0.5	500	4000	0.01	P/ But noise↑	+1 ~ -1
14	V	0.5	500	4000	0.01	P/ But noise↑	+1 ~ -1
15	H	0.5	1000	2000	0.01	P/but overshoot ↑	+6 ~ -6
16	V	0.5	1000	2000	0.01	P/but overshoot ↑	+6 ~ -6
17	H	2	500	500	0.01	P	+4 ~ -4
18	V	2	500	500	0.01	P	+3 ~ -4
19	H	2	500	1000	0.01	P	+2 ~ -1
20	V	2	500	1000	0.01	P	+2 ~ -1
21	H	2	600	1000	0.01	P	+2 ~ -1
22	V	2	600	1000	0.01	P	+2 ~ -1
23	H	2	250	1000	0.01	P/Error ↑	+5 ~ -5
24	V	2	250	1000	0.01	P/Error ↑	+6 ~ -5
⋮	⋮	⋮	⋮	⋮	⋮	⋮	⋮

Note: "H" denote horizontal placement, "V" denotes Vertical placement including upward and downward. If difference, it will be marked separately, otherwise expressed in same row. The error limit is within +10~ -10 counts.

Table 4.4 shows that the PID parameters found from the previous tuning method is appropriate to the control system according to different weights.

The result for one actuator that involved three testing samples is illustrated in WSDk32 (Figure 4.25) where the applied weight is 1kg.

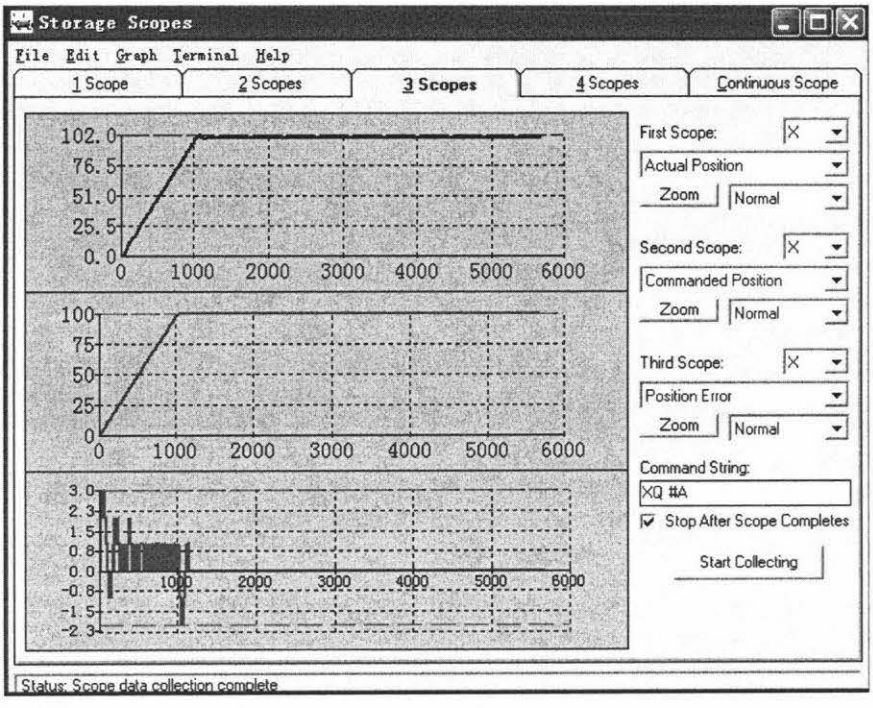

(a) Step response (KP= 516, KD= 1000, KI=0.01)

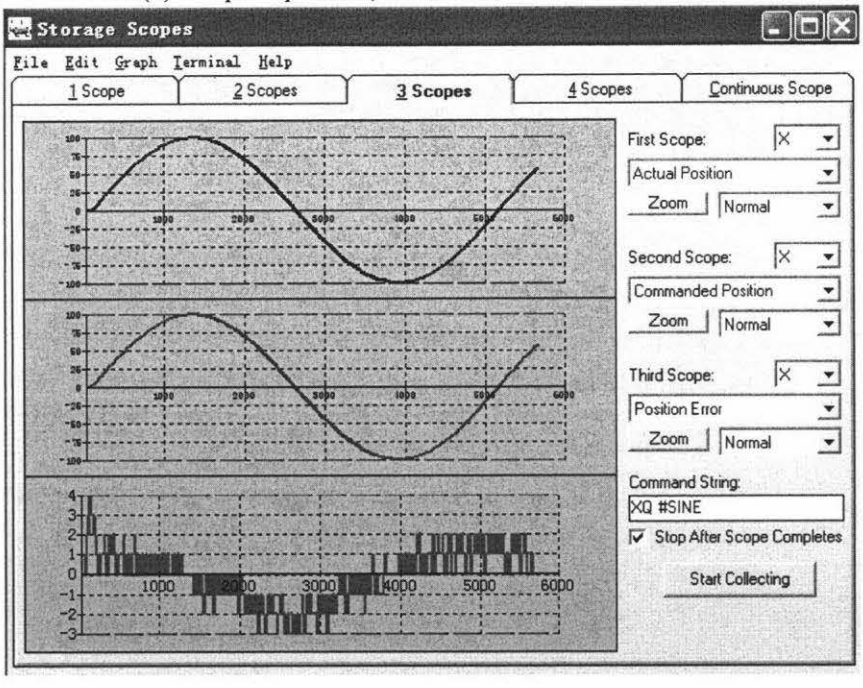

(b) Sinusoids waveform (KP= 516, KD= 1000, KI=0.01)

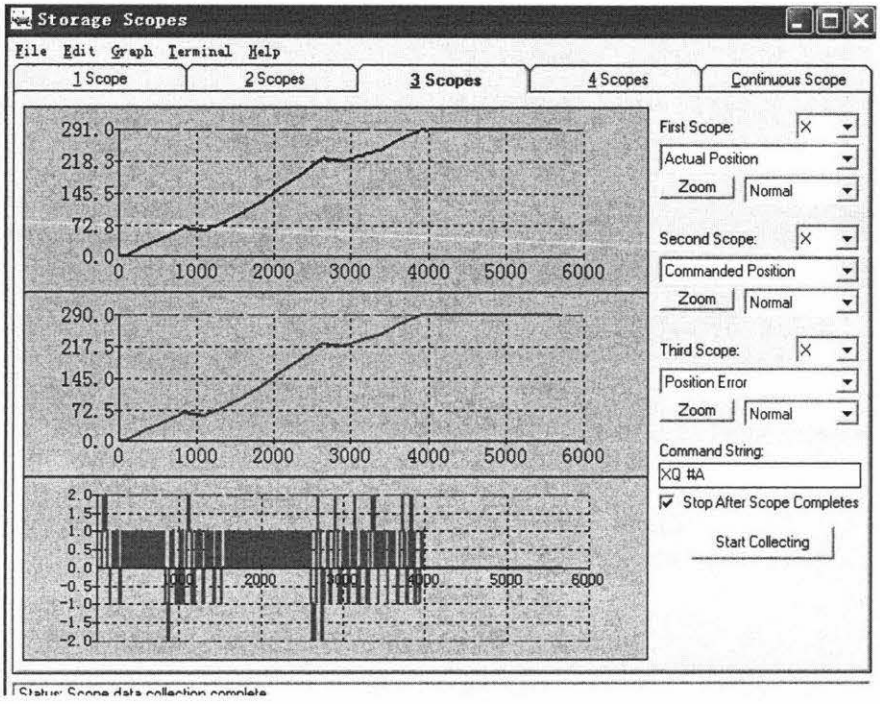

(c) Path following (KP= 516, KD= 1000, KI=0.01)

Figure 4.25 Result shown in WSDK

Figure 4.25 also shows that the average error is within limits, with maximum error 3~4 counts (0.8mm). Therefore, the PID parameters are acceptable.

4.6. Conclusion

In this chapter, the architecture of the motion control has been presented. The hardware and software used for the motion control have been described in details. An improved encoder has enhanced the stability of the system. Contour mode and independent mode have been specified for the motion control. An automatic-manual tuning method has been proposed for PID parameters, which has been demonstrated working well experimentally.

Chapter 5 Operation and performance evaluation

Different from single actuator controlling, operating the 6-UPS robot to perform fracture realignment is quite challenging, where all of six actuators are constrained and move instantaneously. This chapter will examine the validity of the robotic operation based on the previous efforts.

5.1 Practical surgical operation

Since several testing trajectories have been tried on for single actuator, a practical surgical operation seems not so complicated because it just involves a group of motions such as translational and rotary movement.

One of the most common operations can be described as "Pull-Rotate-Push". This kind of action is illustrated in Figure 5.1. Suppose a femur is broken into two pieces A and B as shown in phase A; due to the deforming forces from muscles, tendons and ligaments attached throughout of the bone, bone piece A and B have a displacement in 3D space. Bone piece A could be regarded as being fixed to the human body that lies on the operational table; bone piece B could be seen as a rigid body through a fastened pin at knee joint connecting leg attached on the top plate of the robot.

Phase A: the "Pull" action driven by the retraction of linear actuators pulls the bone piece B to the fracture adjacent zone away from a specified distance determined by surgery so that the second fracture is avoided and a fluoroscope image is taken before the next action come into effect.

Phase B: after "Pull" action, the subsequent action is to rotate bone piece B in realignment with bone piece A in terms of axial direction. The rotation could be started by three actuators in odd or even order resulting in clockwise or anti-clockwise rotation.

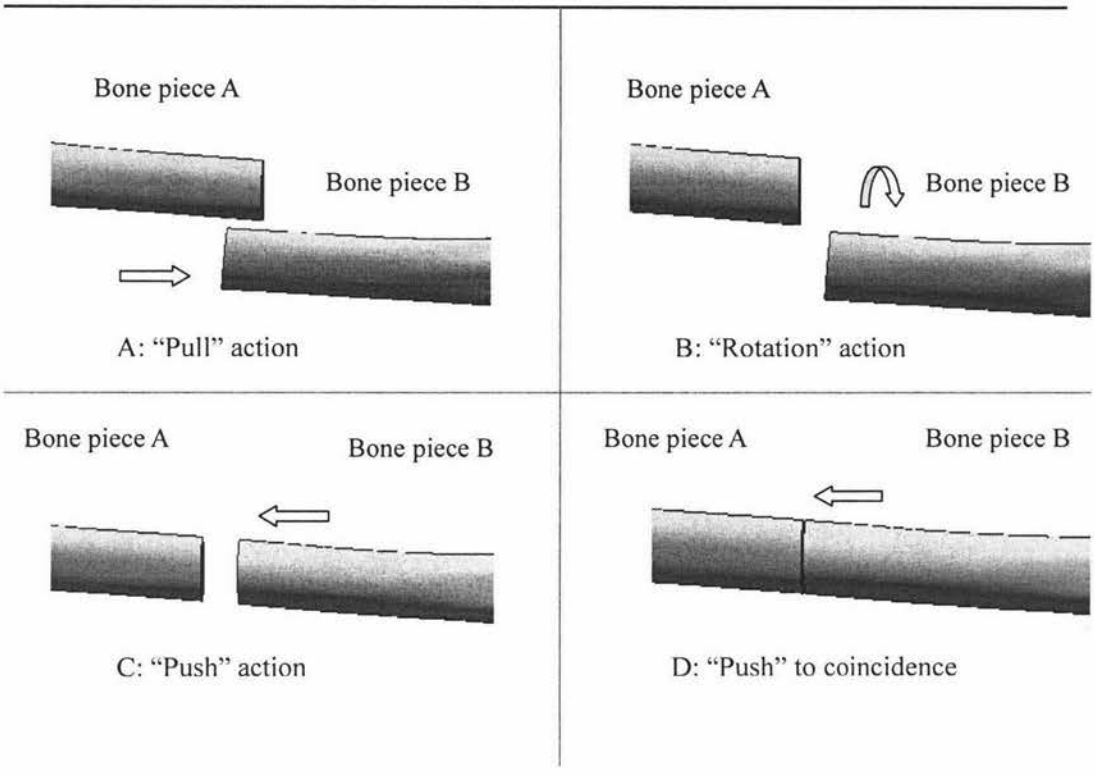

Figure 5.1 "Pull-Rotate-Push" action

Phase C: the "Push" action driven by the extension of linear actuators pushes the bone piece B back to the fracture reunion position by reducing that distance between bone piece A and B.

Phase D: as the distance between two pieces of bone gets into in a permissible value (because it is not possible that two pieces are in a perfect coincidence), the two pieces of bone could be viewed as coincidence, and the surgical operation is complete.

Thus, for the 6-UPS parallel robot, it will have twice translational movements and once rotary movement in the Pull-Rotate-Push" action. With use of inverse kinematics and SolidWorks model, the trajectories could easily be obtained and programmed into controller.

However, to gain a precise result from the real robot, it is very important to do a calibration for robot before doing a practical experiment.

5.2 Calibration

To visually simulate the motion of robot in Cosmos motion environment, a Solidworks' model of the 6-UPS parallel robot was built. Consequently, it introduces

inevitably an error resulted from a theoretical model comparing to the actual robot. Though it is not possible to be eliminated, this type of imperfection can be minimized into an acceptable value by right calibration procedure. The actual meaning of that is strived to obtain an approximately matching result from both theoretical model and actual robot.

5.2.1 Initialized configuration

To calibrate robot, an initialized configuration of the robot in 3D space should be defined in terms of the original design and actual requirement. The original design has been built into SolidWorks model and actual robot in geometry. These features are shown in Figure 5.2.

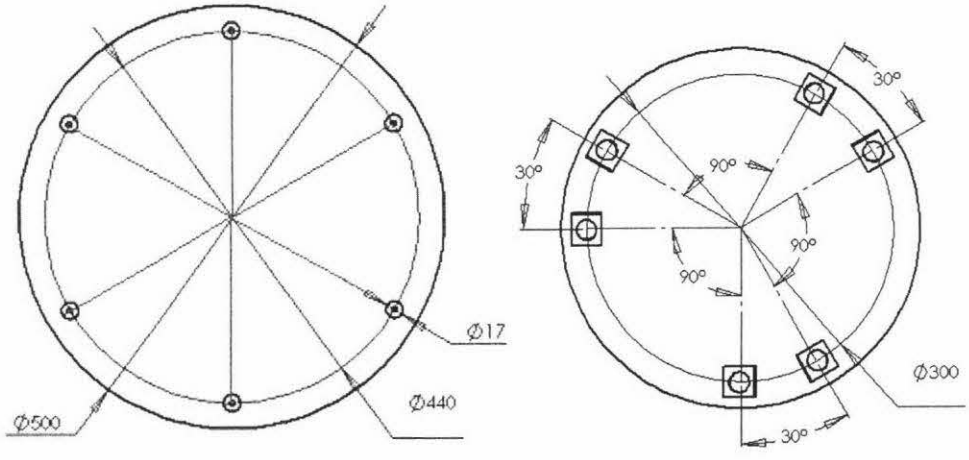

Figure 5.2 Dimension of base plate and top plate

In the base plate, the angular relationship between the any two joints is 60 degree spaced evenly. For the top plate, the angle between any two joints is 30 degree or 90 degree alternatively. Nevertheless, the angular relationship is still not enough to represent the actual relationship between the top and base plates because the top plate has a rotary degree of freedom (rotation) and a vertical translational degree of freedom (height) with respect to the base plate.

Thus, according to actual requirement, the robot becomes initialized when the angular relationship between two joints of each linear actuator is as specified in the

top view plane and the two plates are parallel, (Figure 5.3.)

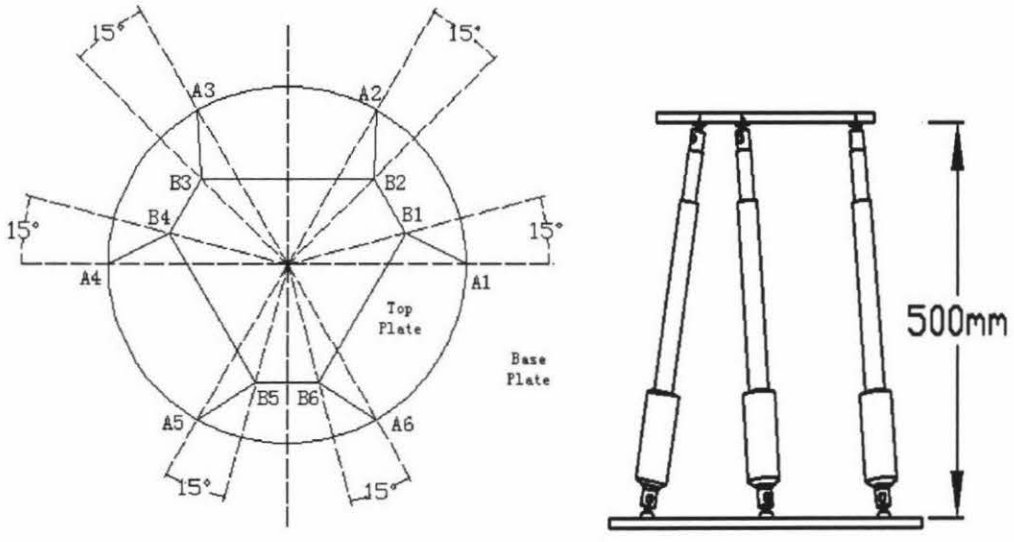

(a) Angular relationships in the Top view (b) Height assignment

Figure 5.3 Initialized configurations for calibration and motion

Based on this configuration, the length of each link may be calculated in the MATLAB inverse kinematics solution. By enter the values into program, the lengths are:

Result

A1B1 = 507.0985

A2B2 = 507.4355

A3B3 = 507.4360

A4B4 = 507.0991

A5B5 = 507.2826

A6B6 = 507.2824

5.2.2 Procedure of calibration

Without index input in the developed encoder, the procedure can only be fulfilled manually using tape measurer, long straight steel ruler, leveler, a ping-pong ball and a plumb line. Although the following procedure is time consuming and complicated, it has proved effective. The procedure is illustrated in Figure 5.4.

1) Firstly, find an even surface to place the robot, and then check the base plate orthogonally with leveler. If air bubble of the leveler in the central, the base is even. Otherwise adjust the surface until the bubble shown in the central.
2) Set control mode into IAP model, with PID setting listed in the Table 4.4. Adjust the length of the links to 506mm~508mm.
3) Check the top plate orthogonally with leveler. If air bubble in the central, the top is even and parallel to the base. Otherwise adjust the length of links manually. The rule to adjust the actuator is: rotating the green item attached on the piston in clockwise is retraction and anticlockwise is extension. Adjust an adjacent couple of the actuators resulting in the height change with respect to other four actuators. Check with the leveler until the top plat is even and parallel to the base.
4) Once the top plate even, measure the vertical distance between the top and the base plates. If the height is less than 500mm, extend slowly all of six actuators in same amount respectively until the height is up to 500mm. If over 500mm, do it reversely. Note that one step is equal to 0.8mm.
5) Once completed, check the concentricity of the two plates with a plumb line that has been fixed at the centre of the top plate. The centre of the base plate has been notched, if the tip of the plumb line does not point at the base centre. Extend the odd labeled or the even labeled actuators for same number of steps against the orientation pointed by the plumb line, which results in an anticlockwise or clockwise rotation without the height change.
6) As the two plates are concentric, repeat 3), 4), 5) to reduce the error from the procedure itself.
7) The calibration is complete when all specifications of initialization are satisfied including height, concentricity, parallelness. Then, measure and record the length of each link and the projective angle at the base plate between two vertexes of each actuator. To reduce an error from the measurement, long straight steel ruler should be as close and parallel to the axes of the actuator as possible. Another short ruler paralleled to the top plate

is useful for intercepting an accurate reading.

8) Notch the initial positions (home position) on the piston and lock with the green item that was designed for the controlling of home position. One of verifications to see whether or not the calibration was successful is to release vertically a Ping-Pong ball above the top plate, if the ball can stops anywhere at the top plate after bounding the calibration was done successfully.

By the calibration, the measured lengths and angles compared to initialized configuration are shown in Table 5.1.

Table 5.1: Comparison of actual robot vs. theoretical model

Link No.	Measure length	Measure angle	Initialize length	Initialize angle
A1B1	507.5mm	16deg.	507.1mm	15deg.
A2B2	507.5mm	14deg.	507.4mm	15deg.
A3B3	508mm	14deg.	507.5mm	15deg.
A4B4	507mm	16deg.	507.3mm	15deg.
A5B5	507mm	15deg.	507.3mm	15deg.
A6B6	507mm	15deg.	507.3mm	15deg.

From Table 4.5, it can be seen that there is small variation between the actual robot and the theoretical model. The reason of this coincidence results from assembly error (less than 1 degree) of the physical robot. Nevertheless, this small variation is still acceptable. Therefore, it concludes that the calibration was successful.

1) Base plate leveling 2) Top plate leveling 3) Length adjustment

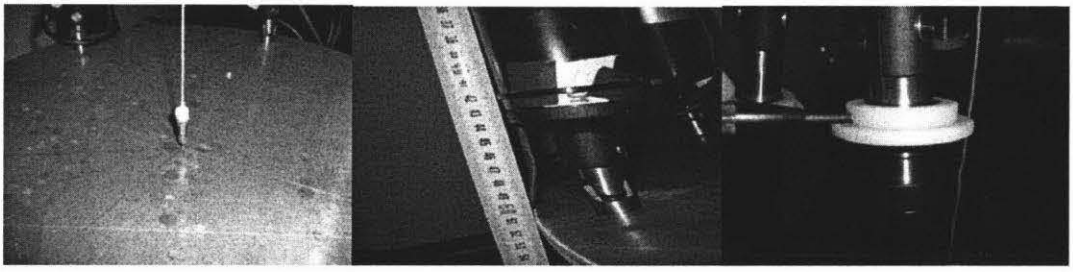

4) Concentricity checking 5) Length measurement 6) Home position Notching

Figure 5.4 Calibration procedure

5.3 Generated trajectories and implementation

5.3.1 Trajectories generation

Once the calibration is complete, the robot model in SolidWorks is able to generate the desired trajectories after initializing the same configuration as that for the actual robot. Such a "Pull-Rotate-Push" action can be started with inverse kinematics calculation, and then enter the displacement of each link into CosmosMotion. Through an appropriate setting in CosmosMotion, the points of the path in each interval (that should be set in same value to Contour mode) are produced in Microsoft excel.

The procedure of a "Push" action with 30mm displacement is demonstrated as below (Figure 5.5):

1) Calculate the length of each link in the inverse kinematics program, input value $\alpha = 15^{\circ}$ and ABO (Height) =530, then the length of each link is obtained as follows:

Table 5.2 Translational displacements

Link No.	Calculated length	Initialize length	Deviation Δ
A1B1	536.7mm	507.1mm	29.6mm
A2B2	537.0mm	507.4mm	29.6mm
A3B3	537.0mm	507.5mm	29.5mm

A4B4	536.7mm	507.3mm	29.4mm
A5B5	536.9mm	507.3mm	29.6mm
A6B6	536.9mm	507.3mm	29.6mm

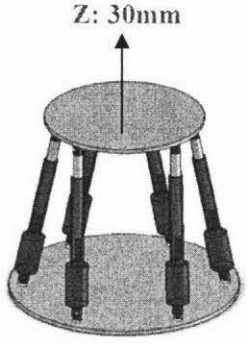

Figure 5.5: Calculation from 30mm displacement along Z axis

2) Enter the deviation Δ into SolidWorks CosmosMotion for simulation and verify the central height between the top and base plate. Note that the initialized position has been assigned to SolidWorks model with $\alpha = 15^{\circ}$ and ABO (Height) =500. After simulation, the height can be measured in the graphical area (Figure 5.6). The measured value is 529.99 mm, which proves the calculated values are correct.

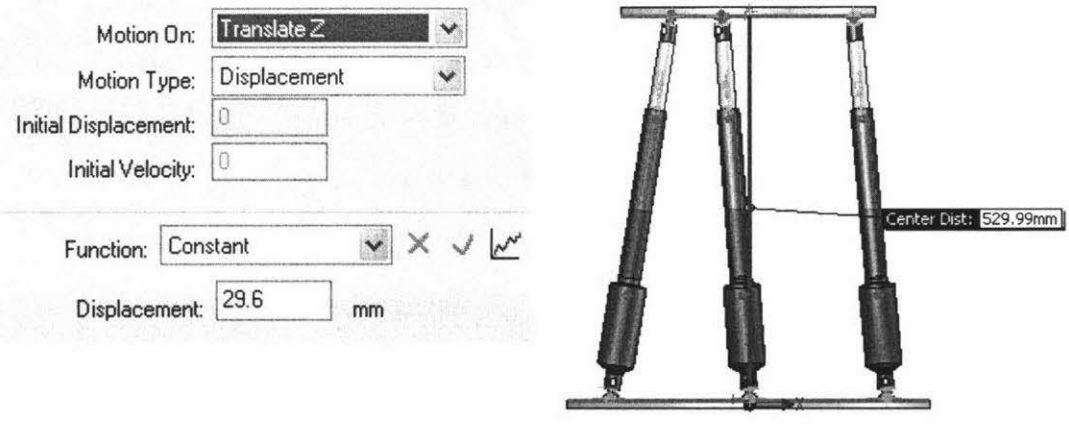

Figure 5.6 Simulation and measurement

3) In CosmosMotion builder, set motion duration of 2.56 or 5.12 seconds and the number of frames of 10 or 20. The reason is that, in Contour mode, the time interval is defined 2^n. As n=8, $T = 2^n = 256$ms. Thus, the minimal sample time should be 256ms. Defining the number of frame, both of two durations can have the minimal sample time (Figure 5.7).

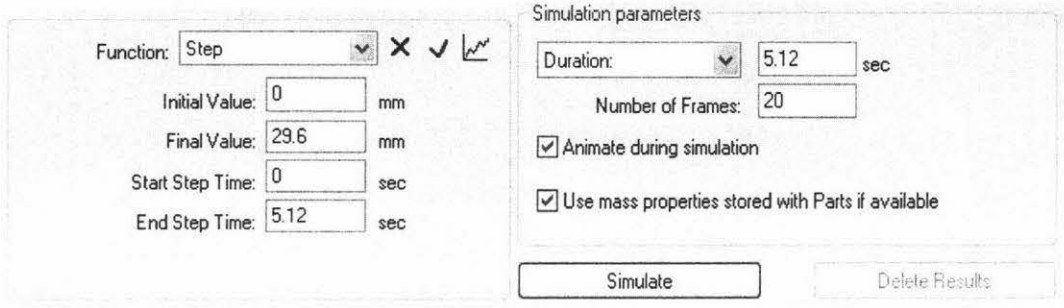

Figure 5.7 Simulation parameters setting

4) Create the relative linear displacement for each actuator (Figure 5.8).

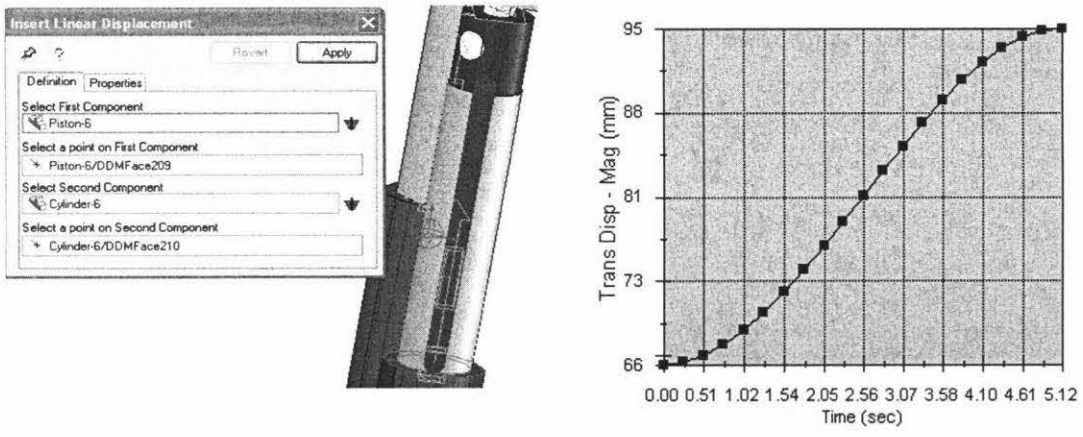

Figure 5.8 Create linear displacement and generated trajectory

5) The trajectory is generated and expressed in Excel. After being edited, it might be transformed into counts recognized by controller (Table 5.3)

Table 5.3: Edited Trajectory

Trans Displacement - Magnitude-Linear Displacement

Time (sec)	Absolute Displacement (mm)	Absolute Δ(mm)	Relative Δ(mm)	RΔ/0.2 (Counts)	Rounded Counts

0	65.73				
0.256	65.95	0.22	0.22	1.1	1
0.512	66.56	0.83	0.61	3.07	3
0.768	67.53	1.8	0.97	4.85	5
1.024	68.81	3.08	1.28	6.4	6
1.28	70.36	4.63	1.55	7.73	8
1.536	72.12	6.39	1.77	8.84	9
1.792	74.07	8.34	1.95	9.73	10
2.048	76.15	10.42	2.08	10.4	10
2.304	78.32	12.59	2.17	10.84	11
2.56	80.53	14.8	2.21	11.06	11
2.816	82.74	17.01	2.21	11.06	11
3.072	84.91	19.18	2.17	10.84	11
3.328	86.99	21.26	2.08	10.4	10
3.584	88.94	23.21	1.95	9.73	10
3.84	90.71	24.98	1.77	8.84	9
4.096	92.25	26.52	1.55	7.73	8
4.352	93.53	27.8	1.28	6.4	6
4.608	94.5	28.77	0.97	4.85	5
4.864	95.12	29.39	0.61	3.07	3
5.12	95.33	29.6	0.21	1.07	1
Total:			**29.61**	**148.03**	**148**

A "rotation" action of α = -30°, ABO (Height) =500mm can also follow and the obtained results are given in Table 5.4 and Figure 5.9.

Table 5.4: Rotary displacement in α = -30 rotation

Link No.	Calculated length	Initialize length	Deviation Δ
A1B1	523.7mm	507.1mm	16.6mm
A2B2	507.3 mm	507.4mm	-0.2mm
A3B3	524.3mm	507.5mm	16.8mm
A4B4	507.1mm	507.3mm	-0.2mm
A5B5	523.8mm	507.3mm	16.5mm
A6B6	507.4mm	507.3mm	0.1mm

Figure 5.9 α = -30 rotation

From Table 5.4, only three actuators are involved in the "rotation" motion, the small deviations in other three actuators could be neglected. The trajectory of one actuator is listed in Table 5.5, after it was implemented in CosmosMotion.

Table 5.5 Displacement for rotation

Time (sec)	Absolute Displacement (mm)	Absolute Δ(mm)	Relative Δ(mm)	RΔ/0.2 (Counts)	Rounded Counts
0	65.73				
0.256	65.85	0.12	0.12	0.6	1
0.512	66.19	0.46	0.34	1.72	2
0.768	66.73	1	0.54	2.7	3
1.024	67.45	1.72	0.71	3.57	4
1.28	68.31	2.58	0.86	4.31	4
1.536	69.3	3.57	0.99	4.93	5
1.792	70.38	4.65	1.08	5.42	5
2.048	71.54	5.81	1.16	5.8	6
2.304	72.75	7.02	1.21	6.04	6
2.56	73.98	8.25	1.23	6.17	6
2.816	75.21	9.48	1.23	6.17	6
3.072	76.42	10.69	1.21	6.04	6
3.328	77.58	11.85	1.16	5.8	6
3.584	78.67	12.94	1.08	5.42	5
3.84	79.65	13.92	0.99	4.93	5
4.096	80.52	14.79	0.86	4.31	4
4.352	81.23	15.5	0.71	3.57	4
4.608	81.77	16.04	0.54	2.7	3
4.864	82.11	16.38	0.34	1.71	2
5.12	82.23	16.5	0.12	0.6	1
Total:			**16.5**	**82.51**	**84**

Since the "Pull" is an inverse action of "Push" operation, the procedure of "Pull" is described here.

5.3.2 Implementation on the robot

With use of the known PID setting and the generated trajectory, a program used to indicated the "Pull-rotation-Push" actions has been developed (Appendix A). The graphical response of one actuator is shown in Figure 5.10.

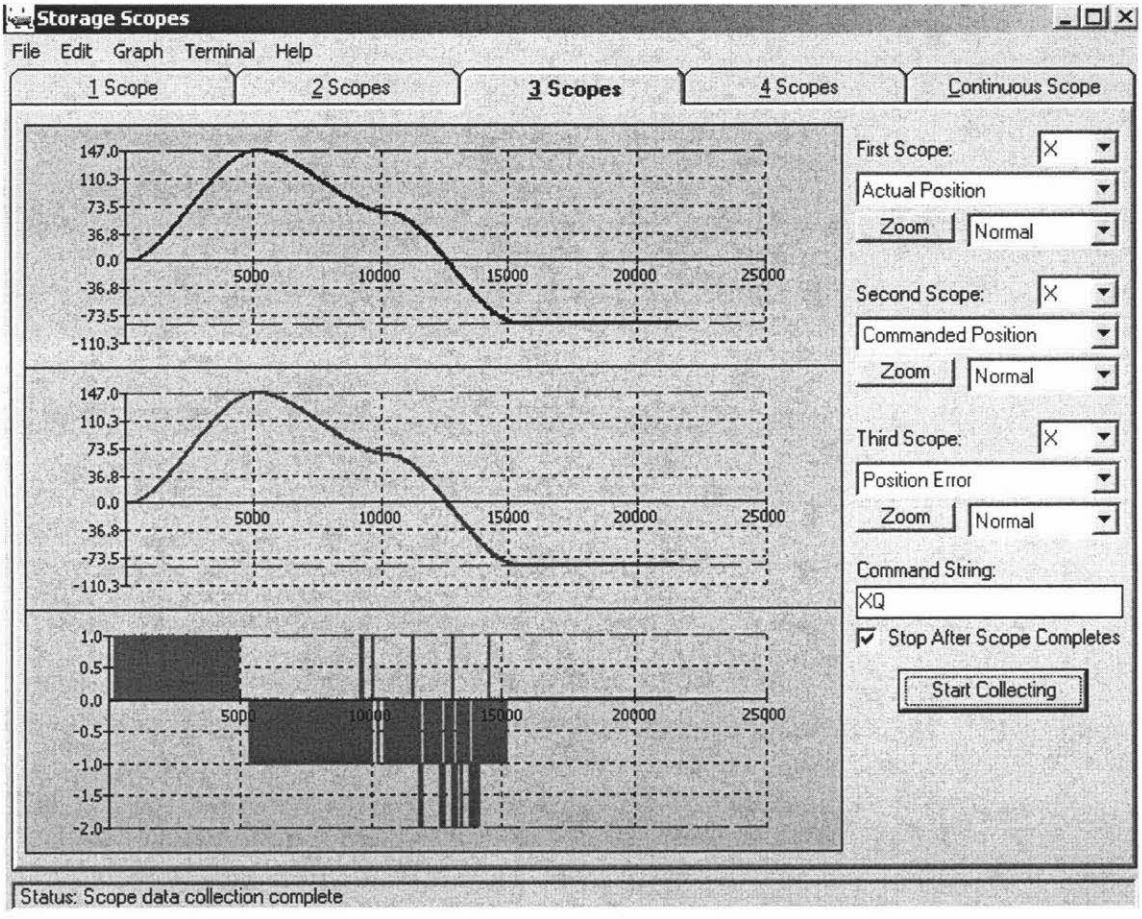

Figure 5.10 Response of a "Pull-Rotate-Push" action

This figure shows the response of one actuator involved in the "Pull-Rotate-Push" action. For the first 5.12 seconds, the actuator retracted (Pull action, in WSDK32), it is defined as positive of 148 counts (29.6mm). And for the subsequent 5.12 seconds, the actuator extended (negative) 84 counts (16.8mm) to complete the "Rotate" action. For the last 5.12 seconds, actuator continued to extend 148 counts (29.6mm) for implementing a "Push" action.

The error limit for all actuators set in the control program is +20 counts ~ -20 counts (+4mm~-4mm) which were typed in two lines of commands as below.

OE1,1,1,1,1,1
ER=20*

The first line denotes the opening error control for all six actuators' and the second line defines the error limit of 20 counts for all six actuators. All six actuators will be stopped automatically and immediately when the actual error reaches the limit and an alarm will be displayed on the controller panel. It can be seen in Figure 5.10 that the maximum error during the motion is +1~-2 counts which is within the error limit. The result demonstrates the PID parameters and trajectories suitable for the motion control of robot.

To simulate vividly, the manikin mounting femur bone and human sciatic joint have been placed on the robot. The entire assembled robot mechanism was successfully demonstrated (Figure 5.11). More photos and video files are available in CD.

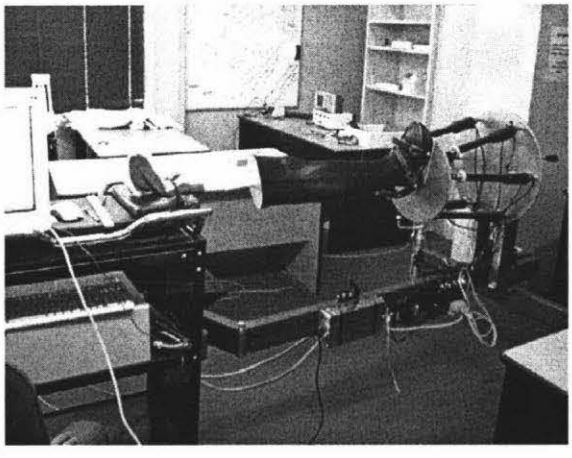

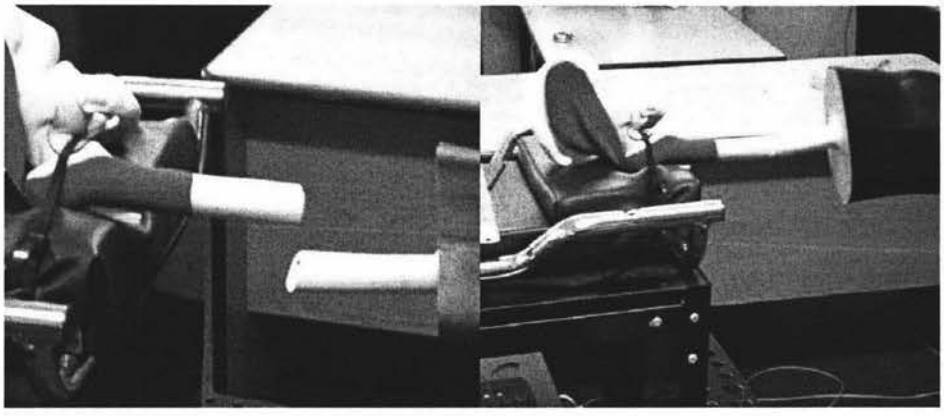

Figure 5.11 Robot system and demonstration

5.4 Existing problems

Although all of six actuators could be able to follow the generated trajectory without exceeding the error limit, an unexpected problem has occurred in the motion test that the actuators have an undesirable vibration as they extend and retract. As a result, the top plate appears vibrating with small amplitude. Another problem detected in the test, some spherical joints were easily damaged. These problems need to be resolved before the further experiments are carried on.

5.4.1 Representation of problems

The vibration represents that a linear movement along the axial direction is not smooth. Some more characteristics of the vibration are as follows:

1) The amplitude of the vibration while extending is higher than retracting.
2) The vibration in pure rotation gets less than the translational movement.
3) The robot that is placed vertically got less vibration.
4) Higher spinning speed cause the vibration easily.
5) The longer the actuator extends the more significant is the vibration.

5.4.2 Possible reasons

Through examining the above characteristics of the vibration, the possible reasons might be related to the following:

1) Inappropriate PID parameters making unsmooth motion.
2) The variation between theoretical model and actual robot.
3) Low resolution of the encoders
4) Overconstaint resulting in large force in the spherical joints
5) Quality of the motors
6) Lubrication failure and mechanical friction.

5.4.3 Analysis and solution

1) Inappropriate PID parameter: reviewing Table 4.3 as below, it was found that the potential factor might be overshoot, so decreasing KP and increasing KD might be useful. After this was done, however, the vibration still existed without any change. In the experiment the KD was increased to the maximum KD=4000, specified by amplifier and the KP was reduced to the critical value which causes the steady-state error increase up to +8~8counts. Therefore, PID factor can be excluded from the reasons of the problem.

Close Loop response	Rise time	overshoot	settling time	Steady-state error
KP↑	Decrease	Increase	Small Change	Decrease
KI↑	Decrease	Increase	Increase	Eliminate
KD↑	Small Change	Decrease	Decrease	Small Change

2) The variation between theoretical model and actual robot: because the inverse kinematics of the parallel robot has a unique solution, this factor reflects on the variation in the actuation of each link, which eventually results in a position error on the top plate. However, the variation between two models is minor, which can not be large enough to cause the vibration. This also was proved in the calibration procedure where the top plate could be positioned within workspace without causing any extra force through adjusting manually a small amount of the displacement on each and every actuator.

3) The resolution of the encoders is too low: the developed encoders only have 4 counts/per revolution without index input comparing to the industrial rotary encoder which has at least 200 lines (4x200=800 counts) per revolution with index input. The encoder with lower resolution affects on the motion control significantly, which makes the curve of control unsmooth like a ladder. Such characteristics obviously could be observed from the partial response of "Pull-Rotate-Push" action (Figure 5.12). The figure shows that the motion trajectory comprises of a series of steps. Higher solution of encoder has an effect on increasing the numbers of step in each time interval and the amplitude of each step will become smaller. As a result, it will smooth the curve remarkable. Adversely, the curve of the motion will become rough like "Cog-cog". Thus, to reduce the vibration, the option is to either change encoder or optimize control program which reduces the spinning speed as much as possible through extending the duration from 2.56 seconds to 5.12 seconds and sampling frames from 10 to 20. A practical test shows that the vibration got less but it could not be eliminated because the lowest spinning speed to keep actuator stable was nearly reached, where in the most of time interval (256ms), the actuator only travelled a few counts. Another evidence of the encoder failure is a wider range bandwidth that the encoder has. An encoder with high or low resolution determines the quality of PID tuning no matter what tuning method is used. A PID tuning running on the rough encoder is easily to be satisfied in a wider range. So, the encoder is the key factor of the system vibration.

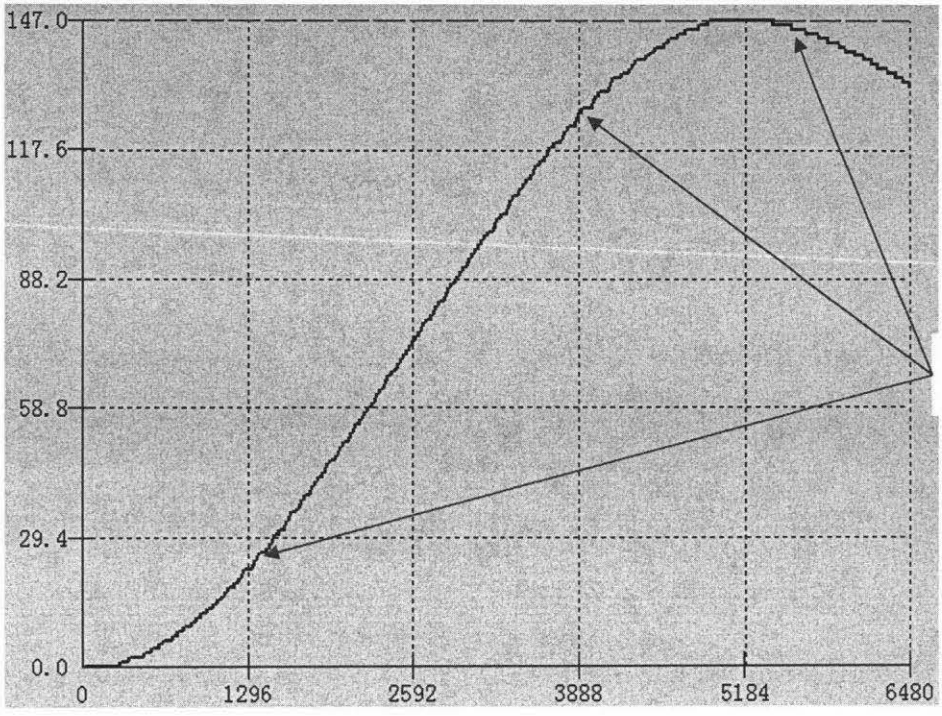

Figure 5.12: Optimized control curve with "Cog-cog"

4) Large force in the spherical joints: during the test, the spherical joints were damaged seriously. Particularly, the ball in the socket could not move freely with a very large resistance. The reason was found that the interface between the ball and socket was deformed. Hence, the spherical joint was no longer a 3-DOF joint. Figure 5.13 shows a damaged spherical joint, the edge of socket has a discernible dented area. Another invisible damage is a little of tiny metal piece found at the bottom socket.

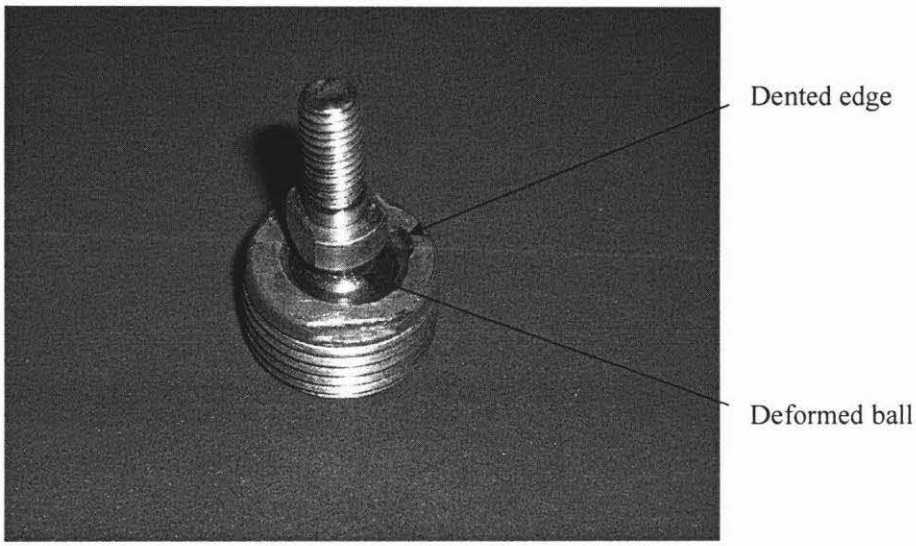

Figure 5.13 Damaged spherical joint

To further confirm the causes, a force and torque analysis for all spherical joints has been carried out in CosmosMotion. The final visible result is illustrated in Figure 5.14. The force (The arrowed straight line) applied on the top six spherical joints are summarized into Table 5.6.

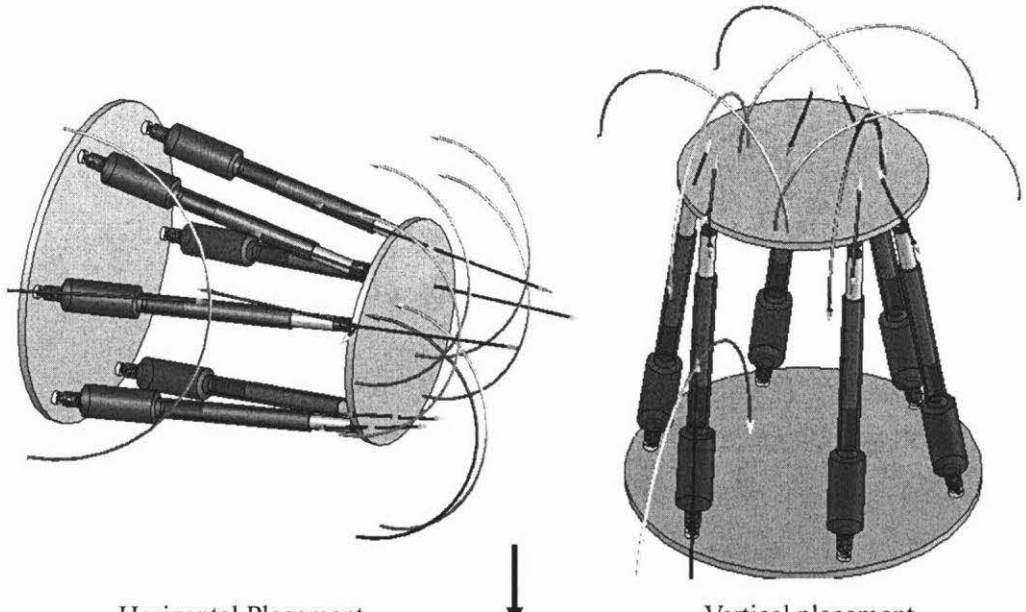

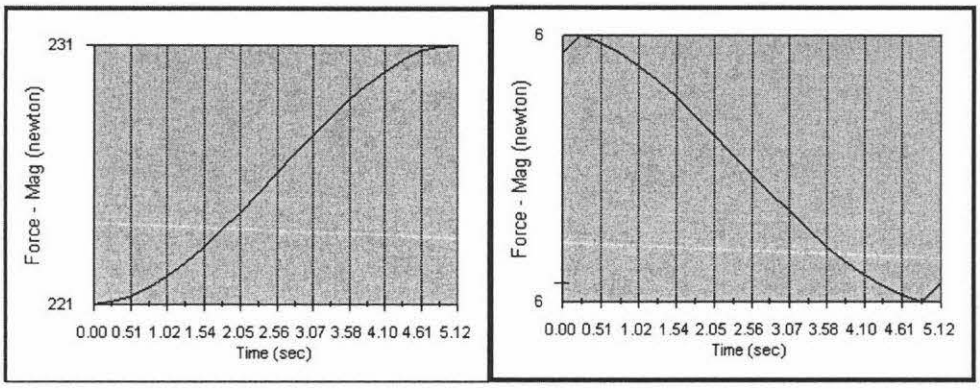

The stress applied on the No.6 actuator in Horizontal (left) and Vertical placement (Right)

Figure 5.14 Force analyses for spherical joints

Table 5.6 Stress on the spherical joints in two placements

Link No.	Maximum Stress (H)	Maximum Stress (V)
A1B1	63.8N	6.3N
A2B2	63.8N	6.3N
A3B3	231N	6.3N
A4B4	168N	6.3N
A5B5	168N	6.3N
A6B6	231N	6.3N

From Table5.6, in the horizontal placement, the spherical joints on No.3 and No.6 actuators have a maximum force up to 231N as the robot extends 29.6 mm. Its value is much greater than the force in the vertical placement (6.3N). This result coincides with the real situation that all of damaged spherical joints are from the two actuators. At the same time, unlike the vertical situation, the forces applied on the joints in the horizontal placement are not equal. It is easily understandable that the vertical placement distributes the weight of the top plate averagely over the six joints. Consequently, in the horizontal placement, an internal force has applied on the top plate. When six actuators are not running synchronously, the uneven internal force might produce the undesired vibration. This has explained why the vertical

placement gains the vibration less. Furthermore, from the force curve, the trend of the curve indicates that the force is going up when the top plate extends. This reveals the fact for characteristics 1) and 5), that is, the longer the force arm the larger the torque and thus the worse the vibration. Hence, the failure of the spherical joint is another key factor that influences the performance of the system.

5) The quality of the motors: A damaged linear motor was dissembled and found that it is simply a normal 24V brush DC motor. The performance is hard to be evaluated without a motor data sheet. By checking the manual of the actuator, the maximum thrust able to be produced by the motor is 400N that is larger than 231N required by the task without considering the patient's leg on the robot. Hence, it is doubted that the robot is strong enough to do deal with a practical operation.
6) Lubrication failure and mechanical factor: there was no apparent change in the situation after the lubrication was applied on the motor shaft and piston. .

To sum up, the existing problems results from the lower resolution of the encoders and the quality of the spherical joints. The improvement can be made by selecting an appropriate encoder and spherical joints. A few other options for improvement will be given in the next chapter.

Chapter 6 Conclusion and future developments

6.1 Conclusion

The incidences of Long bones fracture occur in New Zealand with a ratio of approximate 1 case per 10,000 populations. Due to the long bones such as tibia and femur that have muscles, and other soft tissues attached throughout the length of the bone, the realignment of long bones fracture mainly rely on the human operation with the aid of fluoroscopy at the present day. As the operation also depends highly on the surgeon's experience, the drawbacks of current practice result in long time exposure to radiation, slow recovery due to soft tissue damaged in manual operation and possible morbidity. Hence, to eliminate these drawbacks, a semi-automated long bone fractures reduction system based on a 6-DOF parallel robot platform has being developed since 2004.

As a part of the semi-automated fractures reduction system, the developed 6-DOF parallel robot comprises of six linear actuators driven by 24VDC servo motor with a rotary incremental encoder of 4 counts per revolution built in each actuator. To implement a realignment of long bone fracture, a framework for placing 6-DOF robot has been developed, which consists of links, Jockey roller/standers and other attachments with a feature of keeping a 2-DOF workspace in horizontal and 500mm height adjustment in vertical. A half-manikin with a femur and a human sciatic joint are fixed by a holster attached on the top plate of the robot and patient's table respectively, which simulates real fracture realignment scenarios.

The inverse kinematics and singularity of the 6-DOF parallel robot have been studied to obtain a theoretical support for its motion control and calibration. With assignment of Z-Y-X Euler angle for the robot, the solution of inverse kinematics can calculate the length of each link with a unique solution corresponding to an arbitrary pose of the top plate within 3D workspace. The Jacobin matrix also has been developed. The singular configurations of the 6-DOF parallel robot have been described in both the analytical matrix and the published results. .

In motion control, Galil DMC-1800 series multiple axes motion controller and amplifiers have been used for the 6-DOF parallel robot. The stability and reliability of the encoder have been improved. Contour mode has been used for controlling actuator motion since it can keep a harmonious relationship between actuators in each time interval. PID tuning algorithms including mathematic and automatic methods were discussed. However, both of them could not gain appropriate PID parameters for the system. The PID parameters for the system eventually obtained based on the combination of the general tuning result and the control principle. The PID parameters have been presented in a table according to different weight applied on the actuator. The validity and verification of PID parameters have been proved through a larger numbers of experiments, which were performed in multiple configurations, a range of applied weights and different generated trajectories.

The practical realignment of bone fractures normally requires a "Pull-Rotate-Push" action implemented by the 6-DOF parallel robot. To reduce the undesired error in robotic models and assembly, the procedure of the calibration is detailed. With the help of inverse kinematics and SolidWorks CosmosMotion, the displacement of each actuator has been programmed into Galil controller. The actual result has shown the robot is capable of implementing a "Pull-Rotate-Push" operation with an error of 0.2mm~0.4mm, which demonstrates that the proposed PID tuning, calibration and trajectory generation are acceptable.

A major disadvantage of the robotic operation was the undesired shaking. The reasons found might be the poor resolution of the rotary encoder and the low grade spherical joints. The shaking problem was analyzed through PID experiments and force analysis. The improvements made have reduced the vibration. However, the vibration could not be eliminated fully. The recommendations for future developments have been proposed, which is mainly concerned with the use of miniature rotary encoder and advanced spherical joints.

6.2 Future developments

The encoder and the spherical joint have become the bottlenecks in getting a satisfactory performance of the robotic system. To realize a fine PID tuning and gain a stable motion, future development will be mainly concentrated on the selections of the encoders and spherical joints. The encoders to be chosen should be able to assemble into the current actuators. A few other engineering suggestions are made in the end of the chapter.

6.2.1 Encoder

The encoder issue has not been resolved throughout the project, as they had been built in the actuators by other students. The solution to it is to purchase an industrial mini-rotary encoder. The major requirements of new encoder are listed in the Table 6.1.

Table 6.1 Requirements of encoder

Features	Specifications
Encoder type	Incremental rotary
Resolution	At least 200lines (800 counts) per revolution
Shaft bore	Minimum Φ 10 mm, maximum Φ 15mm
Outer diameter	Less than50mm
Shaft length	Must be through shaft standard
Signal output	Quadrature outputs with index channel
Input Voltage	5VDC~ 12VDC
Output option	RS422

Among the requirements, the resolution of 200 lines is the minimal standard for an industrial encoder, higher resolutions will be costly. To simplify the procedure of the calibration, an index channel is necessary for locating the home position. The hardest requirement to be met is the outer diameter of encode determined by the inner diameter of the actuator.

In terms of these requirements, most candidates are not suitable because of their dimensions, except QD145 optical encoder and ST 38/50 series encoder that meet the

all requirements listed in the table (Figure 6.1). The comparison between QD145 and ST 38/50 series encoders listed as Table 6.2.

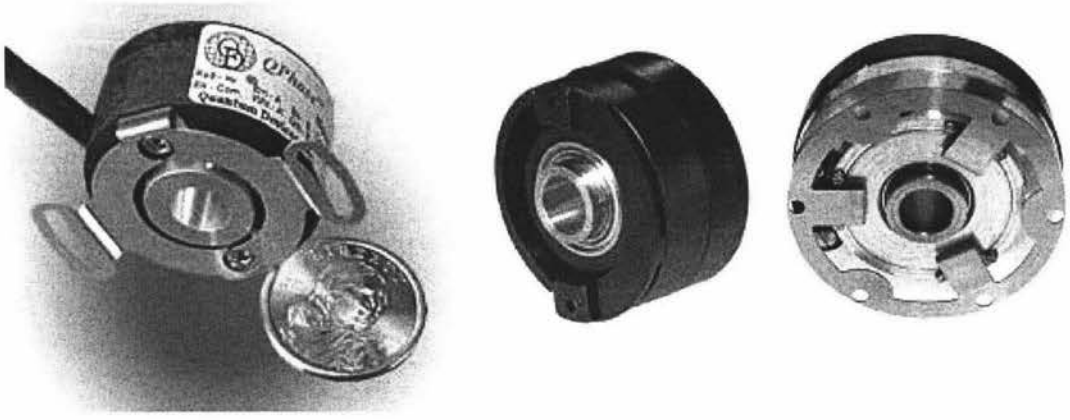

Figure 6.1 QD145 optical encoder (QPhase 2006)& ST38/50 series encoders (ServoTek 2006)

Table 6.2 Specifications of encoders

Features	QD145	ST38	ST50
Encoder type	Incremental	Incremental	Incremental
Resolution	200~5000	200~5000	200~5000
Shaft bore	10mm	10mm	14mm
Outer diameter	36.84mm	38mm	50mm
Shaft length	Through shaft	Through shaft	Through shaft
Signal output	Quadratured with index channel	Quadratured with index channel	Quadratured with index channel
Input Voltage	5V~26VDC	5V~26VDC	5V~26VDC
Output option	RS422	RS422	RS422

From Table6.2, apart from dimension, three miniature encoders have same specifications with QD145 and ST38 that have a smaller size. All datasheets and quotations are included in Appendix C.

6.2.2 Spherical joint

One advanced spherical rolling joint mentioned by Merlet in 2000 is supplied by Seiko (Figure 6.2). The joint allows for misalignment of 30~45 degrees with a size from 7.6mm to 7.6mm and a weight from 15g to 6.73kg. The feature of the spherical rolling joint is given below:

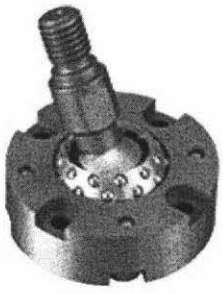

Figure 6.2: Spherical rolling joint supplied by Seiko (Hephaist Seiko 2005)

1) High precision: the movable part has less frictional resistance due to its rolling joint structure under preload, achieving high precision with zero clearance.
2) Downsizing of joints with multiple degrees of freedom: compared with those combining rolling bearings with 3 degrees of freedom, higher rigidity and downsizing has been achieved.
3) Application to parallel mechanism: optimal for achieving high precision, high rigidity and downsizing of parallel mechanism.
4) Superfine inner spherical machining technology: realized with superfine inner spherical machining technology of Hephaist (Hephaist Seiko 2005).

The specifications show that SRJ008C or SRJ012C is suitable for the robot application with a load capacity of 540N or 770N (Appendix C).

6.2.3 Other suggestions

Currently, the controlling of the robot motion is commanded from human-computer interface, as a result, all motions must followed the same procedure involving inverse kinematics, trajectory generation, programming and implementation. Sometimes, for a simple motion such as the calibration that needs only forward few

counts, it is unnecessary to follow the entire procedure. Hence, a manual control mode is great for simple motion control. This function could be realized easily by utilizing the I/O interface provided by DMC-1800 controller. Like other parallel mechanisms, a control unit (panel) will be convenient for manual operation. The basic elements of the control unit should comprise of six INCH (Independent channel Handler) buttons for six actuators, emergency stop, DC current gauge, two AC/DC indicators and buzzer etc. Another usage of the control unit is able to contain power supply, amplifier and electrical wiring into a safety environment.

References

APEX. (2003). "APEX assembly." Max-Planck-Institut für Radioastronomie. http://www.mpifr-bonn.mpg.de/div/mm/apex/may2003/index.html.

Asish, A. (2005). "Position Sensing and Control of a Long Bone Fracture Realignment Medical Robot.",14-31.

Bruyninckx, H. (2005)."Parallel robots." The Robotics WEBook, 2-15, Department of Engineering, Divison PMA, Belgium, http:// www.roble.info.,

Craig, J.J. (2005)."Introduction to Robotics: Mechanics and control," Third Edition, 43-62., 2005 Pearson Prentice Hall, the United States of America.

Chen, J. (2005). "Alternative representations to "Angle-axis" approach: Euler angles." Department of Systems engineering, Research School of Information Sciences and Engineering, Australian National University, http://users.rsise.anu.edu.au/~chen/teaching/Robotics_ENGN4627_2005/lectureNotes/engn4627-Part05.pdf

CyberResearch. (2007). "Quadrature Signals-understanding Quadrature signals", CyberResearch, Inc., Branford, USA. http://www.cyberresearch.com/content/tutorials/tutorial16.htm

Donelan, P. (2005). Singularities of Robot Manipulators." School of Mathematics, statistics and computer science, Victoria University of Wellington, New Zealand

Fichter, E.F. (1986). "A Stewart platform-based manipulator: general theory and practical construction." International Journal of Robotics Research.,

vol.5, No.2, 157-182.

Hunt, K.H. (1978). "Kinematic Geometry of Mechanics." Oxford University.UK.

Heiphaist Seiko®, "Spherical Rolling joint SRJ series." Specification and datasheet, Heiphaist Seiko Inc., Japan. http://www.hephaist.co.jp/e/pro/ball.html.

Galil, Inc (2005). "DMC-1700/1800 user manual, manual Rev.1.21." Galil Motion Control, Inc. Rocklin, California, America

Gosselin C. (1988). "Kinematic analysis optimization and programming of parallel robotic manipulators." Ph.D.Thesis,McGill University, Montreal.

Gough V.E. (1956). "Contribution to discussion of papers on research in automobile stability, control and tyre performance." Proc.Auto Div.Inst. Mech. Eng.

Harib, K., and Srinivasan, K. (2003). "Kinematic and dynamic analysis of Stewart plateform-based machine tool structures." *Journal of Robotica,* Cambridge University Press, volume21, 541-554.

Kim, D., and Chung, W. (1999)."Analytic singularity Equation and Analysis of Six DOF Parallel Manipulators Using Local Structurization Method", IEEE Transactions on robotics and Automation, Vol.15, No.4, 612-621

LINAK Group(2006)."Actuator LA22, Product datasheet", LINAK 06.12 . MA, M9-02-035-K. Chapter 5.02

Lisien, B., Abraham, N., and Wolf, A. et al. (2004). "MiniBone attached Robotic System", Sensor Based Planning Lab, Carnegie Mellon

University.

Ma, O. and Angeles, J. (1990). "Architecture singularities of platform manipulators." in IEEE Int. Conf. Robot. Automat., vol.6, 281-290.

MeanWell. (2005). "750W single output power supply, SP-750 series datasheet", 2-10, TRC Electronics Inc., Australia.

Merlet, J.-P. (2000)."Parallel Robots."second edition, published by Springer, ISBN 1402003854, 7-12.

Michigan. (1997)."Control of tutorials for Matlab, PID Tutorial", The University of Michigan, USA. http://www.engin.umich.edu/group/ctm/PID/PID.html#pid.

Micromega. (2003). "Low-stiffness active isolation interface." Micromega Dynamics. http://www.micromega-dynamics.com/index.htm.

Ogata, K. (1997). "Modern control engineering", 3rd ed., 616-632. Published by Prentice-Hall Inc. the United States of America.

QPhase. (2006) " QD145 (1.45) Diameter optical Encoder Datasheet." rev.050909, Quantum Devices, Inc., Barneveld, Americ.

Sabater, J.M., Saltarén, R. J. and Aracl, R., et al. (2006)."Teleoperated parallel climbing robot in nuclear installations", industrial Robot: An International Journal, vol 33, no.5, 381-386, Emerald Group Publishing Limited.

Shoham, M. (2003). "Bone-mounted miniature robot for surgical procedures: concept and clinical applications." *IEEE Int. Conf. on Robotics and*

Automation, 19(5):893-901.

ServoTek. (2006). "ST 38/50 Series Encoder, Specifications, Datasheet 501/502." Servo-Tek Products Company, Hawthorne, America

Swanson, K. (2004). "Mechatronic design of a medical platform robot for long bone fracture realignment.", 6-25.

Torrance, J. (2004)."Motion control of a Medical Platform Robot for Long Bone Fracture Realignment.", 7-15.

Graham, A.E., Xie, S.Q., Aw, K.C., Xu, W, L., and Mukherjee, S.,(2005). "Design of a Parallel Long Bone Fracture Reduction Robot with Planning Treatment Tool", Proceeding IEEE/RJ international conference on Robots and Intelligent Systems, Beijing, China 9-15 October, pp. 1255-1260.

Appendix A

1. Inverse kinematics solution in MATLAB program

```
%Name:Yimin Wu ID: 03223779
%Date 28 Mar 2007
%ABT is the homogeneous transformation matrix
%AP1 is the 4x1 matrix
%AP is the 3x1 matrix
a=input ('Please enter the angle value of Alpha a= ')
b=input ('Please enter the angle value of Beta b=')
c=input ('Please enter the angle value of Gamma c=')
d=input ('please enter the angle offset between the frame A and frame B at the start
position d=')
ABO=input ('Please enter the origin of the frame B with respect to frame A in format
[x;y;z] APB= ')

%the position of B1~B6 defined by frame B(the top plate)
B1P=[150;0;0;1]
B2P=[129.90;75;0;1]
B3P=[-75;129.90;0;1]
B4P=[-129.90;75;0;1]
B5P=[-75;-129.90;0;1]
B6P=[0;-150;0;1]

%the homogeneous transformation for all six vectors
ABT=[cosd(a+d)*cosd(b)          cosd(a+d)*sind(b)*sind(c)-sind(a-d)*cosd(c)
cosd(a+d)*sind(b)*cosd(c)+sind(a+d)*sind(c) ABO(1,1);
    sind(a+d)*cosd(b)          sind(a+d)*sind(b)*sind(c)+cosd(a+d)*cosd(c)
sind(a+d)*sind(b)*cosd(c)-cosd(a+d)*sind(c) ABO(2,1);
    -sind(b) cosd(b)*sind(c) cosd(b)*cosd(c) ABO(3,1);
    0 0 0 1]

A1P=ABT*B1P
A2P=ABT*B2P
A3P=ABT*B3P
A4P=ABT*B4P
A5P=ABT*B5P
A6P=ABT*B6P
```

```
%A1P=[A1P(1,1);A1P(2,1);A1P(3,1)]
%plot(AP,ABP)
%the position of A1~A6 defined by frame A(the base plate)
A1=[220;0;0]
A2=[110;192.525;0]
A3=[-110;192.525;0]
A4=[-220;0;0]
A5=[-110;-192.525;0]
A6=[110;-192.525;0]

lengthA1x= (A1(1,1)-A1P(1,1))*(A1(1,1)-A1P(1,1))
lengthA1y= (A1(2,1)-A1P(2,1))*(A1(2,1)-A1P(2,1))
lengthA1z= (A1(3,1)-A1P(3,1))*(A1(3,1)-A1P(3,1))

lengthA2x= (A2(1,1)-A2P(1,1))*(A2(1,1)-A2P(1,1))
lengthA2y= (A2(2,1)-A2P(2,1))*(A2(2,1)-A2P(2,1))
lengthA2z= (A2(3,1)-A2P(3,1))*(A2(3,1)-A2P(3,1))

lengthA3x= (A3(1,1)-A3P(1,1))*(A3(1,1)-A3P(1,1))
lengthA3y= (A3(2,1)-A3P(2,1))*(A3(2,1)-A3P(2,1))
lengthA3z= (A3(3,1)-A3P(3,1))*(A3(3,1)-A3P(3,1))

lengthA4x= (A4(1,1)-A4P(1,1))*(A4(1,1)-A4P(1,1))
lengthA4y= (A4(2,1)-A4P(2,1))*(A4(2,1)-A4P(2,1))
lengthA4z= (A4(3,1)-A4P(3,1))*(A4(3,1)-A4P(3,1))

lengthA5x= (A5(1,1)-A5P(1,1))*(A5(1,1)-A5P(1,1))
lengthA5y= (A5(2,1)-A5P(2,1))*(A5(2,1)-A5P(2,1))
lengthA5z= (A5(3,1)-A5P(3,1))*(A5(3,1)-A5P(3,1))

lengthA6x= (A6(1,1)-A6P(1,1))*(A6(1,1)-A6P(1,1))
lengthA6y= (A6(2,1)-A6P(2,1))*(A6(2,1)-A6P(2,1))
lengthA6z= (A6(3,1)-A6P(3,1))*(A6(3,1)-A6P(3,1))

A1B1=sqrt (lengthA1x+lengthA1y+lengthA1z)
A2B2=sqrt (lengthA2x+lengthA2y+lengthA2z)
A3B3=sqrt (lengthA3x+lengthA3y+lengthA3z)
A4B4=sqrt (lengthA4x+lengthA4y+lengthA4z)
A5B5=sqrt (lengthA5x+lengthA5y+lengthA5z)
A6B6=sqrt (lengthA6x+lengthA6y+lengthA6z)
```

2. Programs used in the testing (Push-Rotate-Pull)

#RW
OE1,1,1,1,1,1
ER*=20
IT0.3,0.3,0.3,0.3,0.3,0.3
KP*=700
KD*=800
KI*=0.01
CM ABCDEF
DT8
CD1,1,1,1,1,1
WC
CD3,3,3,3,3,3
WC
CD5,5,5,5,5,5
WC
CD6,6,6,6,6,6
WC
CD8,8,8,8,8,8
WC
CD9,9,9,9,9,9
WC
CD10,10,10,10,10,10
WC
CD10,10,10,10,10,10
WC
CD11,11,11,11,11,11
WC
CD11,11,11,11,11,11
WC
CD11,11,11,11,11,11
WC
CD11,11,11,11,11,11
WC
CD10,10,10,10,10,10
WC
CD10,10,10,10,10,10
WC
CD9,9,9,9,9,9
WC
CD8,8,8,8,8,8
WC
CD6,6,6,6,6,6
WC

CD5,5,5,5,5,5
WC
CD3,3,3,3,3,3
WC
CD1,1,1,1,1,1
WC
WT 1000
CD-1,0,-1,0,-1,0
WC
CD-2,0,-2,0,-2,0
WC
CD-3,0,-3,0,-3,0
WC
CD-4,0,-4,0,-4,0
WC
CD-4,0,-4,0,-4,0
WC
CD-5,0,-5,0,-5,0
WC
CD-5,0,-5,0,-5,0
WC
CD-6,0,-6,0,-6,0
WC
CD-6,0,-6,0,-6,0
WC
CD-6,0,-6,0,-6,0
WC
CD-6,0,-6,0,-6,0
WC
CD-6,0,-6,0,-6,0
WC
CD-6,0,-6,0,-6,0
WC
CD-5,0,-5,0,-5,0
WC
CD-5,0,-5,0,-5,0
WC
CD-4,0,-4,0,-4,0
WC
CD-4,0,-4,0,-4,0
WC
CD-3,0,-3,0,-3,0
WC
CD-2,0,-2,0,-2,0

WC
CD-1,0,-1,0,-1,0
WC
WT 1000
CD-1,-1,-1,-1,-1,-1
WC
CD-3,-3,-3,-3,-3,-3
WC
CD-5,-5,-5,-5,-5,-5
WC
CD-6,-6,-6,-6,-6,-6
WC
CD-8,-8,-8,-8,-8,-8
WC
CD-9,-9,-9,-9,-9,-9
WC
CD-10,-10,-10,-10,-10,-10
WC
CD-10,-10,-10,-10,-10,-10
WC
CD-11,-11,-11,-11,-11,-11
WC
CD-11,-11,-11,-11,-11,-11
WC
CD-11,-11,-11,-11,-11,-11
WC
CD-11,-11,-11,-11,-11,-11
WC
CD-10,-10,-10,-10,-10,-10
WC
CD-10,-10,-10,-10,-10,-10
WC
CD-9,-9,-9,-9,-9,-9
WC
CD-8,-8,-8,-8,-8,-8
WC
CD-6,-6,-6,-6,-6,-6
WC
CD-5,-5,-5,-5,-5,-5
WC
CD-3,-3,-3,-3,-3,-3
WC
CD-1,-1,-1,-1,-1,-1
WC

DT0;
CD 0,0,0,0,0,0
EN

Appendix B

1. Experimental results in PID tuning

Record of PID Testing and Verification							
Date: 06 July 06						**Actuator Number: 05**	
Start time: 9:45 am						**Testing sample: Sine input (+100~-100 counts)**	
No.	Actuator Placement	Weight (kg)	PID Parameters			Pass or Fail? Comments	Error boundary (unit : count)
			KP	KD	KI		
1	H	0.5	30	270	0.01	F	+20 ~ -20
2	V	0.5	30	270	0.01	F	+23 ~ -23
3	H	0.5	180	270	0.01	P	+5 ~ -8
4	V	0.5	180	270	0.01	P	+5 ~ -8
5	H	0.5	500	270	0.01	P	+3 ~ -4
6	V	0.5	500	270	0.01	P	+5 ~ -6
7	H	0.5	500	500	0.01	P	+4 ~ -4
8	V	0.5	500	500	0.01	P	+3 ~ -3
9	H	0.5	500	1000	0.01	P	+1 ~ -1
10	V	0.5	500	1000	0.01	P	+1 ~ -1
11	H	0.5	500	2000	0.01	P	+2 ~ -2
12	V	0.5	500	2000	0.01	P	+1 ~ -2
13	H	0.5	500	4000	0.01	P/ But noise↑	+1 ~ -1
14	V	0.5	500	4000	0.01	P/ But noise↑	+1 ~ -1
15	H	0.5	1000	2000	0.01	P/but overshoot ↑	+6 ~ -6

16	V	0.5	1000	2000	0.01	P/but overshoot ↑	+6 ~ -6
17	H	2	500	500	0.01	P	+4 ~ -4
18	V	2	500	500	0.01	P	+3 ~ -4
19	H	2	500	1000	0.01	P	+2 ~ -1
20	V	2	500	1000	0.01	P	+2 ~ -1
21	H	2	600	1000	0.01	P	+2 ~ -1
22	V	2	600	1000	0.01	P	+2 ~ -1
23	H	2	250	1000	0.01	P/Error ↑	+5 ~ -5
24	V	2	250	1000	0.01	P/Error ↑	+6 ~ -5
25	H	2	1000	1000	0.01	P	+3~-2
26	V	2	1000	1000	0.01	P	+2~-1
27	H	2	1000	2000	0.01	P	+1~-1
28	V	2	1000	2000	0.01	P	+1~-2
29	H	2	800	800	0.01	P	+1~-1
30	V	2	800	800	0.01	P	+1~-1
31	H	5	180	270	0.01	F	+20 ~ -20
32	V	5	180	270	0.01	F	+15 ~ -18
33	H	5	500	270	0.01	F	+18 ~ -16
34	V	5	500	270	0.01	P	+18 ~ -16
35	H	5	500	500	0.01	P	+7 ~ -3
36	V	5	500	500	0.01	P	+10 ~ -6
37	H	5	500	1000	0.01	P	+4 ~ -3
38	V	5	500	1000	0.01	P	+4 ~ -3
39	H	5	500	2000	0.01	P	+2 ~ -2
40	V	5	500	2000	0.01	P	+1 ~ -2
41	H	5	1000	1000	0.01	P	+2~-3
42	V	5	1000	1000	0.01	P	+3~-3
43	H	5	1000	2000	0.01	P/ But noise↑	+2~-2
44	V	5	1000	2000	0.01	P/ But noise↑	+1~-2

45	H	5	800	1000	0.01	P	+1~-1
46	V	5	800	1000	0.01	P	+1~-1
47	H	5	800	2000	0.01	P/ But noise↑	+1~-2
48	V	5	800	2000	0.01	P/ But noise↑	+1~-2

Note: "H" denote horizontal placement, "V" denotes Vertical placement including upward and downward. If difference, it will be marked separately, otherwise expressed in same row. The error limit is within +10~ -10 counts.

Appendix C

1. ST38/50 Series encoders specifications and email quotation

SERVO-TEK®

ST38 Series Encoder

Specifications

DATA SHEET 501

FEATURES:

- Resolutions to 2048 lines, dual channel with index
- 200 kHz bandwidth, -10°C to 100°C operating temperature, RS422 output
- Differential signal processing for increased reliability and accuracy
- Abundant electronic options, shaft bores, and mounting patterns available
- 1.5 OD x 0.9 inches high, bores to 3/8 maximum
- Duplex bearings and easy to install flexible coupling standard
- Low cost and low profile

Electrical:	
Resolution	200 to 2048 lines/revolution
Bandwidth	200 kHz max
Incremental Accuracy	0.5 arc minutes
Mechanical:	
Size (Height x Diameter)	0.90 to 1.50 (23x38mm)
Optical Radius	0.555 (14mm)
Shaft Bore	Up to 3/8 inches
Minimum Shaft Length	0.25 inches
Maximum Shaft Length	Through shaft is standard
Axial Shaft Movement	±0.030 total
Shaft Speed	10,000 RPM max
Environmental:	
Operating Temperature	-10°C to +100°C
Storage Temperature	-25°C to +100°C
Relative Humidity	90% non-condensing
Mechanical Shock	100G for 6mS
Vibration	10-2000 Hz @ 10G

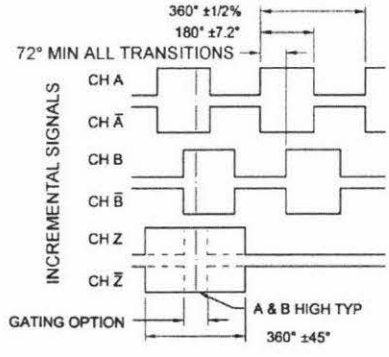

SERVO-TEK PRODUCTS COMPANY • 1086 Goffle Road, Hawthorne, NJ 07506 • Phone: 973-427-3100 • Fax: 973-427-4249
Email: sales@servotek.com • Website: www.servotek.com

Rev. 2

SERVO-TEK®

Specifications

ST50 Series Encoder

DATA SHEET 502

FEATURES:

- Incremental position signals in quadrature
- Brushless commutation signals available
- Differential signal processing for increased reliability and accuracy
- Abundant electronic options, shaft bores, and mounting patterns available
- Easy to install flexible coupling
- 360° alignment rotation
- Overvoltage and polarity reversal protection is standard

Electrical:

Resolution	200 to 5000 lines/revolution
Bandwidth	500 KHz max
Incremental Accuracy	0.5 arc minutes
Commutation Accuracy	±30 arc minutes
Commutation Adjustment	360°

Mechanical:

Size (Height x Diameter)	0.90 to 1.23 x 2.00
Optical Radius	0.780 (20mm)
Shaft Bore	Up to 5/8 inches
Minimum Shaft Length	0.35 bot. clmp.,1.0 top clmp.
Maximum Shaft Length	Through shaft is standard
Axial Shaft Movement	±0.030 total
Shaft Speed	10,000 RPM max

Environmental:

Operating Temperature	-40°C to +125°C
Storage Temperature	-55°C to +150°C
Relative Humidity	90% non-condensing
Mechanical Shock	100 G for 6 ms
Vibration	10-2000 Hz @ 10 G
L_{10} Life Rating	$2x10^8$ revolutions, $1x10^5$ hrs

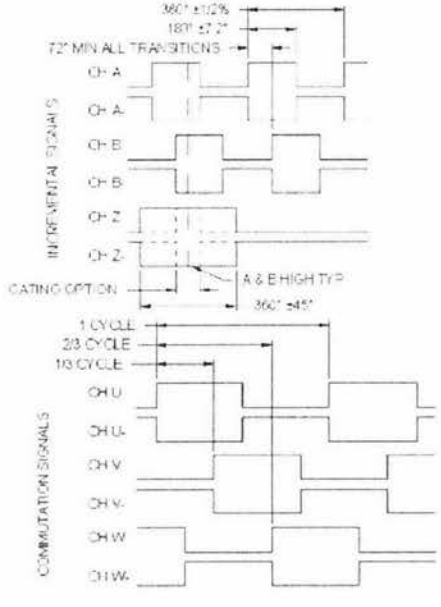

SERVO-TEK PRODUCTS COMPANY • 1086 Goffle Road, Hawthorne, NJ 07506 • Phone: 973-427-3100 • Fax: 973-427-4249
Email: sales@servotek.com • Website: www.servotek.com

Rev. 2

SERVO-TEK®

Specifications

ST50 Series Encoder

DATA SHEET 502

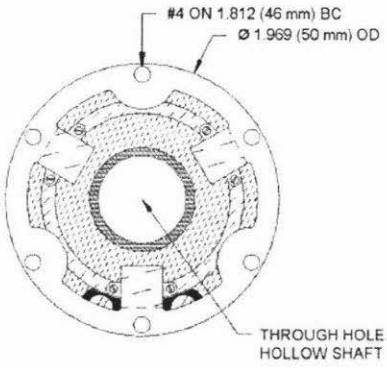

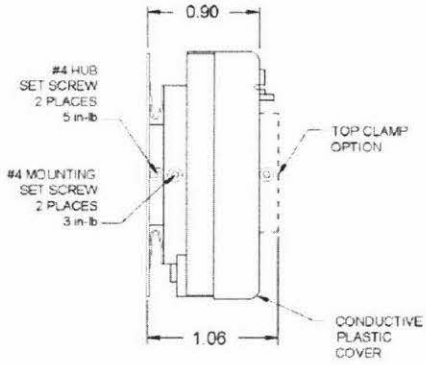

The flexible design concept of the ST50 allows for a great variety of encoder applications while maintaining cost and quality. The model numbering system can be used to configure encoder types using the standard options currently available. However, new models may be configured, by consulting the factory, for specific options not listed here. Any line count and shaft bore are possible within the limits listed. Virtually any electronic circuit or mounting pattern can be made available.

ST50-XXXX/X-XX-XXX-X

Line Count
0200 - 200
0256 - 256
0360 - 360
0500 - 500
0512 - 512
1000 - 1000
1024 - 1024
1250 - 1250
2000 - 2000
2048 - 2048
4096 - 4096
5000 - 5000

Commutation
0 - None
2 - 4 Pole
3 - 6 Pole
4 - 8 Pole
6 - 12 Pole

Shaft Bore
006 - .2362 (6mm)
249 - .2498
250 - .2501
312 - .3123
008 - .3150 (8mm)
374 - .3748
375 - .3751
010 - .3937 (10mm)
012 - .4725 (12mm)
500 - .4998
014 - .5512 (14mm)
625 - .6248

Mounting Pattern	Clamping
A - #4-40 on 1.812 BC	Bot. Clamp
B - Size 21 Servo	Bot. Clamp
C - Size 15 Servo	Bot. Clamp
D - #4-40 on 1.812 BC	Top Clamp
E - Size 21 Servo	Top Clamp
F - Size 15 Servo	Top Clamp

Electronic Output
01 - Incremental & Commutation, both RS422
02 - Incremental only, RS422
03 - Incremental & Commutation, both RS422 with Index Gating option
04 - Incremental only, RS422 with Index Gating option

SERVO-TEK PRODUCTS COMPANY • 1086 Goffle Road, Hawthorne, NJ 07506 • Phone: 973-427-3100 • Fax: 973-427-4249
Email: sales@servotek.com • Website: www.servotek.com

Rev. 2

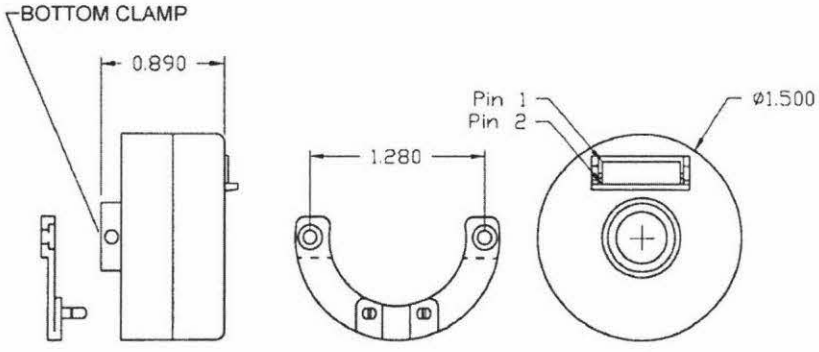

The flexible design concept of the ST38 allows for a great variety of encoder applications while maintaining cost and quality. The model numbering system can be used to configure encoder types using the standard options currently available. However, new models may be configured, by consulting the factory, for specific options not listed here. Almost any line count and shaft bore are possible within the limits listed. Virtually any electronic circuit or mounting pattern can be made available.

ST38-XXXX-XX-XXX-X

Line Count
0200 - 200
0256 - 256
0360 - 360
0500 - 500
0512 - 512
1000 - 1000
1024 - 1024
1250 - 1250
2000 - 2000
2048 - 2048

Shaft Bore
006 - .2362 (6mm)
249 - .2498
250 - .2501
312 - .3123
008 - .3150 (8mm)
374 - .3748
375 - .3751

Mounting Pattern	**Clamping**
A - #2-56 on 1.280 BC	Bot. Clamp

Electronic Output
01 - Incremental only, RS422
02 - Incremental only, RS422 with Index Gating option

SERVO-TEK PRODUCTS COMPANY • 1086 Goffle Road, Hawthorne, NJ 07506 • Phone: 973-427-3100 • Fax: 973-427-4249
Email: sales@servotek.com • Website: www.servotek.com

Rev. 2

Servo-Tek Products Company

1086 GOFFLE ROAD
HAWTHORNE, NJ 07506
TELEPHONE: (973) 427-3100
FAX: (973) 427-4249

EMAIL QUOTATION

QUOTATION NO. 3682
TO: Jason Wu
COMPANY: Massey University
Auckland, New Zealand

DATE:
NO. PAGES: 01
FAX NUMBER:
Email: wu_ym@msn.com
REFERENCE:

FROM: Diane Marsilio, Sales Dept.

ITEM	SERVO-TEK MODEL NUMBER	DESCRIPTION	QTY	UNIT PRICE	TOTAL
A	ST38-0500-02-375 -A	Encoder, line count 500 Incremental only, RS422 with index gating option Shaft bore .3751 Mounting pattern A NOTE: For 2 feet of cable with mating connector add US$ 10.35 to unit price.	6	US$ 155.25	US$ 931.50

B	ST50-0500/0-04-0 14-A	Encoder, line count 500 No commutation Incremental only, RS422 with index gating option Shaft bore .5512 (14mm) Mounting pattern A NOTE: For 2 feet of cable with mating connector add US$ 13.80 to unit price. Shipping & handling charge to be determined. Duties/taxes to be paid by consignee. Payment in advance required. We accept Visa and MasterCard	6	258.75	1552.50

TERMS: Payment in advance – Visa or MasterCard

SHIPMENT: No stock, built to order, 8 weeks

PRICES QUOTED WILL BE HELD FIRM FOR THIRTY DAYS FROM THE DATE OF THIS QUOTATION.

SERVO-TEK'S CONDITIONS OF SALE AND WARRANTY APPLY.

REMARKS: **AREA REPRESENTATIVE:**

2. QD145 diameter optical encoder specifications

Quantum Devices, Inc.
"Improving the Quality of Life through the Power in Light"
®

QPhase™

QD145 (1.45") Diameter Optical Encoder

Design Features:

- 500 kHz Fundamental Frequency Response
- Low profile, 0.87" assembled height
- Bearing design simplifies encoder attachment
- Resolutions up to 5000 lines per revolution direct read
- 4, 6 or 8 pole commutation
- Conductive carbon fiber housing
- Standard 1.812" Bolt Circle mounting
- Through shaft sizes up to 0.375" Diameter
- High Noise Immunity
- Cost Competitive with Modular Encoders

Description:

Quantum Devices, Inc. Model QD145 provides an improved feedback solution in applications typically using modular encoders. With an over all height of just only 0.87" and the stability of a bearing encoder design, the model QD145 can provide significant performance upgrades in applications limited by traditional modular encoder solutions. Outputs consist of a quadrature with reference pulse and three-phase commutation, which can be configured with either the industrial standard 5 volt RS422A Line Driver or the 5 to 26 volt OL7272 line driver. A flexible member allows for much greater tail shaft run out than can be tolerated by modular encoder designs, plus it provides 30 degrees of rotation for commutation timing. A housing constructed of conductive carbon fiber composite provides the EMI shielding of an all metal housing and the performance of a lightweight robust assembly.

Ordering Information:

QD145-05/05-1000-6-01-T3-01-02

Construction
QD145 = Non-RoHS
QR145 = RoHS

Voltage
05/05 = 5VDC +-5%
* 05/26 = 5-26VDC

***Resolution**
200
250
256
500
512
600
1000
1024
1250
2000
2048
2500
4096
5000

***Motor Poles**
0 = No Com
4 = 4 Pole
6 = 6 Pole
8 = 8 Pole

Output Option
01 = RS422A Line Driver
* 02 = OL7272 5-26VDC
03 = TTL Output
* 04 = RS422A for A, B, Z; Open Collector for U, V, W

Bore Size
T1 = 0.250"
T2 = 0.312"
T3 = 0.375"
T4 = 6mm
T5 = 8mm
T6 = 10mm
T11 = 5mm
SS = Special

Mounting
01 = STD 1.812" Flex
02 = Size 15 Resolver Mount
03 = Sealed Housing
04 = STD 1.575" Flex
SS = Special

Index Gating
Blank = Ungated Index
01 = Gated to A, 180°
02 = Gated to A & B, 90°

** Consult Factory for Resolution and Pole Count Availability.*
♦ Not Available with RoHS Construction – Consult Factory

ISO 9001
CERT. NO. FM 52711

Quantum Devices, Inc. 112 Orbison St., P.O. Box 100 , Barneveld, WI 53507
Tel: (608) 924-3000 Fax: (608) 924-3007 URL: www.quantumdev.com E-mail: qdisales@quantumdev.com

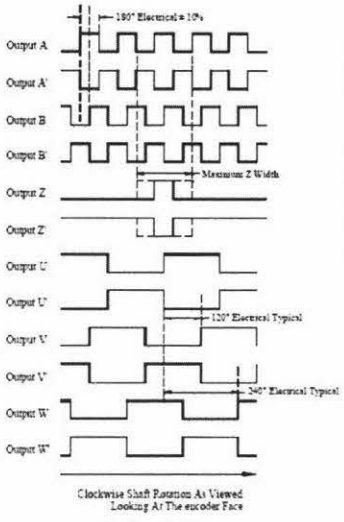

See figure below

Output Waveforms

Note: TTL Output Option consists of +VDC, Common, Case Ground and Output's A, B & Z wires only

QD145 Wiring Diagram

Red -+VDC
Black – Common
Brown – Output A
White – Output A'
Blue – Output B
Green – Output B'
Orange – Output Z
Yellow – Output Z'
Violet – Output U
Gray – Output U'
Brown/White – Output V
Red/White – Output V'
Orange/White – Output W
Yellow/White – Output W'
Black/White – Case Ground
Drain Wire – Cable Shield

Electrical Specifications

Input Voltage	5 VDC ± 5% or 5-26 VDC
Input Current Requirements	125mA Typical @ 5VDC Plus Interface Loads
Input Ripple	2% Peak to Peak @ 5 VDC
Output Circuits	AM26LS31 RS 422A line driver OL7272 High Voltage Line Driver TTL Output
Incremental Output Format	Quadrature with A leading B for CW rotation with Index Pulse centered over A for 2500 line count and below. Index Pulse true over A and B High for 2500 line count and above
Frequency Response	500 kHz
Symmetry	180 Degrees ± 10% Typical
Minimum Edge Separation	54 electrical degrees
Commutation Format	Three Phase 4, 6 or 8 poles
Commutation Accuracy	± 1° mechanical

Environmental Specifications

Storage Temperature	-40 to 125° C
Operating Temperature	-20 to 100° C Typical -20 to 120° C Optional**
Humidity	98% Non-Condensing
Vibration	20 g's @ 50 to 500 CPS
Shock	50 g's @ 11mS Duration

Mechanical Specification

Maximum Shaft Speed	8000 RPM
Through Shaft Diameter	0.250", 0.3125", 0.375", 6mm ,8mm, 10mm, 5mm (-0.0000, + 0.0005)
Radial Shaft Movement	0.007" TIR
Axial Shaft Movement	± 0.030"
Housing	Carbon Fiber Composite (case ground via cable)
Housing Volume Resistivity	10^{-2} ohm-cm
Termination	15 conductor Cable, 28 AWG 18" long, 9 conductor Cable for non-commutated and TTL outputs
Mounting	1.812" Bolt Circle
Moment of Inertia	1.5×10^{-4} oz-in-S^2
Acceleration	$1x10^5$ Radians/S^2
Accuracy	± 1.0 arc minute

** Contact Factory for more information

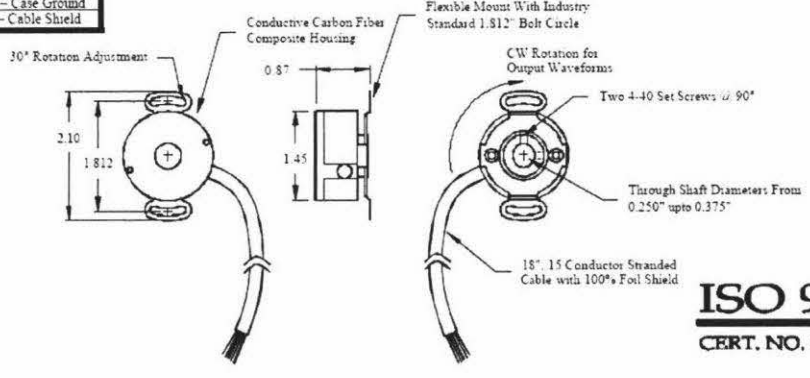

ISO 9001
CERT. NO. FM 52711

Quantum Devices, Inc. 112 Orbison St., P.O. Box 100 , Barneveld, WI 53507

Tel: (608) 924-3000 Fax: (608) 924-3007 URL: www.quantumdev.com E-mail: qdisales@quantumdev.com

3. SP-750 series switched power supply

MEAN WELL 750W Single Output Power Supply **SP-750 series**

■ Features :

- Universal AC input/Full range
- AC input active surge current limiting
- Built-in active PFC function, PF>0.95
- Protections: Short circuit, overload, over voltage, over temperature
- Forced air cooling by built-in DC ball bearing fan
- High power density 5.48/inch^3
- Built-in constant current limiting circuit
- With power good and fail signal output
- Built-in remote ON-OFF control
- Built-in remote sense function
- 3 years warranty

SPECIFICATION

MODEL		SP-750-5	SP-750-12	SP-750-15	SP-750-24	SP-750-27	SP-750-48
OUTPUT	DC VOLTAGE	5V	12V	15V	24V	27V	48V
	RATED CURRENT	120A	62.5A	50A	31.3A	27.8A	15.7A
	CURRENT RANGE	0 ~ 120A	0 ~ 62.5A	0 ~ 50A	0 ~ 31.3A	0 ~ 27.8A	0 ~ 15.7A
	RATED POWER	600W	750W	750W	751.2W	750.6W	753.6W
	RIPPLE & NOISE (max.) Note.2	120mVp-p	120mVp-p	120mVp-p	120mVp-p	120mVp-p	120mVp-p
	VOLTAGE ADJ. RANGE	4.75 ~ 5.5V	10 ~ 13.5V	13.5 ~ 16.5V	22 ~ 26.4V	24 ~ 30V	43 ~ 56V
	VOLTAGE TOLERANCE Note.3	±2.0%	±1.0%	±1.0%	±1.0%	±1.0%	±1.0%
	LINE REGULATION	±0.5%	±0.3%	±0.3%	±0.2%	±0.2%	±0.2%
	LOAD REGULATION	±2.0%	±0.5%	±0.5%	±0.5%	±0.5%	±0.5%
	SETUP, RISE, HOLD TIME	1000ms, 50ms, 16ms/230VAC 1000ms, 50ms, 16ms/115VAC at full load					
INPUT	VOLTAGE RANGE	90 ~ 264VAC 127 ~ 370VDC					
	FREQUENCY RANGE	47 ~ 63Hz					
	POWER FACTOR	0.95/230VAC 0.96/115VAC at full load					
	EFFICIENCY (Typ.)	81%	86%	87%	89%	89%	90%
	AC CURRENT	11A/115VAC 5.3A/230VAC					
	INRUSH CURRENT (max.)	30A/115VAC 50A/230VAC					
	LEAKAGE CURRENT	<2.0mA / 240VAC					
PROTECTION	OVER LOAD	105~125% rated output power Protection type : Constant current limiting, unit will Hiccup after 3 sec.					
	OVER VOLTAGE	5.75 ~ 6.3V	13.8 ~ 16.2V	18 ~ 21V	27.6 ~ 32.4V	31 ~ 36.5V	57.6 ~ 67.2V
		Protection type : Shut down o/p voltage, re-power on to recover					
	OVER TEMPERATURE	85℃±5℃ (TSW1) Detect on heatsink of power transistor 85℃±5℃ (TSW2) Detect on heatsink of power diode Protection type : Shut down o/p voltage, recovers automatically after temperature goes down					
FUNCTION	POWER GOOD/FAIL	50ms/1ms					
	REMOTE CONTROL	RC+/RC- short power on, open power off					
ENVIRONMENT	WORKING TEMP.	-20 ~ +60℃ (Refer to output load derating curve)					
	WORKING HUMIDITY	20~90% RH non-condensing					
	STORAGE TEMP., HUMIDITY	-40 ~ +85℃, 10 ~ 95% RH					
	TEMP. COEFFICIENT	±0.05%/℃ (0 ~ 50℃)					
	VIBRATION	10 ~ 500Hz, 2G 10min./1cycle, 60min. each along X, Y, Z axes					
SAFETY & EMC (Note 4)	SAFETY STANDARDS	UL60950-1, TUV EN60950-1 Approved					
	WITHSTAND VOLTAGE	I/P-O/P:3KVAC I/P-FG:1.5KVAC O/P-FG:0.5KVAC					
	ISOLATION RESISTANCE	I/P-O/P, I/P-FG, O/P-FG:100M Ohms/500VDC					
	EMI CONDUCTION & RADIATION	Compliance to EN55011 (CISPR11), EN55022 (CISPR22) Class B					
	HARMONIC CURRENT	Compliance to EN61000-3-2,-3					
	EMS IMMUNITY	Compliance to EN61000-4-2,3,4,5,6,8,11, ENV50204, EN55024, EN61000-6-2, EN61204-3 Heavy industry level, criteria A					
OTHERS	MTBF	769.3K hrs min. MIL-HDBK-217F (25℃)					
	DIMENSION	276*127*63.5mm (L*W*H)					
	PACKING	2.9Kg; 6pcs / 18.4Kg / 0.98CUFT					
NOTE	1. All parameters NOT specially mentioned are measured at 230VAC input, rated load and 25℃ of ambient temperature. 2. Ripple & noise are measured at 20MHz of bandwidth by using a 12" twisted pair-wire terminated with a 0.1uf & 47uf parallel capacitor. 3. Tolerance : includes set up tolerance, line regulation and load regulation. 4. The power supply is considered a component which will be installed into a final equipment. The final equipment must be re-confirmed that it still meets EMC directives.						

■ Mechanical Specification

Case No.919A Unit:mm

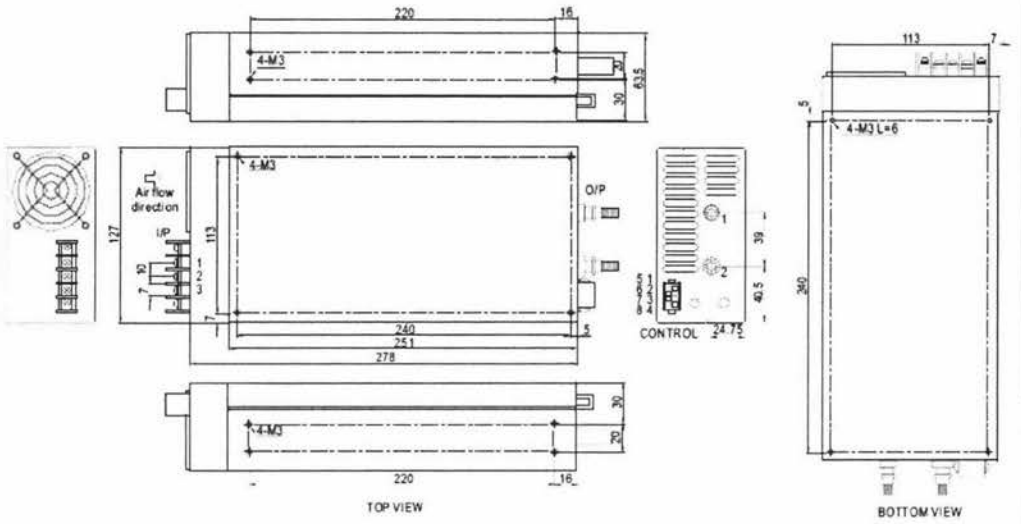

AC Input Terminal Pin. No. Assignment

Pin No.	Assignment
1	AC/L
2	AC/N
3	FG ⏚

DC Output Terminal Pin. No Assignment

Pin No.	Assignment
1	DC OUTPUT +V
2	DC OUTPUT -V

Control Pin. No Assignment : MOLEX 5559-NP uses 5558 male crimp terminal

Pin No.	Assignment	Pin No.	Assignment	Mating connector	Terminal
1	NC	5	NC	MOLEX 5557-NR	MOLEX 5556 Female crimp Terminal receptacle
2	-S	6	PF(Power fail signal)		
3	G	7	+S		
4	RC-	8	RC+		

■ Derating Curve

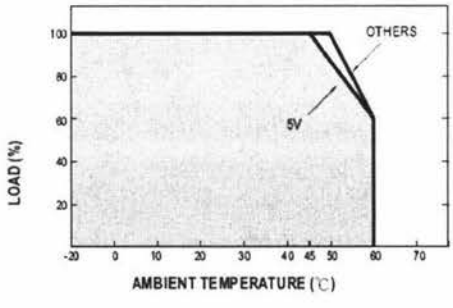

■ Static Characteristics

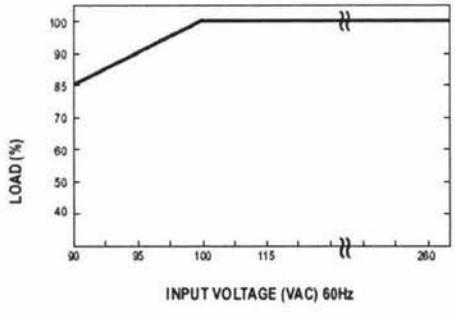

4. Spherical rolling joint specifications

Spherical Rolling Joint

Spherical Rolling Joint SRJ series

Rolling guide with zero clearance has realized high rigidity and high precision.

Joints with multiple degrees of freedom essential to parallel mechanism have conventionally obtained 2~3 degrees of freedom by combining rotational joints.
However, these joints have been characterized by upsizing due to complex structure.
Sliding spherical joints with multiple degrees of freedom have also been available, however, they have had large frictional resistance and inner clearance.
In order to resolve these problems, HEPHAIST SEIKO has developed rolling Spherical Rolling Joint.

Features

1 **High precision**
The movable part has less frictional resistance due to its rolling joint structure under preload, achieving high precision with zero clearance.

2 **Downsizing of joints with multiple degrees of freedom**
Compared with those combining rolling bearings with 3 degrees of freedom, higher rigidity and downsizing has been achieved.

3 **Application to parallel mechanism**
Optimal for achieving high precision, high rigidity and downsizing of parallel mechanism.

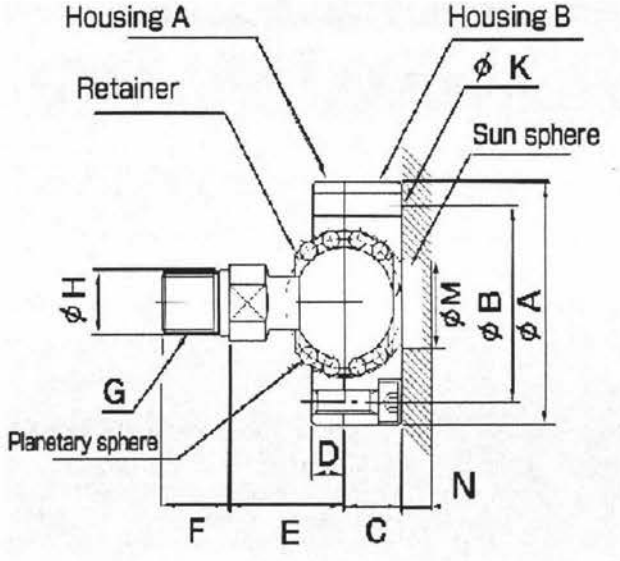

■ **Product specifications**

C series

Type	A	B	C	D	E	F	G	H	K	M	N	C(N)	Co(N)	Spot facing depth	Width across flat	Weight (kg)
SRJ004C	19	15	3.8	2.5	10	6	M3	3.6	2	6	1.5	128	100	1.5	4	0.015
SRJ006C	25	20	5.5	3.8	11.5	8	M4×0.5	4.5	3	10	2	320	280	2.3	5	0.036
SRJ008C	30	24	7	4	16	12	M5×0.5	5.5	3.4	11	2	490	540	2	7	0.06
SRJ012C	42	34	11	6	20	15	M10	11	4.3	14	2	720	770	3.6	14	0.18
SRJ016C	56	45	12	7	32	18	M12	12.6	5.5	25	5	1170	1300	4.6	14	0.37

5. 3141~3144 Hall-effect switches

3141 THRU 3144

Data Sheet 27621.6A*

SENSITIVE HALL-EFFECT SWITCHES FOR HIGH-TEMPERATURE OPERATION

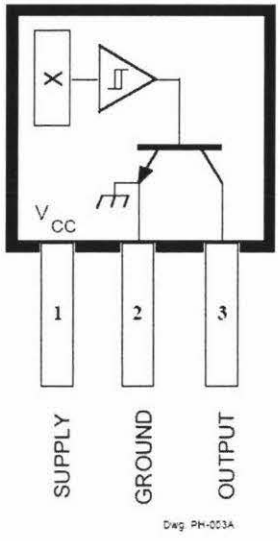

Pinning is shown viewed from branded side.

ABSOLUTE MAXIMUM RATINGS at T_A = +25°C

Supply Voltage, V_{CC} ..... **28 V**
Reverse Battery Voltage, V_{RCC} ..... **-35 V**
Magnetic Flux Density, B ..... **Unlimited**
Output OFF Voltage, V_{OUT} ..... **28 V**
Reverse Output Voltage, V_{OUT} ..... **-0.5 V**
Continuous Output Current, I_{OUT} ..... **25 mA**
Operating Temperature Range, T_A
Suffix 'E–' ..... **-40°C to +85°C**
Suffix 'L–' ..... **-40°C to +150°C**
Storage Temperature Range,
T_S ..... **-65°C to +170°C**

These Hall-effect switches are monolithic integrated circuits with tighter magnetic specifications, designed to operate continuously over extended temperatures to +150°C, and are more stable with both temperature and supply voltage changes. The unipolar switching characteristic makes these devices ideal for use with a simple bar or rod magnet. The four basic devices (3141, 3142, 3143, and 3144) are identical except for magnetic switch points.

Each device includes a voltage regulator for operation with supply voltages of 4.5 to 24 volts, reverse battery protection diode, quadratic Hall-voltage generator, temperature compensation circuitry, small-signal amplifier, Schmitt trigger, and an open-collector output to sink up to 25 mA. With suitable output pull up, they can be used with bipolar or CMOS logic circuits. The A3141– and A3142– are improved replacements for the UGN/UGS3140–; the A3144– is the improved replacement for the UGN/UGS3120–.

The first character of the part number suffix determines the device operating temperature range. Suffix 'E–' is for the automotive and industrial temperature range of -40°C to +85°C. Suffix 'L–' is for the automotive and military temperature range of -40°C to +150°C. Three package styles provide a magnetically optimized package for most applications. Suffix '–LT' is a miniature SOT89/TO-243AA transistor package for surface-mount applications; suffix '–U' is a three-lead plastic mini-SIP, while suffix '–UA' is a three-lead ultra-mini-SIP.

FEATURES and BENEFITS

- Superior Temp. Stability for Automotive or Industrial Applications
- 4.5 V to 24 V Operation ... Needs Only An Unregulated Supply
- Open-Collector 25 mA Output ... Compatible with Digital Logic
- Reverse Battery Protection
- Activate with Small, Commercially Available Permanent Magnets
- Solid-State Reliability
- Small Size
- Resistant to Physical Stress

Always order by complete part number, e.g., **A3141ELT**.

Allegro MicroSystems, Inc.

3141 THRU 3144
SENSITIVE HALL-EFFECT SWITCHES FOR HIGH-TEMP. OPERATION

FUNCTIONAL BLOCK DIAGRAM

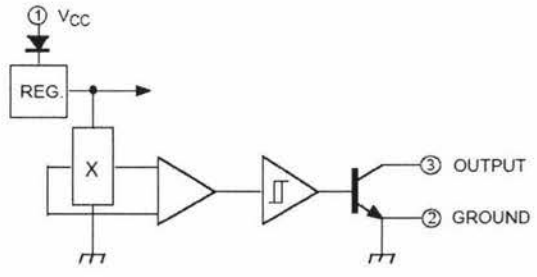

ELECTRICAL CHARACTERISTICS at V_{CC} = 8 V over operating temperature range.

Characteristic	Symbol	Test Conditions	Limits			
			Min.	Typ.	Max.	Units
Supply Voltage	V_{CC}	Operating	4.5	—	24	V
Output Saturation Voltage	$V_{OUT(SAT)}$	I_{OUT} = 20 mA, B > B_{OP}	—	175	400	mV
Output Leakage Current	I_{OFF}	V_{OUT} = 24 V, B < B_{RP}	—	<1.0	10	µA
Supply Current	I_{CC}	B < B_{RP} (Output OFF)	—	4.4	9.0	mA
Output Rise Time	t_r	R_L = 820 Ω, C_L = 20 pF	—	0.04	2.0	µs
Output Fall Time	t_f	R_L = 820 Ω, C_L = 20 pF	—	0.18	2.0	µs

MAGNETIC CHARACTERISTICS in gauss over operating supply voltage range.

Characteristic		Part Numbers*											
		A3141–			A3142–			A3143–			A3144–		
		Min.	Typ.	Max.	Min.	Typ.	Max.	Min.	Typ.	Max.	Min.	Typ.	Max.
B_{OP}	at T_A = 25°C	50	100	160	130	180	230	220	280	340	70	—	350
	over operating temp. range	30	100	175	115	180	245	205	280	355	35	—	450
B_{RP}	at T_A = 25°C	10	45	130	75	125	175	165	225	285	50	—	330
	over operating temp. range	10	45	145	60	125	190	150	225	300	25	—	430
B_{hys}	at T_A = 25°C	20	55	80	30	55	80	30	55	80	20	55	—
	over operating temp. range	20	55	80	30	55	80	30	55	80	20	55	—

NOTES: Typical values are at T_A = +25°C and V_{CC} = 8 V.
B_{OP} = operate point (output turns ON); B_{RP} = release point (output turns OFF); B_{hys} = hysteresis (B_{OP} - B_{RP}).
1 gauss (G) is exactly equal to 0.1 millitesla (mT).
*Complete part number includes a suffix to identify operating temperature range (E- or L-) and package type (-LT, -U, or -UA).

Allegro MicroSystems, Inc.
115 Northeast Cutoff, Box 15036
Worcester, Massachusetts 01615-0036 (508) 853-5000

6. LA22 linear actuator specification

PRODUCT DATA SHEET

ACTUATOR LA22

Features:

- *12/24 V DC permanent magnet motor*
- *Max. thrust 400 N*
- *Stainless steel piston rod and piston rod eye made of reinforced plastic.*
- *Duty cycle: Max. 10% or 2 min. in use followed by 18 min. not in use.*
- *Ambient temperature +5° to +40° C.*
- *Compact construction/design*
- *Protection class: IP 51*
- *Colour: black*
- *1.0 m straight cable without plug (no cable with IP 51)*
- *Speed max. 37 mm/s*
- *Extremely quiet operation*
- *Max. stroke length 200 mm*
- *Storage temperature: - 40° to + 70° C*

Options:

- *Protection class: IP 65 (only back fixture D and E)*

Usage:

- *Should LA22 be used with a non LINAK control unit, please ask the nearest LINAK representative for further details.*

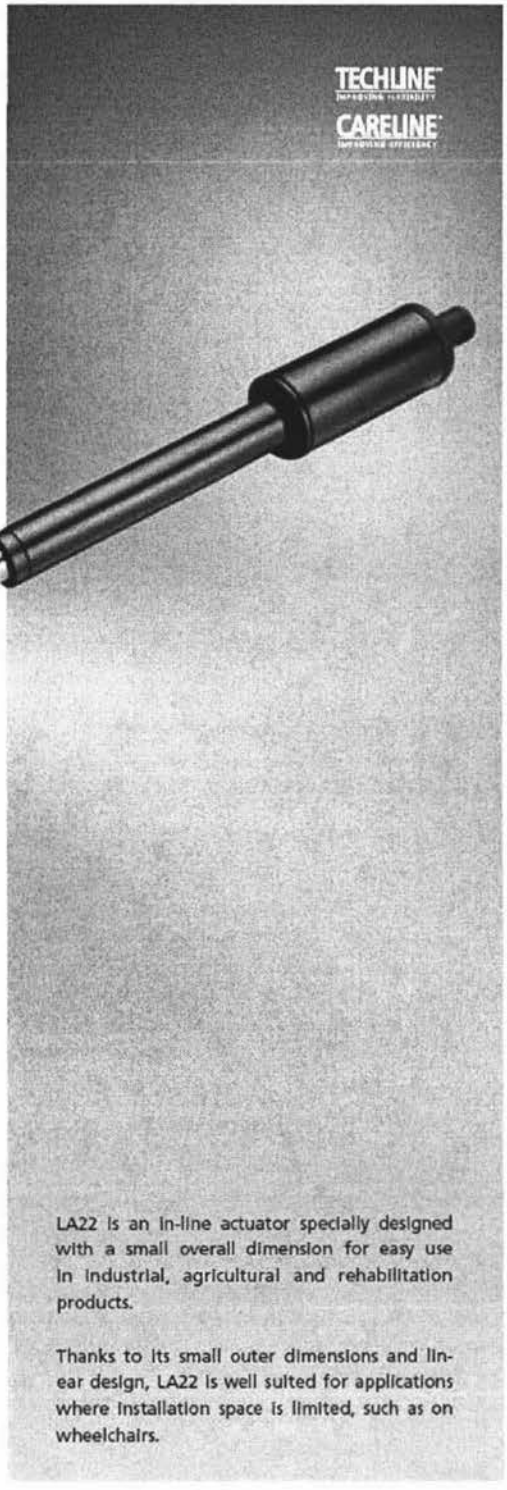

LINAK®
WE IMPROVE YOUR LIFE

Technical specifications:

Type	Thrust max. Push (N)	Self-lock max. Push (N)	Thrust max. Pull (N)	Self-lock max. Pull (N)	Typical speed (mm/s) 0/full load*		Stroke length (mm)				Duty cycle (%)	Typical amp. at full load (A)	
												12V	24V
1 mm pitch	300	300	-	-	37	17.5	50	100	150	200	10	4.5	2.1
0,8 mm pitch	400	400	-	-	27	13.5	50	100	150	200	10	5.9	2.5

** The speed values for both the 12V and 24V motor are the same.*

- *LINAK control boxes are designed so that they will short-circuit the motor terminals (poles) of the actuator(s), when the actuator(s) are not running. This solution give the actuator(s) a higher self-locking ability. If the actuator(s) are not connected to a LINAK control box, the terminals of the motor must be short-circuited to give a higher selflocking ability.*
- *The above figures are with an ambient temperature of 20°C.*
- *If the LA22 0.8mm pitch is connected to a CB8 the max. thrust will be reduced by approx. 25%.*
- *There is no "pull" test data available at the present time, for more information please contact LINAK A/S.*

Dimensions:

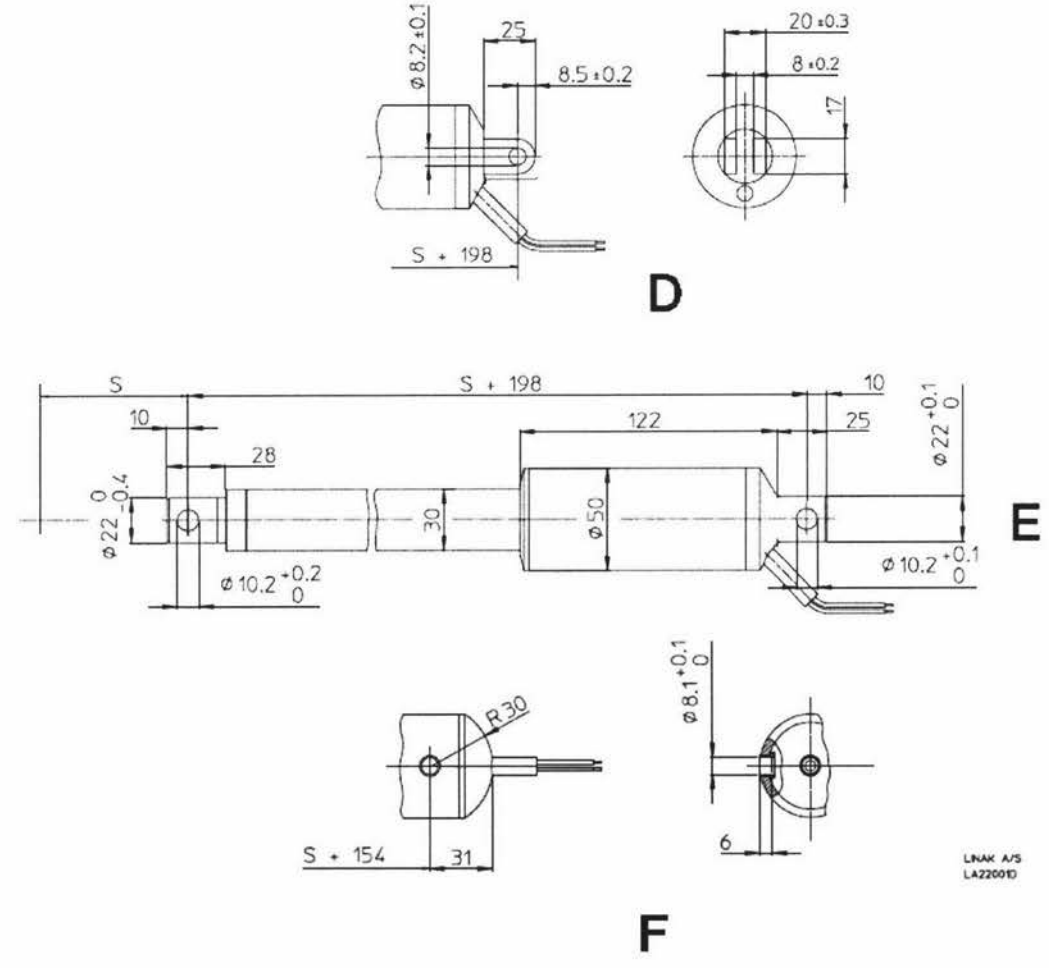

Graph:

LA22 12V motor speed v´s load

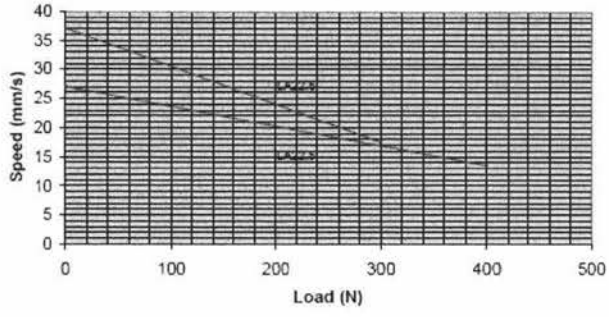

LA22 24V motor speed v´s load

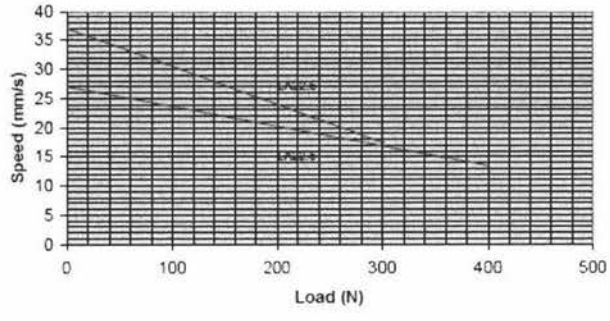

LA22 12V motor current v´s load

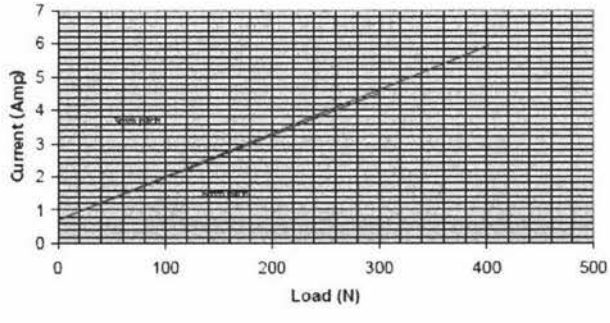

LA22 24V motor current v´s load

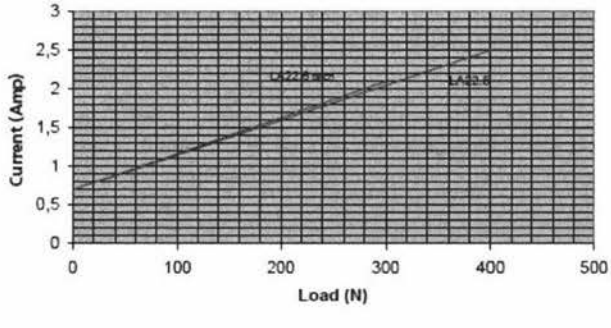

LA22

Ordering example:

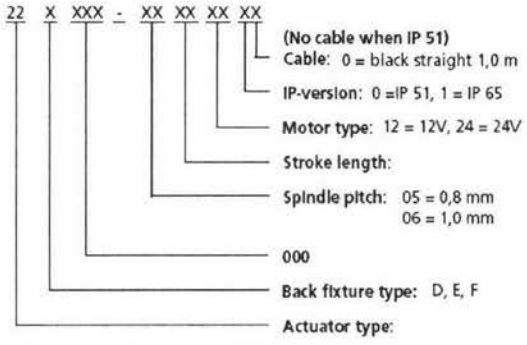

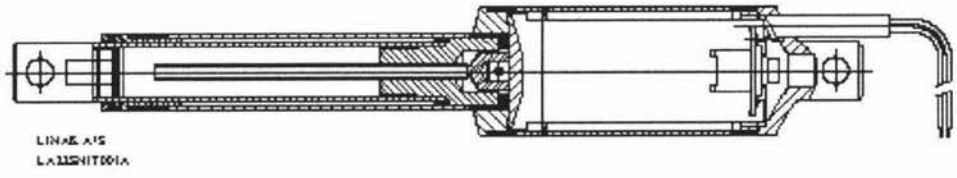

Accessories

- *CS16: electric limit switch, trips out the current to the actuator in the end position*
- *Possibility of connecting a handset to the CS16*
- *LS/LSD: limit switch, to be mounted on the actuator*

Other information

- *LA22 dB (A) 50: measuring method DS/EN ISO 3746, actuator not loaded*

THE CURRENT SUPPLY TO LINEAR ACTUATORS MUST BE CUT OFF IN CASE OF OVERLOAD AND WHEN THE ACTUATORS REACH END POSITION.